

Technical Report Documentation Page

1. Report No.	2. Government Accession No.	3. Recipient's Catalog No.	
4. Title and Subtitle Determining the Sensitivities of an S-Cam Brake		5. Report Date February 27, 1998	6. Performing Organization Code
		8. Performing Organization Report No. UMTRI-98-6	
7. Author(s) Charles C. MacAdam, Thomas D. Gillespie		10. Work Unit No. (TRAIS)	11. Contract or Grant No. Research Agreement
9. Performing Organization Name and Address The University of Michigan Transportation Research Institute 2901 Baxter Road, Ann Arbor, Michigan 48109		13. Type of Report and Period Covered Final 6/1/97 - 2/28/98	
		14. Sponsoring Agency Code	
12. Sponsoring Agency Name and Address Heavy Duty Brake Manufacturers Council c/o Haldex Corporation P.O. Box 4080 Blue Springs, MO 64014-4080			
15. Supplementary Notes Technical Representative: Mr. Randall P. Petresh			
16. Abstract The SAE Recommended Practice J1802, Brake Block Effectiveness Rating [1], has the purpose of establishing a uniform procedure for determination and classification of brake effectiveness for commercial vehicle brakes. The practice provides a means to characterize the friction properties of truck brake lining materials in a representative S-cam brake. However, the test has been found to exhibit an unacceptably large range of variability in the implied friction coefficient for the lining. It has been postulated that some of the variability arises from factors within the brakes that are used for the test—specifically, dimensional tolerances, and possibly friction in the moving parts. A computer model of an S-cam brake was developed under this work to help examine various brake parameter sensitivities. The model calculates brake torque for a specified set of geometry, friction properties, and constant input air chamber force. It assumes that the brake is in a state of equilibrium defined by equalized wear rates on the leading and trailing shoe linings. The parameter sensitivity findings indicate that a potentially significant source of torque variability is related to possible offsets between the drum turning axis and the spider/shoe assembly centerline. Other significant factors include bearing and roller pin friction and the shape of the cam profile. Offsets in the cam shaft center and asymmetric shoe-lining stiffnesses contribute to significant differential wear between the leading and trailing shoes. The issue of torque effectiveness variability and its relationship to the SAE J1802 Recommended Practice is also discussed in the report.			
17. Key Words brake, model, S-cam, parameter, geometry, sensitivity, torque, SAE J1802, effectiveness, lining, wear, commercial, vehicle		18. Distribution Statement This document is available to the public through the National Technical Information Service, Springfield, VA 22161	
19. Security Classif. (of this report) None	20. Security Classif. (of this page) None	21. No. of Pages 90	22. Price

Final Technical Report

for the project

Determining the Sensitivities of
an S-Cam Brake

Sponsored by:

The Heavy Duty Brake Manufacturers Council

Report No. UMTRI-98-6

C. MacAdam
T. Gillespie

February 1998

Executive Summary

The SAE Recommended Practice J1802, Brake Block Effectiveness Rating [1], has the purpose of establishing a uniform procedure for determination and classification of brake effectiveness for commercial vehicle brakes. The practice provides a means to characterize the friction properties of truck brake lining materials in a representative S-cam brake. However, the test has been found to exhibit an unacceptably large range of variability in the implied friction coefficient for the lining. It has been postulated that some of the variability arises from factors within the brakes that are used for the test—specifically, dimensional tolerances, and possibly friction in the moving parts.

The University of Michigan Transportation Research Institute has been funded to conduct a project for the Heavy Duty Brake Manufacturers Council (HDBMC) that would develop a model for an S-cam brake and conduct a sensitivity study to determine the variation in measured lining coefficient as a function of the geometric and friction properties of the brake.

The S-cam brake model developed under this work calculates brake torque for a specified set of geometry, friction properties, and constant input air chamber force. It assumes that the brake is in a state of equilibrium defined by equalized wear rates on the leading and trailing shoe linings. The lining-shoe structure is the only mechanically compliant element and asymmetry is allowed. The cam acts as the distributor of input force to each shoe. The model assumes that equilibrium is reached through sufficient differential wear of the leading and trailing shoe linings, given an initial wear/clearance dimension for the trailing shoe lining. Each input force level defines a unique equilibrium condition (assuming no changes to the brake geometry or its frictional properties). For each specified input force, the model seeks an equilibrium condition consistent with the prescribed geometry and friction properties such that the wear rates of the leading and trailing shoe linings are equalized. At equilibrium, the leading and trailing shoes contribute equal amounts of torque.

The parameter sensitivity findings indicate that a potentially significant source of torque variability is related to possible offsets between the drum turning axis and the spider/shoe assembly centerline. Offsets between these axes can produce significant shifts in the lining pressure distributions of both shoes, thereby altering each shoe's brake factor. This is particularly significant for the leading shoe, which tends to affect torque production more due to its higher self-energizing gain.

Other significant factors include bearing and roller pin friction. Depending upon the amount of lubrication, if any, torque variations can be significant. For example, bearing and roller pin friction levels in the range of 0.1 - 0.2 can reduce brake torque output as much as 17% versus its idealized frictionless counterpart.

The shape of the cam profile is also a potential contributor to brake torque variations.

Movement of the cam center has little effect on torque variation, but does contribute significantly to the amount of differential lining wear between the leading and trailing shoes.

Asymmetry in the effective stiffness of the lining and shoe elements (leading versus trailing) also contributes significantly to differential lining wear. As noted in the report, differential lining wear can be a primary source of non-stationary brake effectiveness.

The remaining geometric parameters are more weakly associated with comparable levels of brake torque variation. However, depending on the amount of potential variation in a particular parameter, significant torque variations may still be possible.

The issue of torque effectiveness variability and its relationship to the SAE J1802 Recommended Practice is also addressed. Since the J1802 burnish procedure acts as a mechanism for achieving (or approaching) equilibrium, the subsequent effectiveness sequence that requires testing at other pressures, may cause the brake to be no longer at, or near, equilibrium. If differential wear exists at equilibrium, this can result in significant changes in torque effectiveness, as defined by the J1802 recommended practice. Under these conditions, if the brake reaches true equilibrium during burnish, the initial stops at pressures of 10, 15 psi, etc. may involve unusual leading shoe-drum contact due to the existing differential lining wear. The brake would then exhibit a lower- or higher-than-expected effectiveness (relative to its equilibrium condition at low pressures). Likewise, at higher-than-burnish pressures (45, 50 psi), the brake is also not in equilibrium and the leading shoe is under- or over-involved depending upon the differential wear state at burnish. This also results in a change in effectiveness relative to equilibrium at the higher pressures. At any non-equilibrium pressure, the S-cam brake seeks equilibrium through the differential wear process of both linings. However, unless enough stops are performed at a fixed pressure to achieve the necessary equilibrium wear rate, the brake effectiveness will be gradually changing. Most variations in brake geometry or structural stiffnesses, away from the idealized symmetric brake, contribute to differential wear.

Recommendations for extending the existing model to include lining wear properties are also suggested. This would permit more extensive examination and analysis of the lining wear process (over time) during a test sequence such as J1802. The extended model would be time and wear dependent and thereby would be more applicable/useful for predicting and analyzing likely S-cam brake torque production during sequential brake applications, as occur in specific brake test procedures or vehicle tests.

Determining the Sensitivities of an S-Cam Brake

Introduction

The SAE Recommended Practice J1802, Brake Block Effectiveness Rating [1], has the purpose of establishing a uniform procedure for determination and classification of brake effectiveness for commercial vehicle brakes. The practice provides a means to characterize the friction properties of truck brake lining materials in a representative S-cam brake. However, the test has been found to exhibit an unacceptably large range of variability in the implied friction coefficient for the lining. It has been postulated that some of the variability arises from factors within the brakes that are used for the test—specifically, dimensional tolerances, and possibly friction in the moving parts.

The University of Michigan Transportation Research Institute has been funded to conduct a project for the Heavy Duty Brake Manufacturers Council (HDBMC) that would develop a model for an S-cam brake and conduct a sensitivity study to determine the variation in measured lining coefficient as a function of the geometric and friction properties of the brake.

Features and Description of Basic Equilibrium Model

Figure 1 describes the basic features and geometry of the S-cam brake. The brake is comprised of leading and trailing shoes that pivot about fixed centers of rotation when activated by the rotating S-cam. The torque input to the cam is provided by an air chamber force acting on the slack adjuster arm. Given this basic geometry and certain frictional quantities within the described assembly, the model calculates a torque output corresponding to a specified input torque acting on the cam. The calculation assumes a state of equilibrium for the brake at which leading and trailing shoe linings are wearing at the same rate. That is, differential lining wear may exist between the leading and trailing shoes at equilibrium, but their respective wear rates are equalized.

The brake calculation starts from some initial position with specified shoe-drum clearances for the leading and trailing shoes. The leading shoe clearance/wear is then iteratively adjusted to bring the brake into the defined equilibrium condition.

Figure 1 depicts a rigid circular drum of radius r surrounding leading and trailing shoes that are also treated as rigid. Linings on each shoe are assumed to be compliant and have a specified friction coefficient. Shoe rollers of radius d_r and corresponding roller pins with radius d_p transmit actuator forces F_a from the cam to the shoe. (The ' primed quantities seen in the figure refer to the trailing shoe counterparts of corresponding dimensions seen on the leading shoe.) The actuator forces are assumed to act on the rollers at an angle α . The shoes pivot about centers located at distances b and c from the brake X-Y origin (spider center). The centerline of each roller is located at dimensions a and d from the pivot centers. The shoe pivot radius is dimension d_{pv} .

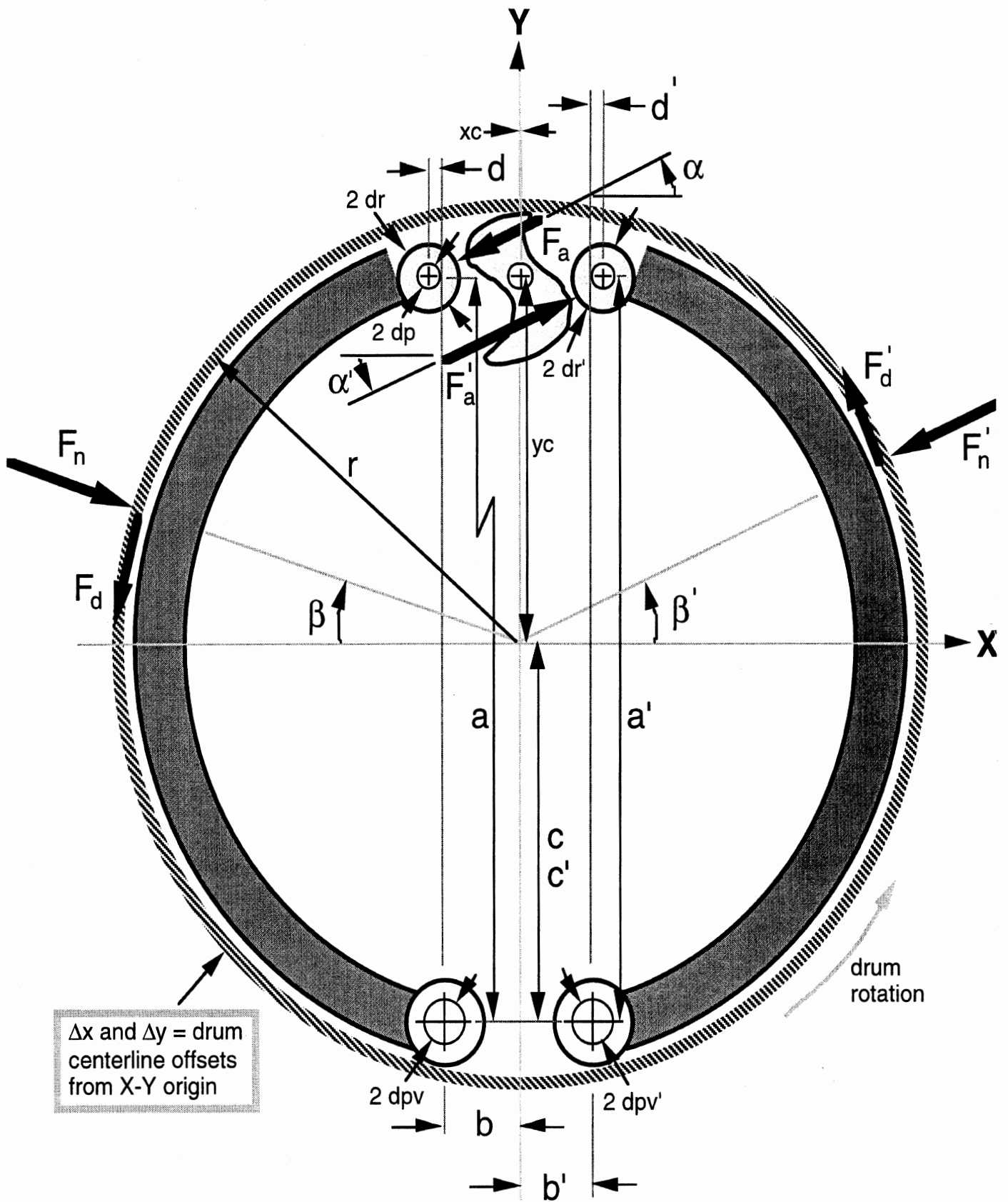


Figure 1. Geometry of the S-Cam Brake Model (not to scale).

The drag force F_d and normal force F_n acting on each shoe are located at centers of pressure β above the X-axis. The cam rotation is in the same direction as the drum.

In addition, friction is assumed to be present at the cam shaft bearing, the roller pins, and at the shoe pivot pin locations. The drum can be offset from the spider X-Y center by amounts Δx and Δy . Likewise, the cam center of rotation is also located by offsets from the X-Y origin by dimension x_c and y_c . The cam geometry is specified by an initial minimum cam radius and specified Archimedes geometry, $r_c = r_{c0} + k \cdot \gamma$, that defines cam radius, r_c , at any cam angle, γ . The initial cam radius is r_{c0} and k is the linear rate of change of cam radius with cam angular rotation γ . These and other model parameters are defined further in Appendices A and C.

The angular parameter α that locates the direction of the actuation force on the roller is obtained through iterative numerical calculations that solve for the equilibrium condition of the brake's moving parts — cam angular rotation and displacement of the shoes. The center of pressure parameter, β , is obtained from a pressure distribution calculation that rotates each shoe about its pivot into the drum to obtain arcs of conflict that define the required lining compression profile. This profile is then numerically integrated to obtain its centroid or effective center of pressure at which the total shoe forces are assumed to act.

No temperature, wheel speed, or lining-pressure influences are present in the model.

Equal Displacement Mechanism

A defining feature of the S-cam brake is the force actuation mechanism. It is essentially an equal displacement device. Since the cam center of rotation is fixed, forces transmitted to the shoe rollers must do so at more or less equal distances. The force actuation mechanism does not “float” allowing equal shoe forces to necessarily develop. Thus, the cam brake develops actuation forces acting on the shoe rollers as a result of the equal displacement properties of the cam — not equal forces, as occurs in wedge type or other floating actuation mechanisms. Consequently, a force imbalance will normally develop across the cam shaft bearing during ordinary operating conditions, and is further modified as unequal (differential) lining wear occurs between the leading and trailing shoes.

Actuator Friction

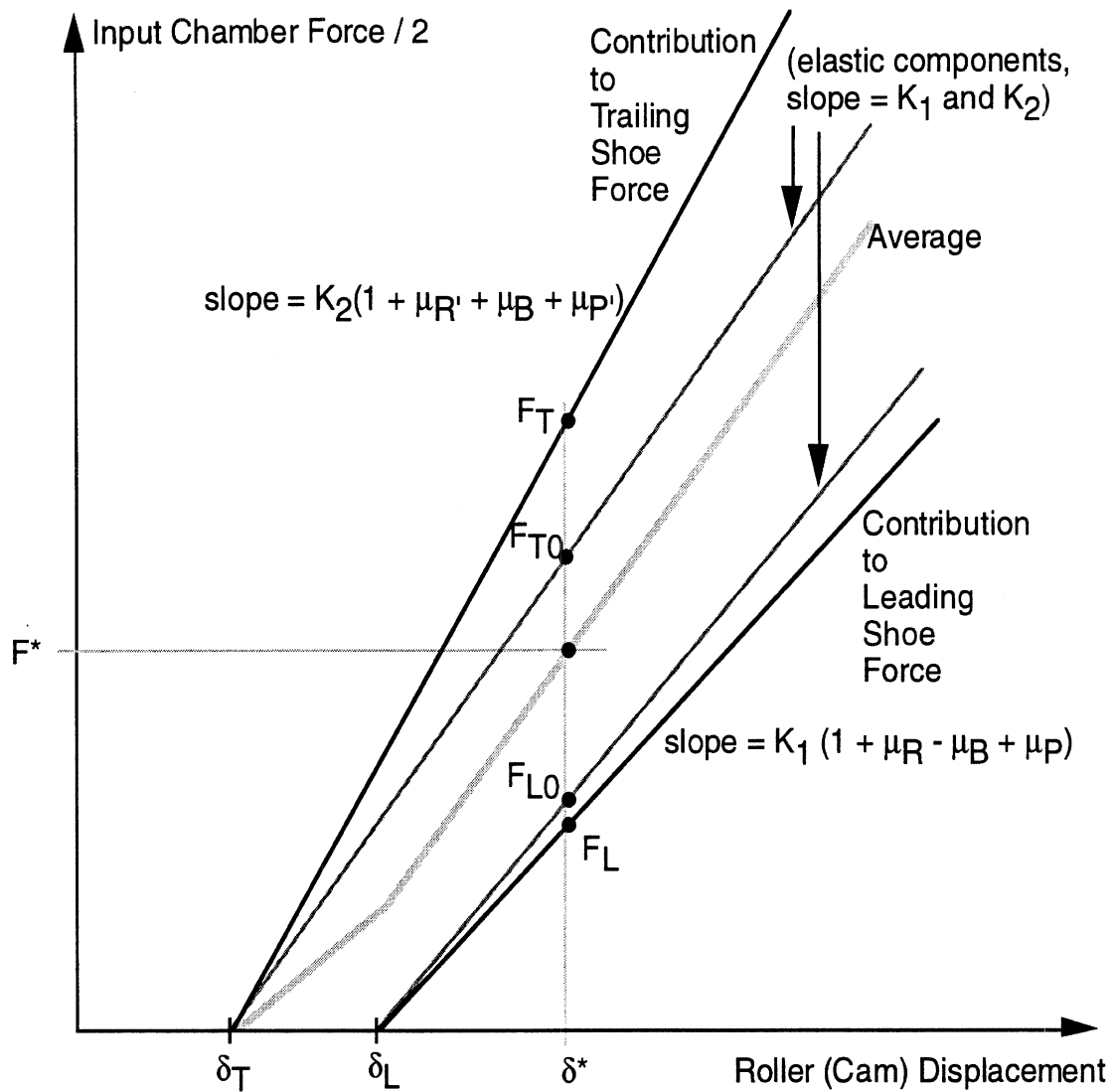
Load-dependent coulomb friction is present in the bearing, roller, and shoe pivot locations. Any increased loads imposed on these points will also increase the friction losses. Since the S-cam brake develops significant force imbalances across the cam bearing as described above, additional

friction losses at the bearing location are incurred as a result. The inputs to the model are the assumed material friction coefficients (e.g., steel on steel) at each location. These are then adjusted internally by the model to account for mechanical gains deriving from the specific component geometry. For example, the influence of roller pin friction is to reduce available input force to the brake shoes. However, since the cam force acting on the roller is resisted by the friction force acting at the smaller radius pin location, the pin friction value input to the model is effectively reduced by the ratio of the pin and roller diameters — thereby lessening its diminishing influence on input force [4]. Similar treatments are applied to the cam shaft bearing friction and the shoe pivot friction locations. (The net result for the nominal SAE J1802 brake geometry is that the actual frictional loss contributed by the bearing friction is about 85% of its input value; the roller pin friction contribution is about 45% of its input value; and the pivot pin friction is about 4%.) These reduced or “adjusted” friction values are those used in subsequent equations or expressions containing friction coefficients.

Differential Lining Wear

New (or equal-thickness) linings, that produce approximately equal displacements to drum contact, can initially produce higher drag forces on one shoe relative to the other. This can be due to a variety of reasons including asymmetry in geometry or structural stiffnesses. If the drag and normal forces on the leading shoe exceed those on the trailing shoe, a higher wear rate will occur initially on the leading shoe lining. As a result, the leading shoe lining thickness will decrease at a faster rate than the trailing shoe lining. The leading shoe actuation force from the cam will also correspondingly diminish further because of the fixed cam (equal displacement) restriction and the accompanying loss of spring force from the diminished lining thickness. As differential lining wear proceeds, additional actuator force imbalances develop across the cam. For a fixed input torque on the cam, the leading shoe wear will eventually reach a level at which its wear rate is equal to that of the trailing shoe wear rate. At this point, the drag and normal forces acting on both shoes will be equalized. This condition is defined in the model as the “equilibrium condition.” From this point on, the leading and trailing shoes will wear at the same rate despite having different amounts of respective wear, as long as the input force and the lining friction coefficient remain unchanged. Both shoes contribute equal amounts of brake torque at this point.

Each equilibrium condition also determines the ratio of actuator forces acting on the cam rollers, referred to as ρ ($0 < \rho < 1$), where $\rho = F_a / F_a'$, the ratio of leading to trailing shoe actuator forces. (ρ is 1.0 for brakes having wedge-type or floating actuator mechanisms). For an S-cam, ρ typically lies in the range of 0.2 to 0.4 and primarily depends on lining friction coefficient and on brake geometry [Appendix C].



$$F_{L0} = \rho \cdot F_{T0} \quad \text{and} \quad F^* = (F_L + F_T) / 2$$

Figure 2. Allocation of Input Force to Each Shoe vs. Roller (Cam) Displacement.

Shoe Forces at Equilibrium

To help further illustrate the equilibrium condition, Figure 2 shows a graph of how input air chamber force is distributed between the leading and trailing shoes as roller/cam displacement changes about equilibrium. For a specified average input force, F^* , and initial trailing shoe clearance/wear, δ_T , an equilibrium condition exists at a roller/cam displacement of δ^* . The top solid line shows the trailing shoe actuator + frictional force requirement increasing linearly from an

initial clearance/wear offset of δ_T . This line represents the amount of input force/torque allocated to the trailing shoe under equilibrium conditions. The slope of this line is $K_2(1+\mu_R'+\mu_B+\mu_P')$, where K_2 includes the stiffness of the lining-shoe elements and a self-energizing gain factor. μ_B is the cam bearing friction, μ_R' is the trailing shoe roller friction, and μ_P' is the corresponding trailing shoe pivot friction. (The friction coefficients referred to here and elsewhere correspond to the “adjusted” friction coefficients derived internally from the roller/pin/cam component geometry and their respective steel-on-steel, or equivalent, input values.) The lower solid line shows the leading shoe actuator + frictional force requirement starting from its clearance/wear value of δ_L . The position of this line is defined by δ_L which is calculated by the model given a specified δ_T , F^* , K_1 , K_2 , and ρ . The slope of this line is $K_1(1+\mu_R-\mu_B+\mu_P)$, where K_1 includes the stiffness of the lining-shoe elements and the self-energizing gain factor of the leading shoe. μ_R is the leading shoe roller friction and μ_P is the corresponding leading shoe pivot friction. The two inner lines correspond to the non-friction elastic force components, $K_1(\delta^*-\delta_T)$ and $K_2(\delta^*-\delta_L)$, needed to compress the lining and balance self-energizing drag forces. The δ^* equilibrium value is the rotation angle of the cam that results in deflections (cam-rise) of the two rollers such that their average force value is equal to F^* and that the ratio of the elastic shoe actuator forces, F_{T0}/F_{L0} , is equal to ρ . These two constraints define the basic assumptions of the model, namely, (1) a force/torque balance across the cam (air chamber force input = frictional force losses + shoe actuator elastic forces) and (2) equalized wear rates of the linings at equilibrium and the equal displacement property of the cam actuator, or, $F_{L0} = \rho \cdot F_{T0}$.

Figure 2 is instructive because it shows graphically how the leading shoe clearance/wear, δ_L , must change as F^* varies over some range. (The diagram holds for a specified set of brake geometry, bearing/roller/pivot friction, and lining friction.) If F^* increases, the two shoe force lines on this specific diagram must spread further apart (implying more wear on the leading shoe lining) in order to satisfy the two constraints that require (1) that *F^* is equal to the average of the two shoes forces*, and (2) *the ratio of the elastic forces is equal to ρ* . If F^* decreases, δ_L must be smaller (or δ_T must increase) moving the two lines closer together in order to likewise satisfy these

equilibrium constraints. (An increased δ_T implies a temporarily higher differential wear rate on the trailing shoe lining until equilibrium is reached.)

Equilibrium Torque Calculation

The brake torque calculation predicted by the model under equilibrium conditions is provided by the expression:

$$\text{Torque} = \text{BF} \cdot [(F_{L0} + F_{T0}) / 2] \cdot r \quad (1)$$

where,

BF is the total brake factor = $4 \cdot \text{BF}_L \cdot \text{BF}_T / (\text{BF}_L + \text{BF}_T)$, [see 2, 3, or Appendix C]

r is the drum radius,

BF_L is the brake factor of the leading shoe

BF_T is the brake factor of the trailing shoe

F_{L0} is the elastic or net (after friction losses) brake force acting on the leading shoe

F_{T0} is the elastic or net (after friction losses) brake force acting on the trailing shoe

Implications of the Equilibrium Condition

Assuming the normal case of imperfect brake geometry and some asymmetry, unique equilibrium conditions exist for each force input and lining friction coefficient combination. That is, for a given lining friction and force input level, the amount of leading shoe wear (beyond or below that of the trailing shoe amount) needed to produce an equilibrium condition can be calculated. If, following a prolonged wear-in procedure at a fixed force input level, the input force is changed, the brake is no longer in equilibrium and must wear into a new equilibrium state at the new force input level. Since this ever-changing force input scenario is the norm under most brake usage conditions, an S-cam brake is never likely to be in a state of true equilibrium by this definition. The only exception to this is perhaps at the end of a burnish procedure.

The above observation may explain in some cases why S-cam brake effectiveness results may be less consistent than desired under changing operating conditions or particular test procedures. This is discussed further in a later section entitled "Relationship of the Equilibrium Model to the SAE Effectiveness Test J1802." In spite of this, the sensitivities of brake torque output to variations in different parameters can still be estimated under equilibrium conditions using the described model. The next section contains results of a parameter sensitivity study using the model under the described equilibrium conditions.

Basic Algorithm

Figure 3 outlines the basic calculation sequence occurring in the S-cam model. The calculation begins by defining the brake geometry, its frictional properties, a lining friction coefficient, an initial clearance/wear for the trailing shoe, and a specified input air chamber force. An iterative calculation loop is then initiated that calculates leading/trailing brake shoe factors and the force actuation ratio parameter, ρ . Roller locations from the cam center are then calculated. The location of the effective force centers, β 's, are next obtained from the pressure distribution calculation (based on the interference of each shoe rotated into the drum as described earlier). The cam is then rotated until contact with the trailing-shoe roller occurs (local iteration). The same is done for the leading-shoe roller. Based on the difference in cam angles obtained for the cam-roller contact conditions, the thickness of the leading shoe lining is either “worn” or “grown” to adjust δ_L . Actuator force angles, α 's, are also calculated at this point in the loop. If the gap/interference between the leading shoe roller and the cam is less than some small threshold value, ϵ , the calculation is completed; otherwise, the iteration continues until it reaches an acceptably small value. Upon convergence, the final values of α , β , δ_L , cam position, and brake torque are obtained.

Summarizing

The S-cam brake model is a static equilibrium model that calculates brake torque for a specified set of geometry, friction properties, and constant input air chamber force. The lining-shoe structure is the only mechanically compliant element and stiffness asymmetry between leading/trailing shoes is allowed. The model assumes that equilibrium is reached through sufficient differential wear of the leading and trailing shoe linings, given an initial clearance/wear dimension for the trailing shoe lining. Each input force level defines a unique equilibrium condition (assuming no changes to the brake geometry or its frictional properties). For each specified input force, the model seeks an equilibrium condition consistent with the prescribed geometry and friction properties such that the wear rates of the leading and trailing shoe linings are equalized.

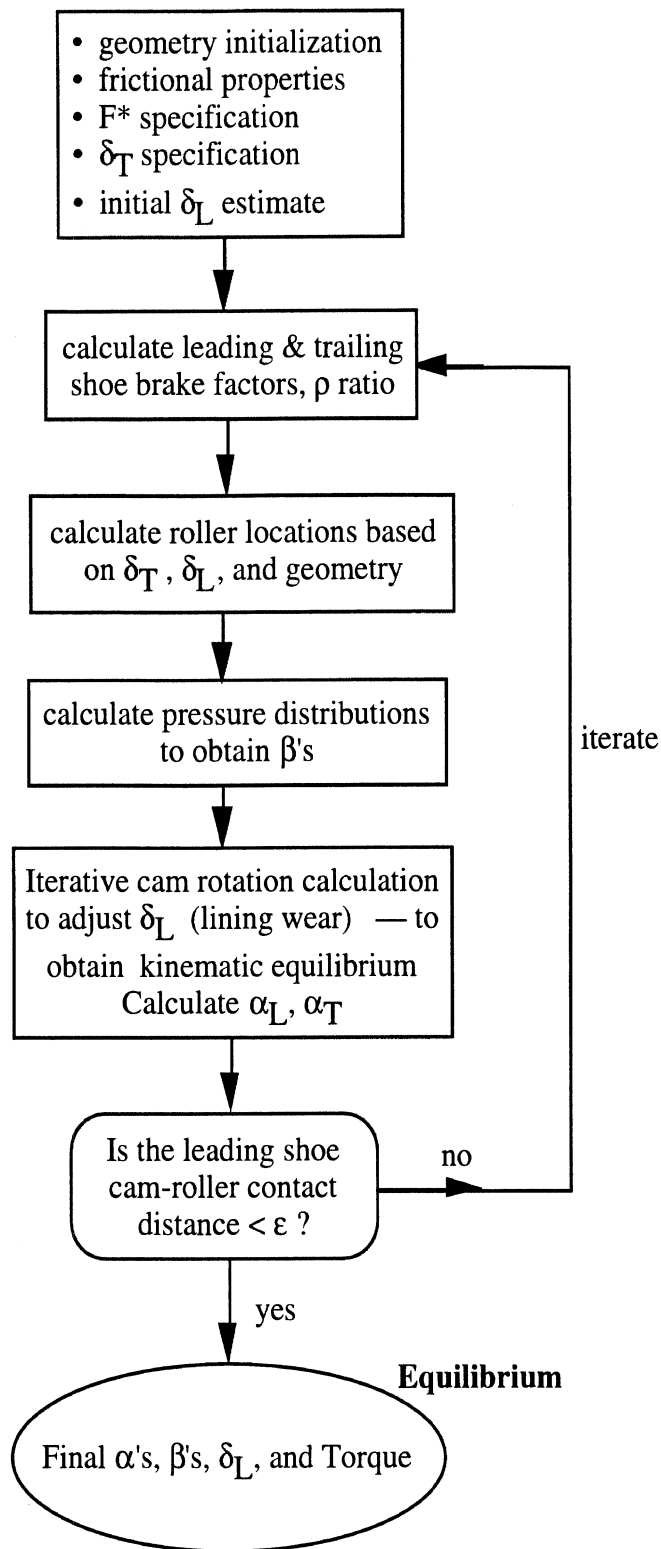


Figure 3. Basic Algorithm of the S-Cam Brake Model.

Parameter Sensitivity Calculations

A numerical sensitivity study was conducted with the equilibrium brake model to determine the likely sensitivity of brake torque output to variations in the nominal design parameters. These parameters included the geometric dimensions appearing in Figure 1 and various friction levels assumed to be present in the moving parts. The calculations were performed at five different lining friction coefficient levels ranging from 0.3 to 0.7 and at four levels of air chamber force inputs: 712.5, 1425, 2137.5, and 2850 lbs. (corresponding approximately to 25, 50, 75, and 100 psi of line pressure). The set of 30 parameters examined in the analysis appear in Table 1. These parameters correspond to the designated brake geometry specified by the SAE J1802 Recommended Practice [1]. Each parameter was varied as a fixed increment and decrement from its reference value. The increment/decrement amount was +/- 0.020 (inches or friction, depending on the parameter; the only exception was for lining stiffness, K, which was varied by +/- 10% in these cases). A 10% level of asymmetry was also assumed between the lining-shoe stiffnesses (leading shoe effective stiffness > trailing shoe effective stiffness) to account for directional differences of the actuator forces on their respective rollers.

The calculated change in brake torque — up or down from the baseline (no parameter change) condition — was normalized by the baseline brake torque and expressed as a net percentage change in brake torque. In cases where the 0.020 parameter variation is considered too large or too small relative to some specified tolerance, the brake torque percentage can be decreased or increased proportionately. For example, if an expected maximum tolerance is 0.010 inches, the indicated torque percentage change would be halved from that shown in the tabular results.

+/- 0.020 Parameter Variations

Table 2 and Table 3 contain exemplary results for +/- 0.020 variations in each of the 30 parameters. Both tables correspond to a lining friction coefficient of 0.50 and an air chamber force input of 1425 lbs. (The entire set of results for other lining friction levels and air chamber force inputs are contained in Appendix D.) The columns in Tables 2 and 3 list the baseline condition and each parameter variation relative to the baseline. The percentage change in brake torque and amount of differential lining wear (displacements relative to cam-roller location) at equilibrium are seen in the last two columns. All “lining wear” or lining thickness variation references in the text are in terms of equivalent roller displacements at the cam-roller location.

The results in these two representative tables indicate particular sensitivity of brake torque to the alignment between the drum centerline and the shoe/spider centerline assembly. Sensitivities of about 3% are indicated, depending upon the direction and polarity of offset. Offsets in drum centerline location have significant influence on the locations of the pressure distributions, β , which in turn, strongly influence the brake factors, particularly for the leading shoe. Potential

Table 1. Brake Parameters Examined in the Numerical Sensitivity Calculations.

Symbol	Parameter Description	Value
a	Distance from leading shoe pivot center to leading shoe roller center	12.75
a'	Distance from trailing shoe pivot center to trailing shoe roller center	12.75
b	Offset of leading shoe pivot from brake (spider) X-Y centerline	1.25
b'	Offset of trailing shoe pivot from brake (spider) X-Y centerline	1.25
c	Distance from leading shoe pivot center to brake (spider) center	6.75
c'	Distance from trailing shoe pivot center to brake (spider) center	6.75
d	Initial X-Offset of leading shoe pivot center from leading shoe roller center	0.41
d'	Initial X-Offset of leading shoe pivot center from leading shoe roller center	0.41
dr	Leading shoe roller radius	0.81
dr'	Trailing shoe roller radius	0.81
dp	Leading shoe roller pin radius	0.371
dp'	Trailing shoe roller pin radius	0.371
dpv	Leading shoe pivot pin radius	0.624
dpv'	Trailing shoe roller pin radius	0.624
r	Radius of drum	8.25
xc	X-offset of cam shaft center from center of brake (spider)	0.0
yc	Y-distance of cam shaft center from center of brake (spider)	6.0
Δx	X-offset of drum center from brake (spider) center	0.0
Δy	Y-offset of drum center from brake (spider) center	0.0
k	Cam rise per radian of rotation	0.497
rc0	Minimum cam radius	0.561
R_B	Radius of cam shaft	0.747
S_L	Length of slack adjuster arm	5.5
μ_B	Cam shaft bearing friction	0.1
μ_R	Leading shoe roller pin friction coefficient	0.2
μ_R'	Trailing shoe roller pin friction coefficient	0.2
μ_P	Leading shoe roller pivot pin friction coefficient	0.2
μ_P'	Trailing shoe roller pivot pin friction coefficient	0.2
δ_T	Initial clearance of trailing shoe (deflection @ cam-roller location)	0.060
K	Stiffness of lining/shoes (as pounds of chamber force per inch of stroke)	2850

Table 2. Result for -0.020 Parameter Variation @ 0.5 μ_L & 1425 lb Force.

Parameter	μ Lining	Chamber Force (lbs)	Parameter Value	Variation	Torque (in-lbs)	% Torque Change	$\delta_L - \delta_T$ (inch)
Baseline	.50	1425.00	0.000	0.000	101913.7	0.00	.008
a	.50	1425.00	12.750	-.020	101834.9	-.08	.003
a'	.50	1425.00	12.750	-.020	102090.5	.17	.004
b	.50	1425.00	1.250	-.020	101925.7	.01	.028
b'	.50	1425.00	1.250	-.020	101843.8	-.07	-.011
c	.50	1425.00	6.750	-.020	102230.0	.31	.013
c'	.50	1425.00	6.750	-.020	101959.8	.05	.013
d	.50	1425.00	.410	-.020	101880.3	-.03	.028
d'	.50	1425.00	.410	-.020	102025.1	.11	-.011
dr	.50	1425.00	.810	-.020	101804.5	-.11	-.012
dr'	.50	1425.00	.810	-.020	101920.2	.01	.029
dp	.50	1425.00	.371	-.020	102286.5	.37	.009
dp'	.50	1425.00	.371	-.020	102286.5	.37	.009
dpv	.50	1425.00	.624	-.020	101923.2	.01	.008
dpv'	.50	1425.00	.624	-.020	101923.2	.01	.008
r	.50	1425.00	8.250	-.020	101675.1	-.23	.008
xc	.50	1425.00	0.000	-.020	101964.7	.05	.048
yc	.50	1425.00	6.000	-.020	101851.6	-.06	.019
Δx	.50	1425.00	0.000	-.020	105117.9	3.14	-.011
Δy	.50	1425.00	0.000	-.020	101627.9	-.28	.009
k	.50	1425.00	.497	-.020	106373.9	4.38	.008
rc0	.50	1425.00	.561	-.020	101809.7	-.10	.008
R_B	.50	1425.00	.747	-.020	101994.2	.08	.009
S_L	.50	1425.00	5.500	-.020	101655.2	-.25	.009
μ_B	.50	1425.00	.100	-.020	102783.9	.85	.008
μ_R	.50	1425.00	.200	-.020	102407.1	.48	.009
μ_R'	.50	1425.00	.200	-.020	102407.1	.48	.009
μ_P	.50	1425.00	.200	-.020	101943.2	.03	.008
μ_P'	.50	1425.00	.200	-.020	101943.2	.03	.008
δ_T	.50	1425.00	.060	-.020	102189.9	.27	.009
K	.50	1425.00	2850.000	-285.000	101916.3	0.00	.009

Table 3. Result for +0.020 Parameter Variation @ $0.5 \mu_L$ & 1425 lb Force.

Parameter	μ Lining	Chamber Force (lbs)	Parameter Value	Variation	Torque (in-lbs)	% Torque Change	$\delta_L - \delta_T$ (inch)
Baseline	.50	1425.00	0.000	0.000	101913.7	0.00	.008
a	.50	1425.00	12.750	.020	101937.9	.02	.013
a'	.50	1425.00	12.750	.020	101935.0	.02	.013
b	.50	1425.00	1.250	.020	101841.6	-.07	-.011
b'	.50	1425.00	1.250	.020	101982.0	.07	.028
c	.50	1425.00	6.750	.020	101764.7	-.15	.003
c'	.50	1425.00	6.750	.020	102122.5	.20	.004
d	.50	1425.00	.410	.020	101886.9	-.03	-.011
d'	.50	1425.00	.410	.020	101949.1	.03	.028
dr	.50	1425.00	.810	.020	101960.5	.05	.029
dr'	.50	1425.00	.810	.020	102069.9	.15	-.012
dp	.50	1425.00	.371	.020	101726.8	-.18	.009
dp'	.50	1425.00	.371	.020	101726.8	-.18	.009
dpv	.50	1425.00	.624	.020	101904.2	-.01	.008
dpv'	.50	1425.00	.624	.020	101904.2	-.01	.008
r	.50	1425.00	8.250	.020	102152.3	.23	.008
xc	.50	1425.00	0.000	.020	101985.5	.07	-.031
yc	.50	1425.00	6.000	.020	102144.0	.23	-.001
Δx	.50	1425.00	0.000	.020	99050.1	-2.81	.028
Δy	.50	1425.00	0.000	.020	105052.1	3.08	.009
k	.50	1425.00	.497	.020	97838.1	-4.00	.009
rc0	.50	1425.00	.561	.020	102014.6	.10	.008
R _B	.50	1425.00	.747	.020	101795.7	-.12	.009
S _L	.50	1425.00	5.500	.020	102360.4	.44	.009
μ_B	.50	1425.00	.100	.020	101018.0	-.88	.008
μ_R	.50	1425.00	.200	.020	101610.2	-.30	.009
μ_R'	.50	1425.00	.200	.020	101610.2	-.30	.009
μ_P	.50	1425.00	.200	.020	101883.9	-.03	.008
μ_P'	.50	1425.00	.200	.020	101883.9	-.03	.008
δ_T	.50	1425.00	.060	.020	101887.5	-.03	.009
K	.50	1425.00	2850.000	285.000	102039.2	.12	.008

sources of drum/spider center offsets can come from allowable machining tolerances. Other sources of offset may be related to possible angular differences in the hub/bearing/drum assembly such that the drum axis is tilted slightly with respect to the spindle thereby offsetting the drum relative to the linings. A 0.1 degree angular misalignment of the drum axis and the spider/shoe normal axis would produce about 0.010 inches of offset between the drum and the center of the linings. This also raises the possibility of corresponding angular deflections deriving from spindle loading during on-vehicle use.

Δy Offset — An upward offset in the drum ($\Delta y = +0.020$ inches, Table 3) shifts the pressure centers of both shoes more towards their shoe centerlines. Appendix B contains model output results for the baseline case and the $\Delta y = +0.020$ inches variation (*Δy Example*) to illustrate how β and the shoe brake factors are altered by this offset. The leading shoe center of pressure moves from about 8 degrees off the center of the shoe to about -2 degrees (nearly on the shoe centerline). This lowers the brake factor on that shoe from about 2.2 to 1.9. The trailing shoe brake factor is increased from about 0.57 to 0.61. The net result is an increase in the total brake factor from 1.80 to 1.85 and a 3.1% increase in torque. (Even though the leading shoe brake factor is reduced from its baseline condition, cam forces are redistributed by this variation such that a higher actuator force is now applied to the leading shoe, thereby increasing the torque output.) Results in Appendix D for other lining friction levels indicate that the variation in torque associated with this parameter is largely independent of lining friction.

Δx Offset — Shifts in drum location in the direction of either shoe center also have significant influences. In this case the pressure distributions on both shoes shift in opposite directions (as opposed to the above case), and result in asymmetric shifts in the pressure distribution locations versus the baseline condition. For example, in the $\Delta x = -0.020$ inches case (Table 2), the drum is shifted toward the center of the leading shoe lining (in the negative X-axis direction), causing the center of pressure for the leading shoe to move more toward the cam. It also causes the center of pressure on the trailing shoe to move away from the cam. Appendix B contains the model output for this case (*Δx Example*). The calculation shows that the leading shoe center of pressure moves to about 11 degrees, from the baseline condition of 8 degrees; the trailing shoe center of pressure moves to about 5 degrees. This results in a higher brake factor for the leading shoe and a 3.1% net increase in torque from the baseline condition. (The model assumes in this case that any drum offset toward/away from the shoe centers is compensated by corresponding differential thicknesses in linings. That is, a $\Delta x = -0.020$ inch offset would produce

leading shoe linings that are 0.020 inches thicker than the corresponding equilibrium thickness calculated for no drum offset.) The results in Appendix D show that the torque variation associated with this parameter strengthens with increased lining friction level.

Bearing, Roller, and Pivot Friction — If nominal values of roller, bearing, and pivot friction are reduced/increased from their 0.1 and 0.2 values by a value of 0.020 (as calculated in Tables 2 and 3), the change in brake torque is seen to be about 1.7% (all five influences summed together). Since likely variations in friction may be several times this level in practice, the likely corresponding torque variations would be about 5% or so. (Again, as noted above, the torque variation results in Tables 2, 3, and Appendix D need to be scaled up or down based upon an anticipated parameter variation relative to the reference variation of 0.020 in these calculations.) When compared with the idealized frictionless brake, the torque of the baseline brake (with the indicated friction values of 0.1 and 0.2) is about 86% as effective.

Cam Profile — The shape of the cam, as defined by its Archimedes spiral gain, k , also shows up as a potentially significant source of torque variation. The nominal value of 0.497 inches of rise per radian of cam rotation is subject to a +/- 4% variation when changed by amounts of +/- 0.020. Not surprisingly, this produces a corresponding +/- 4% variation in torque since it is simply part of the direct mechanical gain of the brake. The only issue raised by this observation relates to the manufacturing consistency and quality control of the desired cam profile and its symmetry.

x_c , y_c , Cam Offsets — Movement of the cam in either direction has no significant effect on torque variation but does affect the level of differential wear at equilibrium. Movement of the cam toward either shoe by +/- 0.020 inches causes the leading shoe to vary from its baseline wear by twice that amount, or +/- 0.040 inches. The factor of two is a result of the cam offset and the corresponding change in cam rotation at equilibrium needed to contact the trailing shoe roller. These cases are shown as examples in Appendix B (+/- x_c Examples).

Movement of the cam away from the line connecting the roller centers (in the Y-direction), results in corresponding adjustment of the differential wear. A +0.020 inch variation away from the brake center reduces the amount of differential wear to about zero for a chamber force input of 1425 lbs and a lining friction level of 0.5. This example output is also in Appendix B (+ y_c Example).

The remaining parameters have less than 1% influence on torque variation for these same parameter variation levels. The lining stiffness parameter, K , appears to play a minimal role in torque variation — at least as a mechanical compliance. It does produce different equilibrium operating conditions in terms of the cam rotation angle and amount of required stroke as seen in the Appendix B example output. The Appendix B example corresponds to a reduction in effective

stiffness from 2850 to 2500 lbs chamber force per inch of chamber stroke (255,000 lb/inch equivalent lining stiffness at the cam-roller location).

Asymmetry Example

The last example calculation in Appendix B (parameter “a” Example) provides a more detailed look at potential asymmetry in brake geometry and corresponds to increasing the leading shoe pivot-to-roller distance, a , by a sizeable 0.1 inches. (By comparing with the baseline example, the influence on roller angle, α , and cam contact angles are more easily seen with variations of this size.) The lengthened leading shoe dimension produces a contact angle, α , on the leading shoe roller that is smaller than the baseline condition, and a corresponding cam contact angle that is larger. This results in a slightly modified leading shoe brake factor and corresponding torque that is about 0.4% larger than the baseline condition. The amount of differential lining wear increases significantly.

Relationship of the Equilibrium Model to the SAE Effectiveness Test J1802

The question of how this equilibrium model relates to the SAE J1802 effectiveness test procedure is important. The equilibrium model is intended to predict likely brake torque effectiveness when input force levels of the same magnitude are repeatedly applied over a long enough time period that differential lining wear between the leading and trailing shoes may develop. It also assumes that the wear rates of both shoes at this time are equalized. Depending on the wear resistance of the lining material, the process of arriving at equilibrium may vary considerably. Since J1802 starts with a burnish procedure that utilizes a repeated input force of constant magnitude, the burnish can be viewed as a mechanism for arriving at equilibrium, provided enough stops are performed to achieve sufficient differential wear. Assuming differential wear exists at equilibrium, the important question is: What happens following the burnish when effectiveness stops are then performed? Since the brake is burnished at a pressure of about 35 psi or so, it is no longer in equilibrium when the effectiveness testing sequence begins at subsequent levels of 10, 15, ..., 50 psi. The required force inputs are no longer at the equilibrium (burnish) level and are changing from stop to stop.

Figure 4 helps to explain this possible sequence with a diagram showing brake torque versus input pressure. The heavy middle line on this diagram represents the equilibrium condition predicted by the model if the brake was tested repeatedly at constant pressure inputs for prolonged periods of time until equilibrium was achieved (at each pressure). The top-most line corresponds to a case of new linings in which no differential wear exists and the brake initially exhibits a higher brake factor because of greater usage of the leading shoe caused by a small geometric or structural asymmetry. At any new-lining starting point, the leading shoe wear rate will initially be greater

than the trailing shoe wear rate and the torque output will gradually trend downward (because of increased leading shoe lining wear and the accompanying reduction in leading shoe actuator force) eventually reaching the indicated equilibrium line. At this point, lining wear rates on both shoes are equalized, but the amount of leading shoe wear is greater than the trailing shoe wear.

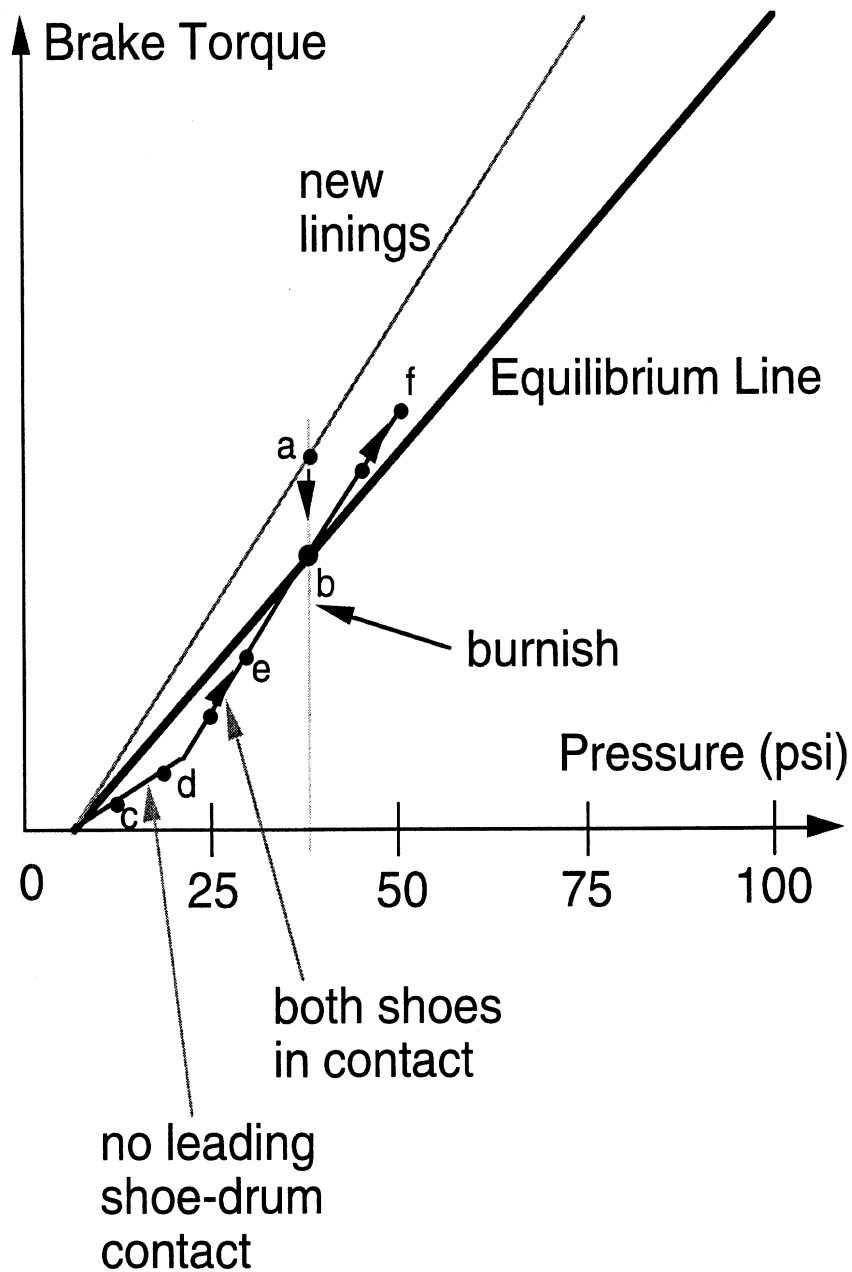


Figure 4. Equilibrium Model and the SAE J1802 Effectiveness Test Procedure.

For the J1802 test procedure, this suggests that at a burnish pressure of 35 psi or so, the brake with new linings described above would start at point **a** and proceed, during repeated burnish stops, eventually to point **b** on the equilibrium line. At this point, the J1802 procedure calls for effectiveness tests to then start at 10 psi and increment by 5 psi amounts until the 50 psi pressure level is reached. The points on the diagram labeled **c**, **d**, **e**, and **f** show this basic sequence. For all of these points, except the 35 psi pressure level, the brake is not in equilibrium. At point **c** (10-15 psi or so), the leading shoe may not be in contact with the drum because of differential wear developed during the prolonged burnish procedure spent at point **b** (35 psi). Consequently, the brake output under these conditions is relying totally on the trailing shoe, and because of its low brake factor, brake torque output suffers. (If the brake remains at this same pressure for numerous repeats, differential lining wear would correct the shoe contact problem by wearing the trailing shoe down until leading shoe contact occurs and wear rates on both shoes are again equalized. Point **c** would move directly upward during this sequence eventually reaching the equilibrium line.) As the J1802 effectiveness sequence continues at increased pressure levels, leading shoe contact will occur at some pressure and begin to contribute towards more brake torque output (point **d**). From this point back up to 35 psi at point **b** (equilibrium), the leading shoe plays an increasingly larger role as the equilibrium condition is re-approached. As pressure now increases beyond equilibrium towards the 50 psi level, the brake again moves away from equilibrium and the leading shoe (possessing a much larger brake factor) is now over-involved, producing brake torque outputs above the equilibrium line (point **f**). (Again, as before, if the brake were to remain at 50 psi for repeated tests, differential lining wear would occur, causing the leading shoe now to wear at a faster rate until equilibrium was reached. This would result in a gradual decrease in torque from point **f** downward to the equilibrium line at 50 psi.)

Another possible scenario is that for very hard or wear-resistant linings with the same brake, full equilibrium is not reached during burnish. In this case, the leading-trailing shoe wear differential is smaller than that required at equilibrium. As a result, effectiveness testing at the lower pressure levels would have lining contact on the leading shoe, thereby utilizing the leading shoe more than the prior scenario, but less than if the brake was in equilibrium at that low pressure. Consequently, the effectiveness points, **c**, **d**, **e**, and **f** in Figure 4 would shift upward by some amount. The degree of upward shift would depend on the amount of net differential wear achieved during the burnish.

The basic thrust of this discussion suggests that, apart from geometric and frictional brake property variations, significant opportunities for variability in S-cam brake effectiveness (as defined by J1802) still exist. Reasons for this variability relate to the basic nature of the S-cam brake design requiring that differential wear be constantly occurring when the brake is not in equilibrium (the usual case) and the influence that lining material wear properties have on this

phenomena.

Hypothetically, an infinitely hard lining material that does not wear, assuming the same lining friction level, would cause the above S-cam brake to exhibit somewhat more gain. The leading shoe would contribute more of the torque and the brake's overall effectiveness would be increased and unchanging — at least with respect to wear phenomena. At the other hypothetical extreme, very soft linings that wear to equilibrium quickly, might also exhibit low variability by staying close to the equilibrium line by means of rapid wear. However, the brake effectiveness would be reduced and the linings replaced frequently. Consequently, real-world linings that wear at a finite rate and lie between these two extremes, do play a role in effectiveness variability insofar as wear history affects subsequent results during a brake testing or brake usage sequence with an S-cam brake design.

To address this issue more rigorously, an extension of the existing model to include lining wear properties as a function of drum rotation, normal force, and so forth would seem to make sense. The extended model would be time-based and allow for wear history to enter the picture as a primary factor in determining what the next prediction of brake torque would be. The SAE J1802 recommended practice might then be more readily evaluated, at least with respect to basic lining material properties. (Known or estimated temperature/pressure/speed influences on lining friction might also be included as an additional feature to evaluate their relative importance as well.) The present equilibrium model could form the basis of this extended time- and wear-dependent model, except that equilibrium would only be the solution if the same input force was applied a sufficient number of times (stops) to achieve equilibrium. The J1802 effectiveness sequence could be simulated with different lining material properties, irrespective of whether or not the brake ever reaches true equilibrium. Potential variability in effectiveness rating could then be examined more quantitatively with respect to lining wear properties and brake geometry variations.

Summary and Conclusions

The S-cam brake model developed under this work calculates brake torque for a specified set of geometry, friction properties, and constant input air chamber force. It assumes that the brake is in a state of equilibrium defined by equalized wear rates on the leading and trailing shoe linings. The lining-shoe structure is the only mechanically compliant element and stiffness asymmetry between leading/trailing shoes is allowed. The cam acts as the distributor of input force to each shoe. The model assumes that equilibrium is reached through sufficient differential wear of the leading and trailing shoe linings, given an initial wear/clearance dimension for the trailing shoe

lining. Each input force level defines a unique equilibrium condition (assuming no changes to the brake geometry or its frictional properties). For each specified input force, the model seeks an equilibrium condition consistent with the prescribed geometry and friction properties such that the wear rates of the leading and trailing shoe linings are equalized. At equilibrium, the leading and trailing shoes contribute equal amounts of torque.

The parameter sensitivity findings indicate that a potentially significant source of torque variability is related to possible offsets between the drum turning axis and the spider/shoe assembly centerline. Offsets between these axes can produce significant shifts in the lining pressure distributions of both shoes, thereby altering each shoe's brake factor. This is particularly significant for the leading shoe, which tends to affect torque production more due to its higher self-energizing gain.

Other significant factors include bearing and roller pin friction. Depending upon the amount of lubrication, if any, torque variations can be significant. For example, bearing and roller pin friction levels in the range of 0.1 - 0.2 can reduce brake torque output as much as 17% versus its idealized frictionless counterpart.

The shape of the cam profile is also a potential contributor to brake torque variations. Movement of the cam center has little effect on torque variation, but does contribute significantly to the amount of differential lining wear between the leading and trailing shoes.

Asymmetry in the effective stiffness of the lining and shoe elements (leading versus trailing) also contributes significantly to differential lining wear. As noted below, differential lining wear can be a primary source of non-stationary brake effectiveness.

The remaining geometric parameters are more weakly associated with comparable levels of brake torque variation. However, depending on the amount of potential variation in a particular parameter, significant torque variations may still be possible.

The issue of torque effectiveness variability and its relationship to the SAE J1802 Recommended Practice is also addressed. Since the J1802 burnish procedure acts as a mechanism for achieving (or approaching) equilibrium, the subsequent effectiveness sequence that requires testing at other pressures, may cause the brake to no longer be at, or near, equilibrium. If differential wear exists at equilibrium, this can result in significant changes in torque effectiveness, as defined by the J1802 recommended practice. Under these conditions, if the brake reaches true equilibrium during burnish, the initial stops at pressures of 10, 15 psi, etc. may involve unusual leading shoe-drum contact due to the existing differential lining wear. The brake would then exhibit a lower- or higher-than-expected effectiveness (relative to its equilibrium condition at low pressures). Likewise, at higher-than-burnish pressures (45, 50 psi), the brake is also not in equilibrium and the leading shoe is under- or over-involved depending upon the differential wear state at burnish. This also results in a change in effectiveness relative to equilibrium at the higher

pressures. At any non-equilibrium pressure, the S-cam brake seeks equilibrium through the differential wear process of both linings. However, unless enough stops are performed at a fixed pressure to achieve the necessary equilibrium wear rate, the brake effectiveness will be gradually changing. Most variations in brake geometry or structural stiffnesses, away from the idealized symmetric brake, contribute to differential wear.

Recommendations for extending the existing model to include lining wear properties are also suggested. This would permit more extensive examination and analysis of the lining wear process (over time) during a test sequence such as J1802. The extended model would be time and wear dependent and thereby would be more applicable/useful for predicting and analyzing likely S-cam brake torque production during sequential brake applications, as occur in specific brake test procedures or vehicle tests.

References

1. "SAE J1802 Recommended Practice, Brake Block Effectiveness Rating," *SAE Handbook*, Volume 2, Parts and Components, SAE, Warrendale, PA, 1996.
2. Limpert, R., *Brake Design and Safety*, SAE, 1992.
3. Adler, U. (ed), *Automotive Handbook (2d Ed)*, Robert Bosch GmbH, Stuttgart, Germany, 1986.
4. Myers, P., "The Effect of 'S' Cam Brake Component Variation on Performance," SAE Paper No. 751012, 1975.

Bibliography

Gillespie, T.D., *Fundamentals of Vehicle Dynamics*, SAE, 1992.

Miller, W., Bailey, J., and Scanlon, R., "S Cam and Shoe Roller Contact Point: An Iteration Procedure," SAE Paper No. 820495, 1982.

Fancher, P., et al., "Evaluation of Brake Adjustment Criteria for Heavy Trucks," Final Report No. FHWA-MC-93-014, UMTRI-93-15, 1995.

McCallum, J. and Tolan, B., "Advances in 'S' Cam Brake Design," *Proceedings of the IMechE*, Paper C36/83, 1983.

Day, A. and Harding, T., "Performance Variation of Cam-Operated Drum Brakes," *Proceedings of the IMechE*, Paper C10/83, 1983.

Day, A., "Drum Brake Interface Pressure Distributions," *Proceedings of the IMechE, Part D: Journal of Automobile Engineering*, Vol. 205, No. D2, 1991.

Day, A., Harding, P., and Newcomb, T., "Combined Thermal and Mechanical Analysis of Drum Brakes," *Proceedings of the IMechE*, Vol. 198D, No. 15, 1984.

Appendix A. Parameter and Symbol Definitions.

a	Distance from Leading Shoe Pivot to Leading Shoe Roller Center
a'	Distance from Trailing Shoe Pivot to Trailing Shoe Roller Center
b	Offset of Leading Shoe Pivot from Centerline
b'	Offset of Trailing Shoe Pivot from Centerline
c	Distance from Leading Shoe Pivot to Centerline
c'	Distance from Trailing Shoe Pivot to Centerline
d	Offset of Leading Shoe Pivot from Leading Shoe Roller Center
d'	Offset of Trailing Shoe Pivot from Trailing Shoe Roller Center
r	Drum Radius
Δx	Offset (towards trailing shoe) of Drum Center from Brake Centerline
Δy	Offset (towards cam) of Drum Center from Brake Centerline
k	Cam Rise to Cam Rotation Ratio (Archimedes spiral gain)
rc0	Cam Radius at Zero Cam Rotation ($\gamma=0$)
Rs	Radius of Cam Shaft
xc	Offset from Center of Cam to Brake Centerline
yc	Distance from Center of Cam to Brake Centerline
dr	Radius of Leading Shoe Roller
dr'	Radius of Trailing Shoe Roller
dp	Radius of Leading Shoe Roller Pin
dp'	Radius of Trailing Shoe Roller Pin
dpv	Radius of Leading Shoe Pivot Pin
dpv'	Radius of Trailing Shoe Pivot Pin
μ_R	Friction Coefficient of Leading Shoe Roller Pin
μ_R'	Friction Coefficient of Trailing Shoe Roller Pin
μ_P	Friction Coefficient of Leading Shoe Pivot Pin
μ_P'	Friction Coefficient of Trailing Shoe Pivot Pin
μ_B	Friction Coefficient of Cam Shaft Bearing
μ_L	Lining Friction Coefficient
S_L	Slack Adjuster Arm Length
CanForce	Air Chamber (Can) Force Application
Kcan	Stiffness of Lining / Mechanical Components Relative to Chamber-Stroke Motion
K	Equivalent Kcan stiffness at roller-cam location (prior to any asymmetry)
z	Percent of Asymmetry Between the Leading/Trailing Lining-Shoe Stiffnesses
K_1	Combined Stiffness of the Lining-Shoe Elements, K_L , and Self-Energizing Gain Factor of the Leading Shoe
K_2	Combined Stiffness of the Lining-Shoe Elements, K_T , and Self-Energizing Gain Factor of the Trailing Shoe
F*	AVERAGE of Leading & Trailing input shoe forces (including friction losses)
δ_L	Leading Shoe-to-Drum Clearance/Wear (displacement at cam-roller location)
δ_T	Trailing Shoe-to-Drum Clearance/Wear (displacement at cam-roller location)
δ^*	Cam-Roller Displacement at Equilibrium (away from initial rest condition)
BF _L	Leading Shoe Brake Factor
BF _T	Trailing Shoe Brake Factor
BF	Combined (total) Brake Factor: $4 \cdot BF_1 \cdot BF_2 / (BF_1 + BF_2)$
F _{L0}	Leading Shoe Actuator Force at Equilibrium (elastic)
F _{T0}	Trailing Shoe Actuator Force at Equilibrium (elastic)

F_L Leading Shoe Actuator Force at Equilibrium (elastic + friction loss)
 F_T Trailing Shoe Actuator Force at Equilibrium (elastic + friction loss)
 ρ Ratio of Leading Shoe Elastic Force to Trailing Elastic Shoe Force, F_{L0}/F_{T0}
 α Angle of Leading Shoe Roller Force, F_a , on Leading Shoe Roller
 α' Angle of Trailing Shoe Roller Force, F_a' , on Trailing Shoe Roller
 β Angle of Effective Center of Pressure from Shoe Center - Leading Shoe
 β' Angle of Effective Center of Pressure from Shoe Center - Trailing Shoe
 γ Angle of Cam Contact at Equilibrium with Respect to Minimum Radius Cam Angle
 γ_0 Initial Angle of Cam at Rest (0-Torque Initial Position)
 $\gamma-\gamma_0$ Net Cam Rotation due to Air Chamber Force Input
 θ Angle Between Cam Center-Contact Point and X-axis at Equilibrium (leading)
 θ' Angle Between Cam Center-Contact Point and X-axis at Equilibrium (trailing)
 ϕ Angle of arc subtended by the lining(s)
 $F_a = F_{L0}$ Leading Shoe Actuator Force (in Figure 1)
 $F_a' = F_{T0}$ Trailing Shoe Actuator Force (in Figure 1)
 F_d Leading Shoe Drag Force
 F_d' Trailing Shoe Drag Force
 F_n Leading Shoe Normal Force
 F_n' Trailing Shoe Normal Force
Torque Brake Torque Output

Note: All "lining wear" or lining thickness variation references in the text are in terms of equivalent roller displacements at the cam-roller location.

Appendix B. Example Model Calculations.

Example calculation results from the S-Cam model are seen in this appendix. The first calculation example corresponds to a baseline example using the nominal parameters of Table 1 and an input can force of 1425 lbs (50 psi) and lining friction coefficient of 0.50. The subsequent examples are also at 1425 lbs and a lining coefficient of 0.50. They include: 1) a Δy variation example (drum/shoe centerline offset) , 2) a Δx variation (drum/shoe centerline offset), 3)-5) +/- x_c , y_c parameter variations (cam center offsets), 6) a -12% lining stiffness K variation, and 7) a parameter "a" variation (leading shoe pivot-to-roller dimension) of 0.1 inches.

The first page of each example output contains a listing of the model input parameters. The second page contains the equilibrium values calculated by the model and the corresponding torque.

S-Cam Brake Model Parameters:

Baseline Example

Shoe Geometry:

a = 12.750 (inches) Leading Shoe Pivot to Leading Shoe Roller Center
 a' = 12.750 (inches) Trailing Shoe Pivot to Trailing Shoe Roller Center
 b = 1.250 (inches) Offset of Leading Shoe Pivot from Centerline
 b' = 1.250 (inches) Offset of Trailing Shoe Pivot from Centerline
 c = 6.750 (inches) Leading Shoe Pivot to Centerline
 c' = 6.750 (inches) Trailing Shoe Pivot to Centerline
 d = 0.410 (inches) Offset of Leading Shoe Pivot from Leading Shoe Roller Center
 d' = 0.410 (inches) Offset of Trailing Shoe Pivot from Trailing Shoe Roller Center
 phi = 55.000 (degrees) Half-Shoe Angle Subtended by Lining Block

Drum Geometry:

r = 8.250 (inches) Drum Radius
 epsx = 0.000 (inches) Offset (towards trailing shoe) of Drum Center from Brake Centerline
 epsy = 0.000 (inches) Offset (towards cam) of Drum Center from Brake Centerline

Cam Geometry:

CamRatio = 0.497 (in/rad) Cam Rise to Cam Rotation Ratio
 CamRadius0 = 0.561 (inches) Cam Radius at Zero Rotation
 ShaftRadius = 0.747 (inches) Radius of Cam Shaft
 xc = 0.000 (inches) Offset from Center of Cam to Brake Centerline
 yc = 6.000 (inches) Distance from Center of Cam to Brake Centerline

Roller & Pivot Geometry:

RollerRadL = 0.810 (inches) Radius of Leading Shoe Roller
 RollerRadT = 0.810 (inches) Radius of Trailing Shoe Roller
 PinRadiusL = 0.371 (inches) Radius of Leading Shoe Roller Pin
 PinRadiusT = 0.371 (inches) Radius of Trailing Shoe Roller Pin
 PivotRadL = 0.624 (inches) Radius of Leading Shoe Pivot Pin
 PivotRadT = 0.624 (inches) Radius of Trailing Shoe Pivot Pin

Friction Values

MuRollerL = 0.200 (-) Friction Coefficient of Leading Shoe Roller Pin
 MuRollerT = 0.200 (-) Friction Coefficient of Trailing Shoe Roller Pin
 MuPivotL = 0.200 (-) Friction Coefficient of Leading Shoe Pivot Pin
 MuPivotT = 0.200 (-) Friction Coefficient of Trailing Shoe Pivot Pin
 MuBearing = 0.100 (-) Friction Coefficient of Cam Shaft Bearing

Chamber & Slack Adjuster:

slackL = 5.50	(inches)	Slack Adjuster Arm Length
CanForce = 1425	(lb)	Air Chamber Force Application
Kcan = 2850	(lb/inch)	Stiffness of Lining and Mechanical Components Relative to Chamber-Stroke Motion
K = 290855	(lb/inch)	Stiffness of Lining and Mechanical Components Relative to Cam-Roller Motion
Asymmetry = 0.10	(-)	Stiffness Asymmetry (+ => leading > trailing)
Fstar = 7884.8	(lb)	AVERAGE of Leading & Trailing input shoe forces, absent friction
deltaT' = 0.060	(inches)	Trailing Shoe to Drum Clearance (displacement at cam-roller location)

Equilibrium Values of S-Cam Brake Model Parameters & Output Torque:

mu-Lining = 0.500	(-)	Lining Friction Coefficient
BF-L = 2.158	(-)	Leading Shoe Brake Factor
BF-T = 0.570	(-)	Trailing Shoe Brake Factor
BF = 1.804	(-)	Combined (total) Brake Factor: $4*BF1*BF2/(BF1+BF2)$
Rho = 0.264	(-)	Ratio of Leading Shoe Force to Trailing Shoe Force
fL = 2861.5	(lbs)	Leading Shoe Force
fT = 10831.2	(lbs)	Trailing Shoe Force
delta* = 0.107	(inches)	Total Cam-Rise Displacement from 0-Torque Initial Position
deltaT = 0.060	(inches)	Trailing Shoe Clearance
deltaL = 0.068	(inches)	Leading Shoe Clearance + Equilibrium Wear
alphaL = 13.1	(degrees)	Angle of Application of Leading Shoe Actuation Force on Roller
alphaT = 13.5	(degrees)	Angle of Application of Trailing Shoe Actuation Force on Roller
betaL = 7.7	(degrees)	Effective Center of Pressure - Leading Shoe
betaT = 7.3	(degrees)	Effective Center of Pressure - Trailing Shoe
Cam Angle = 39.42	(degrees)	Angle of Cam at Equilibrium wrt Minimum Radius Cam Angle
Cam0 = 27.07	(degrees)	Initial Angle of Cam at Rest (0-Torque Initial Position)
Cam Rotation = 12.36	(degrees)	Net Cam Rotation due to Chamber Force Input
Contact AngleL= 10.60	(degrees)	Angle Between Line Connecting Cam Center with Contact Point and X-axis (leading)
Contact AngleT= 10.95	(degrees)	Angle Between Line Connecting Cam Center with Contact Point and X-axis (trailing)
Stroke = 1.19	(inches)	Total Air Chamber Stroke
Torque = 101913.7	(inch-lb)	Brake Torque

S-Cam Brake Model Parameters:

Δy Variation Example

Shoe Geometry:

a = 12.750 (inches) Leading Shoe Pivot to Leading Shoe Roller Center
 a' = 12.750 (inches) Trailing Shoe Pivot to Trailing Shoe Roller Center
 b = 1.250 (inches) Offset of Leading Shoe Pivot from Centerline
 b' = 1.250 (inches) Offset of Trailing Shoe Pivot from Centerline
 c = 6.750 (inches) Leading Shoe Pivot to Centerline
 c' = 6.750 (inches) Trailing Shoe Pivot to Centerline
 d = 0.410 (inches) Offset of Leading Shoe Pivot from Leading Shoe Roller Center
 d' = 0.410 (inches) Offset of Trailing Shoe Pivot from Trailing Shoe Roller Center
 phi = 55.000 (degrees) Half-Shoe Angle Subtended by Lining Block

Drum Geometry:

r = 8.250 (inches) Drum Radius
 epsx = 0.000 (inches) Offset (towards trailing shoe) of Drum Center from Brake Centerline
 epsy = 0.020 (inches) Offset (towards cam) of Drum Center from Brake Centerline

Cam Geometry:

CamRatio = 0.497 (in/rad) Cam Rise to Cam Rotation Ratio
 CamRadius0 = 0.561 (inches) Cam Radius at Zero Rotation
 ShaftRadius = 0.747 (inches) Radius of Cam Shaft
 xc = 0.000 (inches) Offset from Center of Cam to Brake Centerline
 yc = 6.000 (inches) Distance from Center of Cam to Brake Centerline

Roller & Pivot Geometry:

RollerRadL = 0.810 (inches) Radius of Leading Shoe Roller
 RollerRadT = 0.810 (inches) Radius of Trailing Shoe Roller
 PinRadiusL = 0.371 (inches) Radius of Leading Shoe Roller Pin
 PinRadiusT = 0.371 (inches) Radius of Trailing Shoe Roller Pin
 PivotRadL = 0.624 (inches) Radius of Leading Shoe Pivot Pin
 PivotRadT = 0.624 (inches) Radius of Trailing Shoe Pivot Pin

Friction Values

MuRollerL = 0.200 (-) Friction Coefficient of Leading Shoe Roller Pin
 MuRollerT = 0.200 (-) Friction Coefficient of Trailing Shoe Roller Pin
 MuPivotL = 0.200 (-) Friction Coefficient of Leading Shoe Pivot Pin
 MuPivotT = 0.200 (-) Friction Coefficient of Trailing Shoe Pivot Pin
 MuBearing = 0.100 (-) Friction Coefficient of Cam Shaft Bearing

Chamber & Slack Adjuster:

slackL = 5.50	(inches)	Slack Adjuster Arm Length
CanForce = 1425	(lb)	Air Chamber Force Application
Kcan = 2850	(lb/inch)	Stiffness of Lining and Mechanical Components Relative to Chamber-Stroke Motion
K = 290855	(lb/inch)	Stiffness of Lining and Mechanical Components Relative to Cam-Roller Motion
Asymmetry = 0.10	(-)	Stiffness Asymmetry (+ => leading > trailing)
Fstar = 7884.8	(lb)	AVERAGE of Leading & Trailing input shoe forces, absent friction
deltaT' = 0.060	(inches)	Trailing Shoe to Drum Clearance (displacement at cam-roller location)

Equilibrium Values of S-Cam Brake Model Parameters & Output Torque:

mu-Lining = 0.500	(-)	Lining Friction Coefficient
BF-L = 1.881	(-)	Leading Shoe Brake Factor
BF-T = 0.613	(-)	Trailing Shoe Brake Factor
BF = 1.850	(-)	Combined (total) Brake Factor: $4*BF1*BF2/(BF1+BF2)$
Rho = 0.326	(-)	Ratio of Leading Shoe Force to Trailing Shoe Force
fL = 3384.5	(lbs)	Leading Shoe Force
fT = 10384.3	(lbs)	Trailing Shoe Force
delta* = 0.109	(inches)	Total Cam-Rise Displacement from 0-Torque Initial Position
deltaT = 0.060	(inches)	Trailing Shoe Clearance
deltaL = 0.069	(inches)	Leading Shoe Clearance + Equilibrium Wear
alphaL = 13.4	(degrees)	Angle of Application of Leading Shoe Actuation Force on Roller
alphaT = 13.3	(degrees)	Angle of Application of Trailing Shoe Actuation Force on Roller
betaL = -2.2	(degrees)	Effective Center of Pressure - Leading Shoe
betaT = -2.6	(degrees)	Effective Center of Pressure - Trailing Shoe
Cam Angle = 39.60	(degrees)	Angle of Cam at Equilibrium wrt Minimum Radius Cam Angle
Cam0 = 27.07	(degrees)	Initial Angle of Cam at Rest (0-Torque Initial Position)
Cam Rotation = 12.53	(degrees)	Net Cam Rotation due to Chamber Force Input
Contact AngleL= 10.83	(degrees)	Angle Between Line Connecting Cam Center with Contact Point and X-axis
(leading)		
Contact AngleT= 10.76	(degrees)	Angle Between Line Connecting Cam Center with Contact Point and X-axis
(trailing)		
Stroke = 1.20	(inches)	Total Air Chamber Stroke
Torque = 105052.1	(inch-lb)	Brake Torque

S-Cam Brake Model Parameters: Δx Variation Example

Shoe Geometry:
 a = 12.750 (inches) Leading Shoe Pivot to Leading Shoe Roller Center
 a' = 12.750 (inches) Trailing Shoe Pivot to Trailing Shoe Roller Center
 b = 1.250 (inches) Offset of Leading Shoe Pivot from Centerline
 b' = 1.250 (inches) Offset of Trailing Shoe Pivot from Centerline
 c = 6.750 (inches) Leading Shoe Pivot to Centerline
 c' = 6.750 (inches) Trailing Shoe Pivot to Centerline
 d = 0.410 (inches) Offset of Leading Shoe Pivot from Leading Shoe Roller Center
 d' = 0.410 (inches) Offset of Trailing Shoe Pivot from Trailing Shoe Roller Center
 phi = 55.000 (degrees) Half-Shoe Angle Subtended by Lining Block

Drum Geometry:
 r = 8.250 (inches) Drum Radius
 epsx = -0.020 (inches) Offset (towards trailing shoe) of Drum Center from Brake Centerline
 epsy = 0.000 (inches) Offset (towards cam) of Drum Center from Brake Centerline

Cam Geometry:
 CamRatio = 0.497 (in/rad) Cam Rise to Cam Rotation Ratio
 CamRadius0 = 0.561 (inches) Cam Radius at Zero Rotation
 ShaftRadius = 0.747 (inches) Radius of Cam Shaft
 xc = 0.000 (inches) Offset from Center of Cam to Brake Centerline
 yc = 6.000 (inches) Distance from Center of Cam to Brake Centerline

Roller & Pivot Geometry:
 RollerRadL = 0.810 (inches) Radius of Leading Shoe Roller
 RollerRadT = 0.810 (inches) Radius of Trailing Shoe Roller
 PinRadiusL = 0.371 (inches) Radius of Leading Shoe Roller Pin
 PinRadiusT = 0.371 (inches) Radius of Trailing Shoe Roller Pin
 PivotRadL = 0.624 (inches) Radius of Leading Shoe Pivot Pin
 PivotRadT = 0.624 (inches) Radius of Trailing Shoe Pivot Pin

Friction Values
 MuRollerL = 0.200 (-) Friction Coefficient of Leading Shoe Roller Pin
 MuRollerT = 0.200 (-) Friction Coefficient of Trailing Shoe Roller Pin
 MuPivotL = 0.200 (-) Friction Coefficient of Leading Shoe Pivot Pin
 MuPivotT = 0.200 (-) Friction Coefficient of Trailing Shoe Pivot Pin
 MuBearing = 0.100 (-) Friction Coefficient of Cam Shaft Bearing

Chamber & Slack Adjuster:

slackL = 5.50	(inches)	Slack Adjuster Arm Length
CanForce = 1425	(lb)	Air Chamber Force Application
Kcan = 2850	(lb/inch)	Stiffness of Lining and Mechanical Components Relative to Chamber-Stroke Motion
K = 290855	(lb/inch)	Stiffness of Lining and Mechanical Components Relative to Cam-Roller Motion
Asymmetry = 0.10	(-)	Stiffness Asymmetry (+ => leading > trailing)
Fstar = 7884.8	(lb)	AVERAGE of Leading & Trailing input shoe forces, absent friction
deltaT' = 0.060	(inches)	Trailing Shoe to Drum Clearance (displacement at cam-roller location)

Equilibrium Values of S-Cam Brake Model Parameters & Output Torque:

mu-Lining = 0.500	(-)	Lining Friction Coefficient
BF-L = 2.403	(-)	Leading Shoe Brake Factor
BF-T = 0.579	(-)	Trailing Shoe Brake Factor
BF = 1.865	(-)	Combined (total) Brake Factor: $4*BF1*BF2/(BF1+BF2)$
Rho = 0.241	(-)	Ratio of Leading Shoe Force to Trailing Shoe Force
fL = 2650.7	(lbs)	Leading Shoe Force
fT = 11011.4	(lbs)	Trailing Shoe Force
delta* = 0.109	(inches)	Total Cam-Rise Displacement from 0-Torque Initial Position
deltaT = 0.060	(inches)	Trailing Shoe Clearance
deltaL = 0.049	(inches)	Leading Shoe Clearance + Equilibrium Wear
alphaL = 13.4	(degrees)	Angle of Application of Leading Shoe Actuation Force on Roller
alphaT = 13.3	(degrees)	Angle of Application of Trailing Shoe Actuation Force on Roller
betaL = 11.3	(degrees)	Effective Center of Pressure - Leading Shoe
betaT = 5.2	(degrees)	Effective Center of Pressure - Trailing Shoe
Cam Angle = 39.65	(degrees)	Angle of Cam at Equilibrium wrt Minimum Radius Cam Angle
Cam0 = 27.12	(degrees)	Initial Angle of Cam at Rest (0-Torque Initial Position)
Cam Rotation = 12.53	(degrees)	Net Cam Rotation due to Chamber Force Input
Contact AngleL= 10.85	(degrees)	Angle Between Line Connecting Cam Center with Contact Point and X-axis (leading)
Contact AngleT= 10.79	(degrees)	Angle Between Line Connecting Cam Center with Contact Point and X-axis (trailing)
Stroke = 1.20	(inches)	Total Air Chamber Stroke
Torque = 105117.9	(inch-lb)	Brake Torque

S-Cam Brake Model Parameters:

-xc Variation Example

Shoe Geometry:

a = 12.750 (inches) Leading Shoe Pivot to Leading Shoe Roller Center
 a' = 12.750 (inches) Trailing Shoe Pivot to Trailing Shoe Roller Center
 b = 1.250 (inches) Offset of Leading Shoe Pivot from Centerline
 b' = 1.250 (inches) Offset of Trailing Shoe Pivot from Centerline
 c = 6.750 (inches) Leading Shoe Pivot to Centerline
 c' = 6.750 (inches) Trailing Shoe Pivot to Centerline
 d = 0.410 (inches) Offset of Leading Shoe Pivot from Leading Shoe Roller Center
 d' = 0.410 (inches) Offset of Trailing Shoe Pivot from Trailing Shoe Roller Center
 phi = 55.000 (degrees) Half-Shoe Angle Subtended by Lining Block

Drum Geometry:

r = 8.250 (inches) Drum Radius
 epsx = 0.000 (inches) Offset (towards trailing shoe) of Drum Center from Brake Centerline
 epsy = 0.000 (inches) Offset (towards cam) of Drum Center from Brake Centerline

Cam Geometry:

CamRatio = 0.497 (in/rad) Cam Rise to Cam Rotation Ratio
 CamRadius0 = 0.561 (inches) Cam Radius at Zero Rotation
 ShaftRadius = 0.747 (inches) Radius of Cam Shaft
 xc = -0.020 (inches) Offset from Center of Cam to Brake Centerline
 yc = 6.000 (inches) Distance from Center of Cam to Brake Centerline

Roller & Pivot Geometry:

RollerRadL = 0.810 (inches) Radius of Leading Shoe Roller
 RollerRadT = 0.810 (inches) Radius of Trailing Shoe Roller
 PinRadiusL = 0.371 (inches) Radius of Leading Shoe Roller Pin
 PinRadiusT = 0.371 (inches) Radius of Trailing Shoe Roller Pin
 PivotRadL = 0.624 (inches) Radius of Leading Shoe Pivot Pin
 PivotRadT = 0.624 (inches) Radius of Trailing Shoe Pivot Pin

Friction Values

MuRollerL = 0.200 (-) Friction Coefficient of Leading Shoe Roller Pin
 MuRollerT = 0.200 (-) Friction Coefficient of Trailing Shoe Roller Pin
 MuPivotL = 0.200 (-) Friction Coefficient of Leading Shoe Pivot Pin
 MuPivotT = 0.200 (-) Friction Coefficient of Trailing Shoe Pivot Pin
 MuBearing = 0.100 (-) Friction Coefficient of Cam Shaft Bearing

Chamber & Slack Adjuster:

slackL = 5.50	(inches)	Slack Adjuster Arm Length
CanForce = 1425	(lb)	Air Chamber Force Application
Kcan = 2850	(lb/inch)	Stiffness of Lining and Mechanical Components Relative to Chamber-Stroke Motion
K = 290855	(lb/inch)	Stiffness of Lining and Mechanical Components Relative to Cam-Roller Motion
Asymmetry = 0.10	(-)	Stiffness Asymmetry (+ => leading > trailing)
Fstar = 7884.8	(lb)	AVERAGE of Leading & Trailing input shoe forces, absent friction
deltaT' = 0.060	(inches)	Trailing Shoe to Drum Clearance (displacement at cam-roller location)

Equilibrium Values of S-Cam Brake Model Parameters & Output Torque:

mu-Lining = 0.500	(-)	Lining Friction Coefficient
BF-L = 2.156	(-)	Leading Shoe Brake Factor
BF-T = 0.571	(-)	Trailing Shoe Brake Factor
BF = 1.805	(-)	Combined (total) Brake Factor: $4*BF1*BF2/(BF1+BF2)$
Rho = 0.265	(-)	Ratio of Leading Shoe Force to Trailing Shoe Force
fL = 2865.8	(lbs)	Leading Shoe Force
fT = 10827.5	(lbs)	Trailing Shoe Force
delta* = 0.107	(inches)	Total Cam-Rise Displacement from 0-Torque Initial Position
deltaT = 0.060	(inches)	Trailing Shoe Clearance
deltaL = 0.108	(inches)	Leading Shoe Clearance + Equilibrium Wear
alphaL = 13.0	(degrees)	Angle of Application of Leading Shoe Actuation Force on Roller
alphaT = 13.3	(degrees)	Angle of Application of Trailing Shoe Actuation Force on Roller
betaL = 9.4	(degrees)	Effective Center of Pressure - Leading Shoe
betaT = 7.3	(degrees)	Effective Center of Pressure - Trailing Shoe
Cam Angle = 41.85	(degrees)	Angle of Cam at Equilibrium wrt Minimum Radius Cam Angle
Cam0 = 29.49	(degrees)	Initial Angle of Cam at Rest (0-Torque Initial Position)
Cam Rotation = 12.36	(degrees)	Net Cam Rotation due to Chamber Force Input
Contact AngleL= 10.30	(degrees)	Angle Between Line Connecting Cam Center with Contact Point and X-axis (leading)
Contact AngleT= 10.55	(degrees)	Angle Between Line Connecting Cam Center with Contact Point and X-axis (trailing)
Stroke = 1.19	(inches)	Total Air Chamber Stroke
Torque = 101964.7	(inch-lb)	Brake Torque

S-Cam Brake Model Parameters: **+xc Variation Example**

Shoe Geometry:

a = 12.750	(inches)	Leading Shoe Pivot to Leading Shoe Roller Center
a' = 12.750	(inches)	Trailing Shoe Pivot to Trailing Shoe Roller Center
b = 1.250	(inches)	Offset of Leading Shoe Pivot from Centerline
b' = 1.250	(inches)	Offset of Trailing Shoe Pivot from Centerline
c = 6.750	(inches)	Leading Shoe Pivot to Centerline
c' = 6.750	(inches)	Trailing Shoe Pivot to Centerline
d = 0.410	(inches)	Offset of Leading Shoe Pivot from Leading Shoe Roller Center
d' = 0.410	(inches)	Offset of Trailing Shoe Pivot from Trailing Shoe Roller Center
phi = 55.000	(degrees)	Half-Shoe Angle Subtended by Lining Block

Drum Geometry:

r = 8.250	(inches)	Drum Radius
epsx = 0.000	(inches)	Offset (towards trailing shoe) of Drum Center from Brake Centerline
epsy = 0.000	(inches)	Offset (towards cam) of Drum Center from Brake Centerline

Cam Geometry:

CamRatio = 0.497	(in/rad)	Cam Rise to Cam Rotation Ratio
CamRadius0 = 0.561	(inches)	Cam Radius at Zero Rotation
ShaftRadius = 0.747	(inches)	Radius of Cam Shaft
xc = 0.020	(inches)	Offset from Center of Cam to Brake Centerline
yc = 6.000	(inches)	Distance from Center of Cam to Brake Centerline

Roller & Pivot Geometry:

RollerRadL = 0.810	(inches)	Radius of Leading Shoe Roller
RollerRadT = 0.810	(inches)	Radius of Trailing Shoe Roller
PinRadiusL = 0.371	(inches)	Radius of Leading Shoe Roller Pin
PinRadiusT = 0.371	(inches)	Radius of Trailing Shoe Roller Pin
PivotRadL = 0.624	(inches)	Radius of Leading Shoe Pivot Pin
PivotRadT = 0.624	(inches)	Radius of Trailing Shoe Pivot Pin

Friction Values

MuRollerL = 0.200	(-)	Friction Coefficient of Leading Shoe Roller Pin
MuRollerT = 0.200	(-)	Friction Coefficient of Trailing Shoe Roller Pin
MuPivotL = 0.200	(-)	Friction Coefficient of Leading Shoe Pivot Pin
MuPivotT = 0.200	(-)	Friction Coefficient of Trailing Shoe Pivot Pin
MuBearing = 0.100	(-)	Friction Coefficient of Cam Shaft Bearing

Chamber & Slack Adjuster:

slackL = 5.50 (inches) Slack Adjuster Arm Length
 CanForce = 1425 (lb) Air Chamber Force Application
 Kcan = 2850 (lb/inch) Stiffness of Lining and Mechanical Components Relative to Chamber-Stroke Motion
 K = 290855 (lb/inch) Stiffness of Lining and Mechanical Components Relative to Cam-Roller Motion
 Asymmetry = 0.10 (-) Stiffness Asymmetry (+ => leading > trailing)
 Fstar = 7884.8 (lb) AVERAGE of Leading & Trailing input shoe forces, absent friction
 deltaT' = 0.060 (inches) Trailing Shoe to Drum Clearance (displacement at cam-roller location)

Equilibrium Values of S-Cam Brake Model Parameters & Output Torque:

mu-Lining = 0.500 (-) Lining Friction Coefficient
 BF-L = 2.155 (-) Leading Shoe Brake Factor
 BF-T = 0.571 (-) Trailing Shoe Brake Factor
 BF = 1.806 (-) Combined (total) Brake Factor: $4*BF1*BF2/(BF1+BF2)$
 Rho = 0.265 (-) Ratio of Leading Shoe Force to Trailing Shoe Force
 fL = 2867.6 (lbs) Leading Shoe Force
 fT = 10826.0 (lbs) Trailing Shoe Force
 delta* = 0.107 (inches) Total Cam-Rise Displacement from 0-Torque Initial Position
 deltaT = 0.060 (inches) Trailing Shoe Clearance
 deltaL = 0.029 (inches) Leading Shoe Clearance + Equilibrium Wear
 alphaL = 13.2 (degrees) Angle of Application of Leading Shoe Actuation Force on Roller
 alphaT = 13.2 (degrees) Angle of Application of Trailing Shoe Actuation Force on Roller
 betaL = 5.9 (degrees) Effective Center of Pressure - Leading Shoe
 betaT = 7.3 (degrees) Effective Center of Pressure - Trailing Shoe
 Cam Angle = 37.00 (degrees) Angle of Cam at Equilibrium wrt Minimum Radius Cam Angle
 Cam0 = 24.64 (degrees) Initial Angle of Cam at Rest (0-Torque Initial Position)
 Cam Rotation = 12.36 (degrees) Net Cam Rotation due to Chamber Force Input
 Contact AngleL= 10.95 (degrees) Angle Between Line Connecting Cam Center with Contact Point and X-axis
 (leading)
 Contact AngleT= 10.92 (degrees) Angle Between Line Connecting Cam Center with Contact Point and X-axis
 (trailing)
 Stroke = 1.19 (inches) Total Air Chamber Stroke
 Torque = 101985.5 (inch-lb) Brake Torque

S-Cam Brake Model Parameters: **+yc Variation Example**

Shoe Geometry:

a = 12.750	(inches)	Leading Shoe Pivot to Leading Shoe Roller Center
a' = 12.750	(inches)	Trailing Shoe Pivot to Trailing Shoe Roller Center
b = 1.250	(inches)	Offset of Leading Shoe Pivot from Centerline
b' = 1.250	(inches)	Offset of Trailing Shoe Pivot from Centerline
c = 6.750	(inches)	Leading Shoe Pivot to Centerline
c' = 6.750	(inches)	Trailing Shoe Pivot to Centerline
d = 0.410	(inches)	Offset of Leading Shoe Pivot from Leading Shoe Roller Center
d' = 0.410	(inches)	Offset of Trailing Shoe Pivot from Trailing Shoe Roller Center
phi = 55.000	(degrees)	Half-Shoe Angle Subtended by Lining Block

Drum Geometry:

r = 8.250	(inches)	Drum Radius
epsx = 0.000	(inches)	Offset (towards trailing shoe) of Drum Center from Brake Centerline
epsy = 0.000	(inches)	Offset (towards cam) of Drum Center from Brake Centerline

Cam Geometry:

CamRatio = 0.497	(in/rad)	Cam Rise to Cam Rotation Ratio
CamRadius0 = 0.561	(inches)	Cam Radius at Zero Rotation
ShaftRadius = 0.747	(inches)	Radius of Cam Shaft
xc = 0.000	(inches)	Offset from Center of Cam to Brake Centerline
yc = 6.020	(inches)	Distance from Center of Cam to Brake Centerline

Roller & Pivot Geometry:

RollerRadL = 0.810	(inches)	Radius of Leading Shoe Roller
RollerRadT = 0.810	(inches)	Radius of Trailing Shoe Roller
PinRadiusL = 0.371	(inches)	Radius of Leading Shoe Roller Pin
PinRadiusT = 0.371	(inches)	Radius of Trailing Shoe Roller Pin
PivotRadL = 0.624	(inches)	Radius of Leading Shoe Pivot Pin
PivotRadT = 0.624	(inches)	Radius of Trailing Shoe Pivot Pin

Friction Values

MuRollerL = 0.200	(-)	Friction Coefficient of Leading Shoe Roller Pin
MuRollerT = 0.200	(-)	Friction Coefficient of Trailing Shoe Roller Pin
MuPivotL = 0.200	(-)	Friction Coefficient of Leading Shoe Pivot Pin
MuPivotT = 0.200	(-)	Friction Coefficient of Trailing Shoe Pivot Pin
MuBearing = 0.100	(-)	Friction Coefficient of Cam Shaft Bearing

Chamber & Slack Adjuster:

slackL = 5.50	(inches)	Slack Adjuster Arm Length
CanForce = 1425	(lb)	Air Chamber Force Application
Kcan = 2850	(lb/inch)	Stiffness of Lining and Mechanical Components Relative to Chamber-Stroke Motion
K = 290855	(lb/inch)	Stiffness of Lining and Mechanical Components Relative to Cam-Roller Motion
Asymmetry = 0.10	(-)	Stiffness Asymmetry (+ => leading > trailing)
Fstar = 7884.8	(lb)	AVERAGE of Leading & Trailing input shoe forces, absent friction
deltaT' = 0.060	(inches)	Trailing Shoe to Drum Clearance (displacement at cam-roller location)

Equilibrium Values of S-Cam Brake Model Parameters & Output Torque:

mu-Lining = 0.500	(-)	Lining Friction Coefficient
BF-L = 2.150	(-)	Leading Shoe Brake Factor
BF-T = 0.572	(-)	Trailing Shoe Brake Factor
BF = 1.808	(-)	Combined (total) Brake Factor: $4*BF1*BF2/(BF1+BF2)$
Rho = 0.266	(-)	Ratio of Leading Shoe Force to Trailing Shoe Force
fL = 2878.8	(lbs)	Leading Shoe Force
fT = 10816.4	(lbs)	Trailing Shoe Force
delta* = 0.107	(inches)	Total Cam-Rise Displacement from 0-Torque Initial Position
deltaT = 0.060	(inches)	Trailing Shoe Clearance
deltaL = 0.059	(inches)	Leading Shoe Clearance + Equilibrium Wear
alphaL = 14.1	(degrees)	Angle of Application of Leading Shoe Actuation Force on Roller
alphaT = 12.6	(degrees)	Angle of Application of Trailing Shoe Actuation Force on Roller
betaL = 7.3	(degrees)	Effective Center of Pressure - Leading Shoe
betaT = 7.3	(degrees)	Effective Center of Pressure - Trailing Shoe
Cam Angle = 38.85	(degrees)	Angle of Cam at Equilibrium wrt Minimum Radius Cam Angle
Cam0 = 26.48	(degrees)	Initial Angle of Cam at Rest (0-Torque Initial Position)
Cam Rotation = 12.37	(degrees)	Net Cam Rotation due to Chamber Force Input
Contact AngleL= 10.36	(degrees)	Angle Between Line Connecting Cam Center with Contact Point and X-axis (leading)
Contact AngleT= 11.41	(degrees)	Angle Between Line Connecting Cam Center with Contact Point and X-axis (trailing)
Stroke = 1.19	(inches)	Total Air Chamber Stroke
Torque = 102144.0	(inch-lb)	Brake Torque

S-Cam Brake Model Parameters:

K Variation Example

Shoe Geometry:

a = 12.750 (inches) Leading Shoe Pivot to Leading Shoe Roller Center
 a' = 12.750 (inches) Trailing Shoe Pivot to Trailing Shoe Roller Center
 b = 1.250 (inches) Offset of Leading Shoe Pivot from Centerline
 b' = 1.250 (inches) Offset of Trailing Shoe Pivot from Centerline
 c = 6.750 (inches) Leading Shoe Pivot to Centerline
 c' = 6.750 (inches) Trailing Shoe Pivot to Centerline
 d = 0.410 (inches) Offset of Leading Shoe Pivot from Leading Shoe Roller Center
 d' = 0.410 (inches) Offset of Trailing Shoe Pivot from Trailing Shoe Roller Center
 phi = 55.000 (degrees) Half-Shoe Angle Subtended by Lining Block

Drum Geometry:

r = 8.250 (inches) Drum Radius
 epsx = 0.000 (inches) Offset (towards trailing shoe) of Drum Center from Brake Centerline
 epsy = 0.000 (inches) Offset (towards cam) of Drum Center from Brake Centerline

Cam Geometry:

CamRatio = 0.497 (in/rad) Cam Rise to Cam Rotation Ratio
 CamRadius0 = 0.561 (inches) Cam Radius at Zero Rotation
 ShaftRadius = 0.747 (inches) Radius of Cam Shaft
 xc = 0.000 (inches) Offset from Center of Cam to Brake Centerline
 yc = 6.000 (inches) Distance from Center of Cam to Brake Centerline

Roller & Pivot Geometry:

RollerRadL = 0.810 (inches) Radius of Leading Shoe Roller
 RollerRadT = 0.810 (inches) Radius of Trailing Shoe Roller
 PinRadiusL = 0.371 (inches) Radius of Leading Shoe Roller Pin
 PinRadiusT = 0.371 (inches) Radius of Trailing Shoe Roller Pin
 PivotRadL = 0.624 (inches) Radius of Leading Shoe Pivot Pin
 PivotRadT = 0.624 (inches) Radius of Trailing Shoe Pivot Pin

Friction Values

MuRollerL = 0.200 (-) Friction Coefficient of Leading Shoe Roller Pin
 MuRollerT = 0.200 (-) Friction Coefficient of Trailing Shoe Roller Pin
 MuPivotL = 0.200 (-) Friction Coefficient of Leading Shoe Pivot Pin
 MuPivotT = 0.200 (-) Friction Coefficient of Trailing Shoe Pivot Pin
 MuBearing = 0.100 (-) Friction Coefficient of Cam Shaft Bearing

Chamber & Slack Adjuster:

slackL = 5.50	(inches)	Slack Adjuster Arm Length
CanForce = 1425	(lb)	Air Chamber Force Application
Kcan = 2500	(lb/inch)	Stiffness of Lining and Mechanical Components Relative to Chamber-Stroke Motion
K = 255136	(lb/inch)	Stiffness of Lining and Mechanical Components Relative to Cam-Roller Motion
Asymmetry = 0.10	(-)	Stiffness Asymmetry (+ => leading > trailing)
Fstar = 7884.8	(lb)	AVERAGE of Leading & Trailing input shoe forces, absent friction
deltaT' = 0.060	(inches)	Trailing Shoe to Drum Clearance (displacement at cam-roller location)

Equilibrium Values of S-Cam Brake Model Parameters & Output Torque:

mu-Lining = 0.500	(-)	Lining Friction Coefficient
BF-L = 2.157	(-)	Leading Shoe Brake Factor
BF-T = 0.571	(-)	Trailing Shoe Brake Factor
BF = 1.807	(-)	Combined (total) Brake Factor: $4*BF1*BF2/(BF1+BF2)$
Rho = 0.265	(-)	Ratio of Leading Shoe Force to Trailing Shoe Force
fL = 2867.0	(lbs)	Leading Shoe Force
fT = 10826.5	(lbs)	Trailing Shoe Force
delta* = 0.114	(inches)	Total Cam-Rise Displacement from 0-Torque Initial Position
deltaT = 0.060	(inches)	Trailing Shoe Clearance
deltaL = 0.070	(inches)	Leading Shoe Clearance + Equilibrium Wear
alphaL = 13.4	(degrees)	Angle of Application of Leading Shoe Actuation Force on Roller
alphaT = 13.2	(degrees)	Angle of Application of Trailing Shoe Actuation Force on Roller
betaL = 7.7	(degrees)	Effective Center of Pressure - Leading Shoe
betaT = 7.3	(degrees)	Effective Center of Pressure - Trailing Shoe
Cam Angle = 40.25	(degrees)	Angle of Cam at Equilibrium wrt Minimum Radius Cam Angle
Cam0 = 27.12	(degrees)	Initial Angle of Cam at Rest (0-Torque Initial Position)
Cam Rotation = 13.13	(degrees)	Net Cam Rotation due to Chamber Force Input
Contact AngleL= 10.75	(degrees)	Angle Between Line Connecting Cam Center with Contact Point and X-axis (leading)
Contact AngleT= 10.67	(degrees)	Angle Between Line Connecting Cam Center with Contact Point and X-axis (trailing)
Stroke = 1.26	(inches)	Total Air Chamber Stroke
Torque = 102043.2	(inch-lb)	Brake Torque

S-Cam Brake Model Parameters:		Parameter	"a" Variation	Example
Shoe Geometry:				
a	= 12.850	(inches)	Leading Shoe Pivot to Leading Shoe Roller Center	
a'	= 12.750	(inches)	Trailing Shoe Pivot to Trailing Shoe Roller Center	
b	= 1.250	(inches)	Offset of Leading Shoe Pivot from Centerline	
b'	= 1.250	(inches)	Offset of Trailing Shoe Pivot from Centerline	
c	= 6.750	(inches)	Leading Shoe Pivot to Centerline	
c'	= 6.750	(inches)	Trailing Shoe Pivot to Centerline	
d	= 0.410	(inches)	Offset of Leading Shoe Pivot from Leading Shoe Roller Center	
d'	= 0.410	(inches)	Offset of Trailing Shoe Pivot from Trailing Shoe Roller Center	
phi	= 55.000	(degrees)	Half-Shoe Angle Subtended by Lining Block	
Drum Geometry:				
r	= 8.250	(inches)	Drum Radius	
epsx	= 0.000	(inches)	Offset (towards trailing shoe) of Drum Center from Brake Centerline	
epsy	= 0.000	(inches)	Offset (towards cam) of Drum Center from Brake Centerline	
Cam Geometry:				
CamRatio	= 0.497	(in/rad)	Cam Rise to Cam Rotation Ratio	
CamRadius0	= 0.561	(inches)	Cam Radius at Zero Rotation	
ShaftRadius	= 0.747	(inches)	Radius of Cam Shaft	
xc	= 0.000	(inches)	Offset from Center of Cam to Brake Centerline	
yc	= 6.000	(inches)	Distance from Center of Cam to Brake Centerline	
Roller & Pivot Geometry:				
RollerRadL	= 0.810	(inches)	Radius of Leading Shoe Roller	
RollerRadT	= 0.810	(inches)	Radius of Trailing Shoe Roller	
PinRadiusL	= 0.371	(inches)	Radius of Leading Shoe Roller Pin	
PinRadiusT	= 0.371	(inches)	Radius of Trailing Shoe Roller Pin	
PivotRadL	= 0.624	(inches)	Radius of Leading Shoe Pivot Pin	
PivotRadT	= 0.624	(inches)	Radius of Trailing Shoe Pivot Pin	
Friction Values				
MuRollerL	= 0.200	(-)	Friction Coefficient of Leading Shoe Roller Pin	
MuRollerT	= 0.200	(-)	Friction Coefficient of Trailing Shoe Roller Pin	
MuPivotL	= 0.200	(-)	Friction Coefficient of Leading Shoe Pivot Pin	
MuPivotT	= 0.200	(-)	Friction Coefficient of Trailing Shoe Pivot Pin	
MuBearing	= 0.100	(-)	Friction Coefficient of Cam Shaft Bearing	

Chamber & Slack Adjuster:

slackL = 5.50 (inches) Slack Adjuster Arm Length
 CanForce = 1425 (lb) Air Chamber Force Application
 Kcan = 2850 (lb/inch) Stiffness of Lining and Mechanical Components Relative to Chamber-Stroke Motion
 K = 290855 (lb/inch) Stiffness of Lining and Mechanical Components Relative to Cam-Roller Motion
 Asymmetry = 0.10 (-) Stiffness Asymmetry (+ => leading > trailing)
 Fstar = 7884.8 (lb) AVERAGE of Leading & Trailing input shoe forces, absent friction
 deltaT' = 0.060 (inches) Trailing Shoe to Drum Clearance (displacement at cam-roller location)

Equilibrium Values of S-Cam Brake Model Parameters & Output Torque:

mu-Lining = 0.500 (-) Lining Friction Coefficient
 BF-L = 2.194 (-) Leading Shoe Brake Factor
 BF-T = 0.571 (-) Trailing Shoe Brake Factor
 BF = 1.812 (-) Combined (total) Brake Factor: $4*BF1*BF2/(BF1+BF2)$
 Rho = 0.260 (-) Ratio of Leading Shoe Force to Trailing Shoe Force
 fL = 2826.5 (lbs) Leading Shoe Force
 fT = 10861.6 (lbs) Trailing Shoe Force
 delta* = 0.107 (inches) Total Cam-Rise Displacement from 0-Torque Initial Position
 deltaT = 0.060 (inches) Trailing Shoe Clearance
 deltaL = 0.091 (inches) Leading Shoe Clearance + Equilibrium Wear
 alphaL = 9.8 (degrees) Angle of Application of Leading Shoe Actuation Force on Roller
 alphaT = 13.2 (degrees) Angle of Application of Trailing Shoe Actuation Force on Roller
 betaL = 8.7 (degrees) Effective Center of Pressure - Leading Shoe
 betaT = 7.3 (degrees) Effective Center of Pressure - Trailing Shoe
 Cam Angle = 39.40 (degrees) Angle of Cam at Equilibrium wrt Minimum Radius Cam Angle
 Cam0 = 27.02 (degrees) Initial Angle of Cam at Rest (0-Torque Initial Position)
 Cam Rotation = 12.38 (degrees) Net Cam Rotation due to Chamber Force Input
 Contact AngleL= 13.47 (degrees) Angle Between Line Connecting Cam Center with Contact Point and X-axis
 (leading)
 Contact AngleT= 10.71 (degrees) Angle Between Line Connecting Cam Center with Contact Point and X-axis
 (trailing)
 Stroke = 1.19 (inches) Total Air Chamber Stroke
 Torque = 102300.9 (inch-lb) Brake Torque

Appendix C. S-Cam Brake Model Equations.

The equations appearing in this appendix utilize Figures 1 and 2 and the symbols defined in Appendix A.

Leading Shoe Moment Equilibrium —

Summing moments about the pivot =>

$$-(a + dr \sin \alpha)F_a \cos \alpha - F_d \cos \beta (r \cos \beta - b) + (dr \cos \alpha - d) F_a \sin \alpha - F_d \sin \beta (r \sin \beta + c) + F_n \cos \beta (r \sin \beta + c) - F_n \sin \beta (r \cos \beta - b) = 0 \quad (C-1)$$

If, $F_d = \mu_L F_n \Rightarrow F_n = F_d / \mu_L$ and substituting into (C-1) => (C-2)

$$F_d / F_a = ((dr \cos \alpha - d) \sin \alpha - (a + dr \sin \alpha) \cos \alpha) / [r - b (\cos \beta + \sin \beta / \mu_L) + c (\sin \beta - \cos \beta / \mu_L)] \quad (C-3)$$

Trailing Shoe Moment Equilibrium —

Likewise for the trailing shoe:

$$F_d' / F_a' = ((dr' \cos \alpha' - d') \sin \alpha' + (a' - dr' \sin \alpha') \cos \alpha') / [r - b' (\cos \beta' - \sin \beta' / \mu_L) + c' (\sin \beta' + \cos \beta' / \mu_L)] \quad (C-4)$$

Equilibrium Condition —

Equalization of drag (normal) forces on the leading and trailing shoes (equalized wear rates) =>

$$F_d = F_d' \quad (C-5)$$

or, from (C-1), C-4), and (C-5),

$$\rho = F_a / F_a' = \{ [r - b (\cos \beta + \sin \beta / \mu_L) + c (\sin \beta - \cos \beta / \mu_L)] \cdot ((dr' \cos \alpha' - d') \sin \alpha' + (a' - dr' \sin \alpha') \cos \alpha') \} / \{ [r - b' (\cos \beta' - \sin \beta' / \mu_L) + c' (\sin \beta' + \cos \beta' / \mu_L)] \cdot ((dr \cos \alpha - d) \sin \alpha - (a + dr \sin \alpha) \cos \alpha) \} \quad (C-6)$$

$$\text{If, } F_n = K_L (\delta - \delta_L) \quad \text{and} \quad F_n' = K_T (\delta - \delta_T), \quad (\text{C-7})$$

and substituting into (C-3) and (C-4) to solve for F_a and F_a' :

$$F_a = K_L (\delta - \delta_L) \mu_L [r - b (\cos \beta + \sin \beta / \mu_L) + c (\sin \beta - \cos \beta / \mu_L)] / \\ ((dr \cos \alpha - d) \sin \alpha - (a + dr \sin \alpha) \cos \alpha) \quad (\text{C-8})$$

$$F_a' = K_T (\delta - \delta_T) \mu_L [r - b' (\cos \beta' - \sin \beta' / \mu_L) + c' (\sin \beta' + \cos \beta' / \mu_L)] / \\ ((dr' \cos \alpha' - d') \sin \alpha' + (a' - dr' \sin \alpha') \cos \alpha') \quad (\text{C-9})$$

Combining the self-energizing terms and leading/trailing lining-shoe stiffnesses, K_L and K_T , into effective leading and trailing stiffnesses, K_1 and K_2 , and adding the friction forces from the roller, bearing, and pivot:

$$F_a = K_1 (\delta - \delta_L) (1 + \mu_R + \mu_P - \mu_B) \quad (\text{C-10})$$

and,

$$F_a' = K_2 (\delta - \delta_T) (1 + \mu_R' + \mu_P' + \mu_B) \quad (\text{C-11})$$

Requiring 1) a force balance across the cam at equilibrium :

$$2 F^* = F_a + F_a' = K_1 (\delta - \delta_L) (1 + \mu_R + \mu_P - \mu_B) + K_2 (\delta - \delta_T) (1 + \mu_R' + \mu_P' + \mu_B) \quad (\text{C-12})$$

and, 2) $F_a / F_a' = \rho$ (less the friction terms) =>

$$\rho = K_1 (\delta - \delta_L) / K_2 (\delta - \delta_T) \quad (\text{C-13})$$

If, $\mu_R = \mu_R'$ and $\mu_P = \mu_P'$, solving (C-11) and (C-12) for δ (= δ^* at equilibrium)

and δ_L (given δ_T) provides:

$$\delta^* = \delta_T + 2 F^* / \{ K_2 [(1 + \rho)(1 + \mu_R + \mu_P) + (1 - \rho) \mu_B] \} \quad (\text{C-14})$$

and,

$$\delta_L = (1 - \rho K_2 / K_1) + \rho K_2 / K_1 \delta_T \quad (C-15)$$

The Special Case of No Differential Wear —

For $\delta_L = \delta_T$, equation (C-14) implies,

$$K_1 = \rho K_2 \quad (C-16)$$

Notes —

$$2 F^* = \text{CanForce } S_L / k \quad (C-17)$$

Appendix D. Parameter Sensitivity Calculations

Two tables appear in this Appendix containing parameter sensitivity results for each of the 30 parameters defined in Table 1 of the report. The matrix of conditions include five lining friction coefficients of 0.3, 0.4, 0.5, 0.6, and 0.7, each at four air chamber force levels of 712.5, 1425, 2137.5, and 2850 lbs. Each table corresponds to plus and minus parameter variation amounts of 0.020.

The seven tabular columns refer to: 1) the parameter being varied, 2) lining friction level, 3) chamber force application, 4) size of parameter variation, 5) corresponding torque, 6) the percentage torque variation due to the particular parameter variation, and 7) the amount of differential lining wear between the leading and trailing shoes at equilibrium (negative values imply less wear on the leading shoe relative to the baseline 0.060 trailing shoe amount). *The differential lining wear indicated in the tables is measured relative to the cam-roller displacement location. The lining wear at the center of the shoes is about half this amount.*

Table D-1. Parameter Sensitivity Calculations for -0.020 Variations.

Parameter	μ Lining	Chamber Force (lbs)	Parameter Value	Variation	Torque (in-lbs)	% Torque Change	$\delta_L - \delta_T$ (in)
Baseline	.30	712.50	0.000	0.000	31151.7	0.00	.004
a	.30	712.50	12.750	-.020	31112.4	-.13	0.000
a'	.30	712.50	12.750	-.020	31171.2	.06	0.000
b	.30	712.50	1.250	-.020	31158.6	.02	.024
b'	.30	712.50	1.250	-.020	31144.7	-.02	-.015
c	.30	712.50	6.750	-.020	31200.7	.16	.009
c'	.30	712.50	6.750	-.020	31113.8	-.12	.009
d	.30	712.50	.410	-.020	31145.6	-.02	.024
d'	.30	712.50	.410	-.020	31150.4	0.00	-.015
dr	.30	712.50	.810	-.020	31112.4	-.13	-.016
dr'	.30	712.50	.810	-.020	31092.0	-.19	.024
dp	.30	712.50	.371	-.020	31210.6	.19	.004
dp'	.30	712.50	.371	-.020	31210.6	.19	.004
dpv	.30	712.50	.624	-.020	31155.4	.01	.004
dpv'	.30	712.50	.624	-.020	31155.4	.01	.004
r	.30	712.50	8.250	-.020	31078.1	-.24	.004
xc	.30	712.50	0.000	-.020	31163.9	.04	.044
yc	.30	712.50	6.000	-.020	31086.0	-.21	.014
Δx	.30	712.50	0.000	-.020	31726.3	1.84	-.015
Δy	.30	712.50	0.000	-.020	31137.4	-.05	.004
k	.30	712.50	.497	-.020	32505.2	4.35	.004
rc0	.30	712.50	.561	-.020	31126.4	-.08	.004
R _B	.30	712.50	.747	-.020	31171.0	.06	.004
S _L	.30	712.50	5.500	-.020	31022.9	-.41	.004
μ_B	.30	712.50	.100	-.020	31330.0	.57	.004

μ_R	.30	712.50	.200	-.020	31237.1	.27	.004
μ_R'	.30	712.50	.200	-.020	31237.1	.27	.004
μ_P	.30	712.50	.200	-.020	31163.3	.04	.004
μ_P'	.30	712.50	.200	-.020	31163.3	.04	.004
δ_T	.30	712.50	.060	-.020	31179.7	.09	.004
K	.30	712.50	2850.000	-285.000	31120.3	-.10	.004
Baseline	.40	712.50	0.000	0.000	41106.0	0.00	.004
a	.40	712.50	12.750	-.020	41085.4	-.05	-.001
a'	.40	712.50	12.750	-.020	41137.8	.08	0.000
b	.40	712.50	1.250	-.020	41122.3	.04	.024
b'	.40	712.50	1.250	-.020	41099.2	-.02	-.015
c	.40	712.50	6.750	-.020	41185.0	.19	.009
c'	.40	712.50	6.750	-.020	41120.3	.03	.010
d	.40	712.50	.410	-.020	41104.2	0.00	.024
d'	.40	712.50	.410	-.020	41109.9	.01	-.015
dr	.40	712.50	.810	-.020	41079.2	-.07	-.016
dr'	.40	712.50	.810	-.020	41097.7	-.02	.025
dp	.40	712.50	.371	-.020	41181.4	.18	.004
dp'	.40	712.50	.371	-.020	41181.4	.18	.004
dpv	.40	712.50	.624	-.020	41110.8	.01	.004
dpv'	.40	712.50	.624	-.020	41110.8	.01	.004
r	.40	712.50	8.250	-.020	41009.7	-.23	.004
xc	.40	712.50	0.000	-.020	41129.2	.06	.044
yc	.40	712.50	6.000	-.020	40995.6	-.27	.014
Δx	.40	712.50	0.000	-.020	42169.7	2.59	-.015
Δy	.40	712.50	0.000	-.020	41035.1	-.17	.004
k	.40	712.50	.497	-.020	42889.6	4.34	.004
rc0	.40	712.50	.561	-.020	41064.7	-.10	.004

Table D-1

R_B	.40	712.50	.747	-.020	41138.9	.08	.004
S_L	.40	712.50	5.500	-.020	40952.3	-.37	.004
μ_B	.40	712.50	.100	-.020	41403.1	.72	.004
μ_R	.40	712.50	.200	-.020	41295.2	.46	.004
μ_R'	.40	712.50	.200	-.020	41295.2	.46	.004
μ_P	.40	712.50	.200	-.020	41121.0	.04	.004
μ_P'	.40	712.50	.200	-.020	41121.0	.04	.004
δ_T	.40	712.50	.060	-.020	41147.9	.10	.004
K	.40	712.50	2850.000	-285.000	41147.4	.10	.005
Baseline	.50	712.50	0.000	0.000	50974.6	0.00	.004
a	.50	712.50	12.750	-.020	50928.1	-.09	-.001
a'	.50	712.50	12.750	-.020	51006.9	.06	-.001
b	.50	712.50	1.250	-.020	50986.8	.02	.024
b'	.50	712.50	1.250	-.020	50950.7	-.05	-.015
c	.50	712.50	6.750	-.020	51038.1	.12	.009
c'	.50	712.50	6.750	-.020	50889.1	-.17	.009
d	.50	712.50	.410	-.020	50962.8	-.02	.024
d'	.50	712.50	.410	-.020	50967.4	-.01	-.015
dr	.50	712.50	.810	-.020	50912.3	-.12	-.016
dr'	.50	712.50	.810	-.020	50866.1	-.21	.024
dp	.50	712.50	.371	-.020	51069.9	.19	.004
dp'	.50	712.50	.371	-.020	51069.9	.19	.004
dpv	.50	712.50	.624	-.020	50980.7	.01	.004
dpv'	.50	712.50	.624	-.020	50980.7	.01	.004
r	.50	712.50	8.250	-.020	50856.4	-.23	.004
xc	.50	712.50	0.000	-.020	50902.1	-.14	.043
yc	.50	712.50	6.000	-.020	50833.9	-.28	.014
Δx	.50	712.50	0.000	-.020	52422.2	2.84	-.015

Table D-1

Δy	.50	712.50	0.000	-.020	50824.1	-.30	.004
k	.50	712.50	.497	-.020	53180.1	4.33	.004
rc0	.50	712.50	.561	-.020	50915.9	-.12	.004
R_B	.50	712.50	.747	-.020	51026.4	.10	.004
S_L	.50	712.50	5.500	-.020	50764.9	-.41	.004
μ_B	.50	712.50	.100	-.020	51416.7	.87	.004
μ_R	.50	712.50	.200	-.020	51101.0	.25	.004
μ_R'	.50	712.50	.200	-.020	51101.0	.25	.004
μ_P	.50	712.50	.200	-.020	50993.5	.04	.004
μ_P'	.50	712.50	.200	-.020	50993.5	.04	.004
δ_T	.50	712.50	.060	-.020	51030.7	.11	.004
K	.50	712.50	2850.000	-285.000	50912.5	-.12	.005
Baseline	.60	712.50	0.000	0.000	60545.8	0.00	.004
a	.60	712.50	12.750	-.020	60524.1	-.04	-.001
a'	.60	712.50	12.750	-.020	60592.3	.08	-.001
b	.60	712.50	1.250	-.020	60569.7	.04	.024
b'	.60	712.50	1.250	-.020	60520.7	-.04	-.015
c	.60	712.50	6.750	-.020	60619.5	.12	.009
c'	.60	712.50	6.750	-.020	60410.6	-.22	.009
d	.60	712.50	.410	-.020	60540.0	-.01	.024
d'	.60	712.50	.410	-.020	60545.0	0.00	-.015
dr	.60	712.50	.810	-.020	60496.5	-.08	-.016
dr'	.60	712.50	.810	-.020	60411.5	-.22	.024
dp	.60	712.50	.371	-.020	60655.7	.18	.004
dp'	.60	712.50	.371	-.020	60655.7	.18	.004
dpv	.60	712.50	.624	-.020	60552.8	.01	.004
dpv'	.60	712.50	.624	-.020	60552.8	.01	.004
r	.60	712.50	8.250	-.020	60406.4	-.23	.004

Table D-1

xc	.60	712.50	0.000	-.020	60578.8	.05	.044
yc	.60	712.50	6.000	-.020	60364.3	-.30	.014
Δx	.60	712.50	0.000	-.020	62698.4	3.56	-.015
Δy	.60	712.50	0.000	-.020	60293.3	-.42	.004
k	.60	712.50	.497	-.020	63162.0	4.32	.004
rc0	.60	712.50	.561	-.020	60465.0	-.13	.004
R _B	.60	712.50	.747	-.020	60617.2	.12	.004
S _L	.60	712.50	5.500	-.020	60292.6	-.42	.004
μ_B	.60	712.50	.100	-.020	61155.1	1.01	.004
μ_R	.60	712.50	.200	-.020	60819.8	.45	.004
μ_R'	.60	712.50	.200	-.020	60819.8	.45	.004
μ_P	.60	712.50	.200	-.020	60567.6	.04	.004
μ_P'	.60	712.50	.200	-.020	60567.6	.04	.004
δ_T	.60	712.50	.060	-.020	60619.3	.12	.004
K	.60	712.50	2850.000	-285.000	60487.1	-.10	.004
Baseline	.70	712.50	0.000	0.000	69919.9	0.00	.004
a	.70	712.50	12.750	-.020	69904.2	-.02	-.001
a'	.70	712.50	12.750	-.020	70129.8	.30	-.001
b	.70	712.50	1.250	-.020	70102.5	.26	.024
b'	.70	712.50	1.250	-.020	69898.1	-.03	-.016
c	.70	712.50	6.750	-.020	70149.6	.33	.009
c'	.70	712.50	6.750	-.020	69935.8	.02	.009
d	.70	712.50	.410	-.020	69924.7	.01	.023
d'	.70	712.50	.410	-.020	69931.1	.02	-.016
dr	.70	712.50	.810	-.020	69862.4	-.08	-.016
dr'	.70	712.50	.810	-.020	69921.0	0.00	.024
dp	.70	712.50	.371	-.020	70213.3	.42	.004
dp'	.70	712.50	.371	-.020	70213.3	.42	.004

Table D-1

dpv	.70	712.50	.624	-.020	69927.7	.01	.004
dpv'	.70	712.50	.624	-.020	69927.7	.01	.004
r	.70	712.50	8.250	-.020	69760.1	-.23	.004
xc	.70	712.50	0.000	-.020	69971.0	.07	.043
yc	.70	712.50	6.000	-.020	69847.2	-.10	.014
Δx	.70	712.50	0.000	-.020	72928.6	4.30	-.015
Δy	.70	712.50	0.000	-.020	69537.7	-.55	.004
k	.70	712.50	.497	-.020	72937.1	4.32	.004
rc0	.70	712.50	.561	-.020	69979.9	.09	.004
R _B	.70	712.50	.747	-.020	70181.8	.37	.004
S _L	.70	712.50	5.500	-.020	69796.4	-.18	.004
μ_B	.70	712.50	.100	-.020	70892.1	1.39	.004
μ_R	.70	712.50	.200	-.020	70228.6	.44	.004
μ_R'	.70	712.50	.200	-.020	70228.6	.44	.004
μ_P	.70	712.50	.200	-.020	69944.2	.03	.004
μ_P'	.70	712.50	.200	-.020	69944.2	.03	.004
δ_T	.70	712.50	.060	-.020	70013.1	.13	.004
K	.70	712.50	2850.000	-285.000	70020.4	.14	.005
Baseline	.30	1425.00	0.000	0.000	62372.9	0.00	.009
a	.30	1425.00	12.750	-.020	62290.6	-.13	.004
a'	.30	1425.00	12.750	-.020	62364.1	-.01	.004
b	.30	1425.00	1.250	-.020	62361.4	-.02	.028
b'	.30	1425.00	1.250	-.020	62324.5	-.08	-.011
c	.30	1425.00	6.750	-.020	62433.3	.10	.014
c'	.30	1425.00	6.750	-.020	62312.6	-.10	.014
d	.30	1425.00	.410	-.020	62337.0	-.06	.028
d'	.30	1425.00	.410	-.020	62336.0	-.06	-.011
dr	.30	1425.00	.810	-.020	62206.6	-.27	-.012

Table D-1

dr'	.30	1425.00	.810	-.020	62268.0	-.17	.029
dp	.30	1425.00	.371	-.020	62472.2	.16	.009
dp'	.30	1425.00	.371	-.020	62472.2	.16	.009
dpv	.30	1425.00	.624	-.020	62379.2	.01	.009
dpv'	.30	1425.00	.624	-.020	62379.2	.01	.009
r	.30	1425.00	8.250	-.020	62225.0	-.24	.009
xc	.30	1425.00	0.000	-.020	62300.2	-.12	.048
yc	.30	1425.00	6.000	-.020	62254.5	-.19	.019
Δx	.30	1425.00	0.000	-.020	63508.2	1.82	-.011
Δy	.30	1425.00	0.000	-.020	62359.4	-.02	.009
k	.30	1425.00	.497	-.020	65009.9	4.23	.008
rc0	.30	1425.00	.561	-.020	62327.6	-.07	.009
R _B	.30	1425.00	.747	-.020	62405.8	.05	.009
S _L	.30	1425.00	5.500	-.020	62082.9	-.46	.009
μ_B	.30	1425.00	.100	-.020	62640.2	.43	.008
μ_R	.30	1425.00	.200	-.020	62546.9	.28	.009
μ_R'	.30	1425.00	.200	-.020	62546.9	.28	.009
μ_P	.30	1425.00	.200	-.020	62392.7	.03	.009
μ_P'	.30	1425.00	.200	-.020	62392.7	.03	.009
δ_T	.30	1425.00	.060	-.020	62400.0	.04	.009
K	.30	1425.00	2850.000	-285.000	62339.9	-.05	.010
Baseline	.40	1425.00	0.000	0.000	82262.4	0.00	.008
a	.40	1425.00	12.750	-.020	82201.0	-.07	.003
a'	.40	1425.00	12.750	-.020	82402.5	.17	.004
b	.40	1425.00	1.250	-.020	82402.1	.17	.028
b'	.40	1425.00	1.250	-.020	82340.8	.10	-.011
c	.40	1425.00	6.750	-.020	82484.9	.27	.013
c'	.40	1425.00	6.750	-.020	82319.6	.07	.013

Table D-1

d	.40	1425.00	.410	-.020	82247.9	-.02	.028
d'	.40	1425.00	.410	-.020	82361.6	.12	-.011
dr	.40	1425.00	.810	-.020	82187.0	-.09	-.012
dr'	.40	1425.00	.810	-.020	82270.3	.01	.029
dp	.40	1425.00	.371	-.020	82558.1	.36	.009
dp'	.40	1425.00	.371	-.020	82558.1	.36	.009
dpv	.40	1425.00	.624	-.020	82270.0	.01	.008
dpv'	.40	1425.00	.624	-.020	82270.0	.01	.008
r	.40	1425.00	8.250	-.020	82068.4	-.24	.008
xc	.40	1425.00	0.000	-.020	82313.6	.06	.048
yc	.40	1425.00	6.000	-.020	82237.6	-.03	.019
Δx	.40	1425.00	0.000	-.020	84307.2	2.49	-.011
Δy	.40	1425.00	0.000	-.020	82134.4	-.16	.009
k	.40	1425.00	.497	-.020	85861.1	4.37	.008
rc0	.40	1425.00	.561	-.020	82189.5	-.09	.008
R _B	.40	1425.00	.747	-.020	82484.1	.27	.009
S _L	.40	1425.00	5.500	-.020	82046.3	-.26	.009
μ_B	.40	1425.00	.100	-.020	82870.8	.74	.008
μ_R	.40	1425.00	.200	-.020	82656.4	.48	.009
μ_R'	.40	1425.00	.200	-.020	82656.4	.48	.009
μ_P	.40	1425.00	.200	-.020	82452.5	.23	.009
μ_P'	.40	1425.00	.200	-.020	82452.5	.23	.009
δ_T	.40	1425.00	.060	-.020	82471.4	.25	.009
K	.40	1425.00	2850.000	-285.000	82407.9	.18	.010
Baseline	.50	1425.00	0.000	0.000	101913.7	0.00	.008
a	.50	1425.00	12.750	-.020	101834.9	-.08	.003
a'	.50	1425.00	12.750	-.020	102090.5	.17	.004
b	.50	1425.00	1.250	-.020	101925.7	.01	.028

Table D-1

b'	.50	1425.00	1.250	-.020	101843.8	-.07	-.011
c	.50	1425.00	6.750	-.020	102230.0	.31	.013
c'	.50	1425.00	6.750	-.020	101959.8	.05	.013
d	.50	1425.00	.410	-.020	101880.3	-.03	.028
d'	.50	1425.00	.410	-.020	102025.1	.11	-.011
dr	.50	1425.00	.810	-.020	101804.5	-.11	-.012
dr'	.50	1425.00	.810	-.020	101920.2	.01	.029
dp	.50	1425.00	.371	-.020	102286.5	.37	.009
dp'	.50	1425.00	.371	-.020	102286.5	.37	.009
dpv	.50	1425.00	.624	-.020	101923.2	.01	.008
dpv'	.50	1425.00	.624	-.020	101923.2	.01	.008
r	.50	1425.00	8.250	-.020	101675.1	-.23	.008
xc	.50	1425.00	0.000	-.020	101964.7	.05	.048
yc	.50	1425.00	6.000	-.020	101851.6	-.06	.019
Δx	.50	1425.00	0.000	-.020	105117.9	3.14	-.011
Δy	.50	1425.00	0.000	-.020	101627.9	-.28	.009
k	.50	1425.00	.497	-.020	106373.9	4.38	.008
rc0	.50	1425.00	.561	-.020	101809.7	-.10	.008
R _B	.50	1425.00	.747	-.020	101994.2	.08	.009
S _L	.50	1425.00	5.500	-.020	101655.2	-.25	.009
μ_B	.50	1425.00	.100	-.020	102783.9	.85	.008
μ_R	.50	1425.00	.200	-.020	102407.1	.48	.009
μ_R'	.50	1425.00	.200	-.020	102407.1	.48	.009
μ_P	.50	1425.00	.200	-.020	101943.2	.03	.008
μ_P'	.50	1425.00	.200	-.020	101943.2	.03	.008
δ_T	.50	1425.00	.060	-.020	102189.9	.27	.009
K	.50	1425.00	2850.000	-285.000	101916.3	0.00	.009
Baseline	.60	1425.00	0.000	0.000	121181.8	0.00	.008

Table D-1

a	.60	1425.00	12.750	-.020	121118.4	-.05	.003
a'	.60	1425.00	12.750	-.020	121483.3	.25	.004
b	.60	1425.00	1.250	-.020	121214.6	.03	.028
b'	.60	1425.00	1.250	-.020	121064.3	-.10	-.012
c	.60	1425.00	6.750	-.020	121571.1	.32	.013
c'	.60	1425.00	6.750	-.020	121241.2	.05	.013
d	.60	1425.00	.410	-.020	121157.5	-.02	.028
d'	.60	1425.00	.410	-.020	121113.6	-.06	-.012
dr	.60	1425.00	.810	-.020	121066.9	-.09	-.012
dr'	.60	1425.00	.810	-.020	120963.2	-.18	.028
dp	.60	1425.00	.371	-.020	121387.8	.17	.009
dp'	.60	1425.00	.371	-.020	121387.8	.17	.009
dpv	.60	1425.00	.624	-.020	121192.9	.01	.008
dpv'	.60	1425.00	.624	-.020	121192.9	.01	.008
r	.60	1425.00	8.250	-.020	120899.7	-.23	.008
xc	.60	1425.00	0.000	-.020	121261.2	.07	.048
yc	.60	1425.00	6.000	-.020	121104.8	-.06	.018
Δx	.60	1425.00	0.000	-.020	125814.9	3.82	-.011
Δy	.60	1425.00	0.000	-.020	120703.5	-.39	.008
k	.60	1425.00	.497	-.020	126519.5	4.40	.008
rc0	.60	1425.00	.561	-.020	121042.0	-.12	.008
R _B	.60	1425.00	.747	-.020	121327.5	.12	.008
S _L	.60	1425.00	5.500	-.020	120916.3	-.22	.009
μ_B	.60	1425.00	.100	-.020	122664.0	1.22	.009
μ_R	.60	1425.00	.200	-.020	121805.8	.51	.008
μ_R'	.60	1425.00	.200	-.020	121805.8	.51	.008
μ_P	.60	1425.00	.200	-.020	121248.1	.05	.008
μ_P'	.60	1425.00	.200	-.020	121248.1	.05	.008

Table D-1

δ_T	.60	1425.00	.060	-.020	121294.7	.09	.009
K	.60	1425.00	2850.000	-285.000	121225.0	.04	.009
Baseline	.70	1425.00	0.000	0.000	140145.1	0.00	.008
a	.70	1425.00	12.750	-.020	140058.7	-.06	.003
a'	.70	1425.00	12.750	-.020	140473.8	.23	.004
b	.70	1425.00	1.250	-.020	140156.5	.01	.028
b'	.70	1425.00	1.250	-.020	139972.8	-.12	-.011
c	.70	1425.00	6.750	-.020	140228.9	.06	.013
c'	.70	1425.00	6.750	-.020	140171.8	.02	.013
d	.70	1425.00	.410	-.020	140087.0	-.04	.028
d'	.70	1425.00	.410	-.020	140039.0	-.08	-.012
dr	.70	1425.00	.810	-.020	139981.8	-.12	-.012
dr'	.70	1425.00	.810	-.020	139860.3	-.20	.028
dp	.70	1425.00	.371	-.020	140368.8	.16	.008
dp'	.70	1425.00	.371	-.020	140368.8	.16	.008
dpv	.70	1425.00	.624	-.020	140158.0	.01	.008
dpv'	.70	1425.00	.624	-.020	140158.0	.01	.008
r	.70	1425.00	8.250	-.020	139821.2	-.23	.008
xc	.70	1425.00	0.000	-.020	140210.6	.05	.048
yc	.70	1425.00	6.000	-.020	139748.0	-.28	.018
Δx	.70	1425.00	0.000	-.020	146050.5	4.21	-.011
Δy	.70	1425.00	0.000	-.020	139425.4	-.51	.008
k	.70	1425.00	.497	-.020	146304.7	4.40	.008
rc0	.70	1425.00	.561	-.020	139964.4	-.13	.008
R_B	.70	1425.00	.747	-.020	140320.6	.13	.008
S_L	.70	1425.00	5.500	-.020	139836.4	-.22	.008
μ_B	.70	1425.00	.100	-.020	142026.8	1.34	.008
μ_R	.70	1425.00	.200	-.020	140859.4	.51	.008

Table D-1

μ_R'	.70	1425.00	.200	-.020	140859.4	.51	.008
μ_P	.70	1425.00	.200	-.020	140185.4	.03	.008
μ_P'	.70	1425.00	.200	-.020	140185.4	.03	.008
δ_T	.70	1425.00	.060	-.020	140252.9	.08	.008
K	.70	1425.00	2850.000	-285.000	140238.0	.07	.009
Baseline	.30	2137.50	0.000	0.000	93541.1	0.00	.013
a	.30	2137.50	12.750	-.020	93427.1	-.12	.008
a'	.30	2137.50	12.750	-.020	93605.3	.07	.008
b	.30	2137.50	1.250	-.020	93507.8	-.04	.032
b'	.30	2137.50	1.250	-.020	93570.4	.03	-.006
c	.30	2137.50	6.750	-.020	93757.8	.23	.018
c'	.30	2137.50	6.750	-.020	93589.8	.05	.018
d	.30	2137.50	.410	-.020	93470.8	-.08	.032
d'	.30	2137.50	.410	-.020	93566.0	.03	-.006
dr	.30	2137.50	.810	-.020	93444.0	-.10	-.007
dr'	.30	2137.50	.810	-.020	93372.4	-.18	.033
dp	.30	2137.50	.371	-.020	93834.5	.31	.013
dp'	.30	2137.50	.371	-.020	93834.5	.31	.013
dpv	.30	2137.50	.624	-.020	93548.1	.01	.013
dpv'	.30	2137.50	.624	-.020	93548.1	.01	.013
r	.30	2137.50	8.250	-.020	93318.1	-.24	.013
xc	.30	2137.50	0.000	-.020	93548.4	.01	.053
yc	.30	2137.50	6.000	-.020	93396.9	-.15	.023
Δx	.30	2137.50	0.000	-.020	95431.3	2.02	-.006
Δy	.30	2137.50	0.000	-.020	93508.9	-.03	.013
k	.30	2137.50	.497	-.020	97688.7	4.43	.012
rc0	.30	2137.50	.561	-.020	93480.7	-.06	.013
R_B	.30	2137.50	.747	-.020	93576.8	.04	.013

Table D-1

S_L	.30	2137.50	5.500	-.020	93231.8	-.33	.013
μ_B	.30	2137.50	.100	-.020	94101.7	.60	.013
μ_R	.30	2137.50	.200	-.020	94028.1	.52	.013
μ_R'	.30	2137.50	.200	-.020	94028.1	.52	.013
μ_P	.30	2137.50	.200	-.020	93562.7	.02	.013
μ_P'	.30	2137.50	.200	-.020	93562.7	.02	.013
δ_T	.30	2137.50	.060	-.020	93711.4	.18	.013
K	.30	2137.50	2850.000	-285.000	93559.3	.02	.014
Baseline	.40	2137.50	0.000	0.000	123740.4	0.00	.013
a	.40	2137.50	12.750	-.020	123517.6	-.18	.008
a'	.40	2137.50	12.750	-.020	123806.3	.05	.009
b	.40	2137.50	1.250	-.020	123676.4	-.05	.033
b'	.40	2137.50	1.250	-.020	123505.9	-.19	-.007
c	.40	2137.50	6.750	-.020	123751.8	.01	.017
c'	.40	2137.50	6.750	-.020	123569.1	-.14	.018
d	.40	2137.50	.410	-.020	123624.9	-.09	.033
d'	.40	2137.50	.410	-.020	123541.2	-.16	-.007
dr	.40	2137.50	.810	-.020	123598.2	-.11	-.007
dr'	.40	2137.50	.810	-.020	123471.7	-.22	.033
dp	.40	2137.50	.371	-.020	123896.5	.13	.013
dp'	.40	2137.50	.371	-.020	123896.5	.13	.013
dpv	.40	2137.50	.624	-.020	123750.6	.01	.013
dpv'	.40	2137.50	.624	-.020	123750.6	.01	.013
r	.40	2137.50	8.250	-.020	123447.6	-.24	.013
xc	.40	2137.50	0.000	-.020	123573.0	-.14	.052
yc	.40	2137.50	6.000	-.020	123440.7	-.24	.023
Δx	.40	2137.50	0.000	-.020	126872.0	2.53	-.006
Δy	.40	2137.50	0.000	-.020	123538.5	-.16	.013

Table D-1

k	.40	2137.50	.497	-.020	128979.8	4.23	.013
rc0	.40	2137.50	.561	-.020	123645.5	-.08	.013
R _B	.40	2137.50	.747	-.020	123810.1	.06	.013
S _L	.40	2137.50	5.500	-.020	123094.5	-.52	.013
μ _B	.40	2137.50	.100	-.020	124414.3	.54	.013
μ _R	.40	2137.50	.200	-.020	124150.3	.33	.013
μ _R '	.40	2137.50	.200	-.020	124150.3	.33	.013
μ _P	.40	2137.50	.200	-.020	123772.3	.03	.013
μ _P '	.40	2137.50	.200	-.020	123772.3	.03	.013
δ _T	.40	2137.50	.060	-.020	123749.2	.01	.013
K	.40	2137.50	2850.000	-285.000	123559.2	-.15	.014
Baseline	.50	2137.50	0.000	0.000	153175.2	0.00	.012
a	.50	2137.50	12.750	-.020	152980.0	-.13	.008
a'	.50	2137.50	12.750	-.020	153349.6	.11	.008
b	.50	2137.50	1.250	-.020	153068.2	-.07	.032
b'	.50	2137.50	1.250	-.020	153200.5	.02	-.007
c	.50	2137.50	6.750	-.020	153509.8	.22	.018
c'	.50	2137.50	6.750	-.020	152958.9	-.14	.018
d	.50	2137.50	.410	-.020	153026.4	-.10	.032
d'	.50	2137.50	.410	-.020	153256.5	.05	-.007
dr	.50	2137.50	.810	-.020	152931.2	-.16	-.008
dr'	.50	2137.50	.810	-.020	152835.4	-.22	.033
dp	.50	2137.50	.371	-.020	153408.4	.15	.013
dp'	.50	2137.50	.371	-.020	153408.4	.15	.013
dpv	.50	2137.50	.624	-.020	153187.0	.01	.012
dpv'	.50	2137.50	.624	-.020	153187.0	.01	.012
r	.50	2137.50	8.250	-.020	152814.2	-.24	.012
xc	.50	2137.50	0.000	-.020	153311.5	.09	.053

Table D-1

yc	.50	2137.50	6.000	-.020	152821.9	-.23	.022
Δx	.50	2137.50	0.000	-.020	158009.5	3.16	-.006
Δy	.50	2137.50	0.000	-.020	152723.4	-.29	.013
k	.50	2137.50	.497	-.020	159694.3	4.26	.012
rc0	.50	2137.50	.561	-.020	153041.2	-.09	.012
R_B	.50	2137.50	.747	-.020	153273.7	.06	.013
S_L	.50	2137.50	5.500	-.020	152748.5	-.28	.013
μ_B	.50	2137.50	.100	-.020	154468.0	.84	.013
μ_R	.50	2137.50	.200	-.020	153664.4	.32	.013
μ_R'	.50	2137.50	.200	-.020	153664.4	.32	.013
μ_P	.50	2137.50	.200	-.020	153211.7	.02	.012
μ_P'	.50	2137.50	.200	-.020	153211.7	.02	.012
δ_T	.50	2137.50	.060	-.020	153188.5	.01	.013
K	.50	2137.50	2850.000	-285.000	153063.4	-.07	.014
Baseline	.60	2137.50	0.000	0.000	182008.5	0.00	.013
a	.60	2137.50	12.750	-.020	182211.7	.11	.008
a'	.60	2137.50	12.750	-.020	182485.1	.26	.008
b	.60	2137.50	1.250	-.020	182305.3	.16	.032
b'	.60	2137.50	1.250	-.020	182148.3	.08	-.007
c	.60	2137.50	6.750	-.020	182504.5	.27	.017
c'	.60	2137.50	6.750	-.020	182031.4	.01	.018
d	.60	2137.50	.410	-.020	182255.6	.14	.032
d'	.60	2137.50	.410	-.020	182021.0	.01	-.007
dr	.60	2137.50	.810	-.020	182149.3	.08	-.008
dr'	.60	2137.50	.810	-.020	182119.6	.06	.033
dp	.60	2137.50	.371	-.020	182690.0	.37	.012
dp'	.60	2137.50	.371	-.020	182690.0	.37	.012
dpv	.60	2137.50	.624	-.020	182069.1	.03	.013

Table D-1

dpv'	.60	2137.50	.624	-.020	182069.1	.03	.013
r	.60	2137.50	8.250	-.020	181628.7	-.21	.013
xc	.60	2137.50	0.000	-.020	181983.9	-.01	.052
yc	.60	2137.50	6.000	-.020	181587.3	-.23	.022
Δx	.60	2137.50	0.000	-.020	188871.7	3.77	-.006
Δy	.60	2137.50	0.000	-.020	181235.9	-.42	.013
k	.60	2137.50	.497	-.020	190078.4	4.43	.012
rc0	.60	2137.50	.561	-.020	181833.8	-.10	.013
R _B	.60	2137.50	.747	-.020	182607.9	.33	.013
S _L	.60	2137.50	5.500	-.020	181523.9	-.27	.012
μ_B	.60	2137.50	.100	-.020	184185.6	1.20	.012
μ_R	.60	2137.50	.200	-.020	183049.5	.57	.013
μ_R'	.60	2137.50	.200	-.020	183049.5	.57	.013
μ_P	.60	2137.50	.200	-.020	182096.1	.05	.013
μ_P'	.60	2137.50	.200	-.020	182096.1	.05	.013
δ_T	.60	2137.50	.060	-.020	182510.7	.28	.013
K	.60	2137.50	2850.000	-285.000	182365.3	.20	.014
Baseline	.70	2137.50	0.000	0.000	210809.0	0.00	.012
a	.70	2137.50	12.750	-.020	210396.3	-.20	.008
a'	.70	2137.50	12.750	-.020	210907.2	.05	.008
b	.70	2137.50	1.250	-.020	210479.5	-.16	.032
b'	.70	2137.50	1.250	-.020	210706.9	-.05	-.007
c	.70	2137.50	6.750	-.020	211119.7	.15	.017
c'	.70	2137.50	6.750	-.020	210313.1	-.24	.017
d	.70	2137.50	.410	-.020	210423.9	-.18	.032
d'	.70	2137.50	.410	-.020	210812.6	0.00	-.007
dr	.70	2137.50	.810	-.020	210487.4	-.15	-.008
dr'	.70	2137.50	.810	-.020	210180.1	-.30	.033

Table D-1

dp	.70	2137.50	.371	-.020	211065.0	.12	.013
dp'	.70	2137.50	.371	-.020	211065.0	.12	.013
dpv	.70	2137.50	.624	-.020	210825.9	.01	.012
dpv'	.70	2137.50	.624	-.020	210825.9	.01	.012
r	.70	2137.50	8.250	-.020	210318.6	-.23	.012
xc	.70	2137.50	0.000	-.020	210850.5	.02	.052
yc	.70	2137.50	6.000	-.020	210106.5	-.33	.023
Δx	.70	2137.50	0.000	-.020	219812.1	4.27	-.006
Δy	.70	2137.50	0.000	-.020	209651.1	-.55	.012
k	.70	2137.50	.497	-.020	219578.7	4.16	.012
rc0	.70	2137.50	.561	-.020	210571.9	-.11	.012
R _B	.70	2137.50	.747	-.020	211005.3	.09	.013
S _L	.70	2137.50	5.500	-.020	209702.8	-.52	.013
μ_B	.70	2137.50	.100	-.020	213006.8	1.04	.013
μ_R	.70	2137.50	.200	-.020	211477.4	.32	.013
μ_R'	.70	2137.50	.200	-.020	211477.4	.32	.013
μ_P	.70	2137.50	.200	-.020	210861.4	.02	.012
μ_P'	.70	2137.50	.200	-.020	210861.4	.02	.012
δ_T	.70	2137.50	.060	-.020	210882.4	.03	.013
K	.70	2137.50	2850.000	-285.000	210788.0	-.01	.014
Baseline	.30	2850.00	0.000	0.000	124929.5	0.00	.017
a	.30	2850.00	12.750	-.020	124649.7	-.22	.013
a'	.30	2850.00	12.750	-.020	124970.3	.03	.013
b	.30	2850.00	1.250	-.020	124768.9	-.13	.037
b'	.30	2850.00	1.250	-.020	124884.3	-.04	-.002
c	.30	2850.00	6.750	-.020	125191.5	.21	.022
c'	.30	2850.00	6.750	-.020	124779.6	-.12	.022
d	.30	2850.00	.410	-.020	124718.7	-.17	.037

Table D-1

d'	.30	2850.00	.410	-.020	124916.8	-.01	-.002
dr	.30	2850.00	.810	-.020	124626.5	-.24	-.003
dr'	.30	2850.00	.810	-.020	124783.1	-.12	.038
dp	.30	2850.00	.371	-.020	125109.5	.14	.018
dp'	.30	2850.00	.371	-.020	125109.5	.14	.018
dpv	.30	2850.00	.624	-.020	124937.1	.01	.017
dpv'	.30	2850.00	.624	-.020	124937.1	.01	.017
r	.30	2850.00	8.250	-.020	124630.6	-.24	.017
xc	.30	2850.00	0.000	-.020	124958.7	.02	.057
yc	.30	2850.00	6.000	-.020	124673.1	-.21	.027
Δx	.30	2850.00	0.000	-.020	127364.4	1.95	-.002
Δy	.30	2850.00	0.000	-.020	124922.5	-.01	.017
k	.30	2850.00	.497	-.020	130278.8	4.28	.017
rc0	.30	2850.00	.561	-.020	124860.1	-.06	.017
R _B	.30	2850.00	.747	-.020	124967.6	.03	.018
S _L	.30	2850.00	5.500	-.020	124514.7	-.33	.017
μ_B	.30	2850.00	.100	-.020	125480.1	.44	.017
μ_R	.30	2850.00	.200	-.020	125414.4	.39	.017
μ_R'	.30	2850.00	.200	-.020	125414.4	.39	.017
μ_P	.30	2850.00	.200	-.020	124952.8	.02	.017
μ_P'	.30	2850.00	.200	-.020	124952.8	.02	.017
δ_T	.30	2850.00	.060	-.020	124856.9	-.06	.018
K	.30	2850.00	2850.000	-285.000	124866.3	-.05	.019
Baseline	.40	2850.00	0.000	0.000	165197.3	0.00	.017
a	.40	2850.00	12.750	-.020	164929.4	-.16	.013
a'	.40	2850.00	12.750	-.020	165172.6	-.01	.013
b	.40	2850.00	1.250	-.020	164950.1	-.15	.037
b'	.40	2850.00	1.250	-.020	165015.6	-.11	-.002

Table D-1

c	.40	2850.00	6.750	-.020	165410.7	.13	.022
c'	.40	2850.00	6.750	-.020	164860.2	-.20	.022
d	.40	2850.00	.410	-.020	165055.8	-.09	.037
d'	.40	2850.00	.410	-.020	165071.3	-.08	-.002
dr	.40	2850.00	.810	-.020	164926.4	-.16	-.003
dr'	.40	2850.00	.810	-.020	164930.9	-.16	.037
dp	.40	2850.00	.371	-.020	165354.9	.10	.017
dp'	.40	2850.00	.371	-.020	165354.9	.10	.017
dpv	.40	2850.00	.624	-.020	165208.2	.01	.017
dpv'	.40	2850.00	.624	-.020	165208.2	.01	.017
r	.40	2850.00	8.250	-.020	164804.4	-.24	.017
xc	.40	2850.00	0.000	-.020	165170.5	-.02	.057
yc	.40	2850.00	6.000	-.020	164530.1	-.40	.027
Δx	.40	2850.00	0.000	-.020	169448.8	2.57	-.002
Δy	.40	2850.00	0.000	-.020	164966.7	-.14	.017
k	.40	2850.00	.497	-.020	172248.8	4.27	.017
rc0	.40	2850.00	.561	-.020	164753.4	-.27	.017
R_B	.40	2850.00	.747	-.020	165270.1	.04	.017
S_L	.40	2850.00	5.500	-.020	164321.4	-.53	.017
μ_B	.40	2850.00	.100	-.020	166124.2	.56	.017
μ_R	.40	2850.00	.200	-.020	165834.3	.39	.017
μ_R'	.40	2850.00	.200	-.020	165834.3	.39	.017
μ_P	.40	2850.00	.200	-.020	165230.9	.02	.017
μ_P'	.40	2850.00	.200	-.020	165230.9	.02	.017
δ_T	.40	2850.00	.060	-.020	165135.8	-.04	.017
K	.40	2850.00	2850.000	-285.000	165236.8	.02	.019
Baseline	.50	2850.00	0.000	0.000	204360.7	0.00	.017
a	.50	2850.00	12.750	-.020	204391.2	.01	.012

Table D-1

a'	.50	2850.00	12.750	-.020	204605.4	.12	.012
b	.50	2850.00	1.250	-.020	204550.4	.09	.036
b'	.50	2850.00	1.250	-.020	204473.0	.05	-.002
c	.50	2850.00	6.750	-.020	204943.2	.29	.022
c'	.50	2850.00	6.750	-.020	204217.3	-.07	.022
d	.50	2850.00	.410	-.020	204466.7	.05	.037
d'	.50	2850.00	.410	-.020	204515.5	.08	-.002
dr	.50	2850.00	.810	-.020	204309.6	-.02	-.003
dr'	.50	2850.00	.810	-.020	204314.0	-.02	.037
dp	.50	2850.00	.371	-.020	204993.1	.31	.017
dp'	.50	2850.00	.371	-.020	204993.1	.31	.017
dpv	.50	2850.00	.624	-.020	204370.7	0.00	.017
dpv'	.50	2850.00	.624	-.020	204370.7	0.00	.017
r	.50	2850.00	8.250	-.020	203874.4	-.24	.017
xc	.50	2850.00	0.000	-.020	204626.0	.13	.057
yc	.50	2850.00	6.000	-.020	203779.1	-.28	.027
Δx	.50	2850.00	0.000	-.020	210761.7	3.13	-.002
Δy	.50	2850.00	0.000	-.020	203788.8	-.28	.017
k	.50	2850.00	.497	-.020	213054.7	4.25	.016
rc0	.50	2850.00	.561	-.020	204144.1	-.11	.017
R _B	.50	2850.00	.747	-.020	204901.7	.26	.017
S _L	.50	2850.00	5.500	-.020	203628.1	-.36	.017
μ_B	.50	2850.00	.100	-.020	206054.4	.83	.017
μ_R	.50	2850.00	.200	-.020	205133.2	.38	.017
μ_R'	.50	2850.00	.200	-.020	205133.2	.38	.017
μ_P	.50	2850.00	.200	-.020	204391.4	.02	.017
μ_P'	.50	2850.00	.200	-.020	204391.4	.02	.017
δ_T	.50	2850.00	.060	-.020	204743.1	.19	.017

Table D-1

K	.50	2850.00	2850.000	-285.000	204473.2	.06	.019
Baseline	.60	2850.00	0.000	0.000	243128.7	0.00	.017
a	.60	2850.00	12.750	-.020	243107.5	-.01	.012
a'	.60	2850.00	12.750	-.020	243573.1	.18	.012
b	.60	2850.00	1.250	-.020	243273.2	.06	.036
b'	.60	2850.00	1.250	-.020	242953.2	-.07	-.003
c	.60	2850.00	6.750	-.020	243423.5	.12	.021
c'	.60	2850.00	6.750	-.020	243208.7	.03	.022
d	.60	2850.00	.410	-.020	243172.0	.02	.037
d'	.60	2850.00	.410	-.020	243299.1	.07	-.003
dr	.60	2850.00	.810	-.020	242989.7	-.06	-.003
dr'	.60	2850.00	.810	-.020	242992.7	-.06	.037
dp	.60	2850.00	.371	-.020	243956.2	.34	.017
dp'	.60	2850.00	.371	-.020	243956.2	.34	.017
dpv	.60	2850.00	.624	-.020	243141.0	.01	.017
dpv'	.60	2850.00	.624	-.020	243141.0	.01	.017
r	.60	2850.00	8.250	-.020	242552.3	-.24	.017
xc	.60	2850.00	0.000	-.020	243144.5	.01	.056
yc	.60	2850.00	6.000	-.020	242312.1	-.34	.027
Δx	.60	2850.00	0.000	-.020	252501.3	3.85	-.002
Δy	.60	2850.00	0.000	-.020	242152.8	-.40	.017
k	.60	2850.00	.497	-.020	253442.6	4.24	.016
rc0	.60	2850.00	.561	-.020	242935.9	-.08	.017
R_B	.60	2850.00	.747	-.020	243312.3	.08	.017
S_L	.60	2850.00	5.500	-.020	242346.7	-.32	.017
μ_B	.60	2850.00	.100	-.020	245947.1	1.16	.017
μ_R	.60	2850.00	.200	-.020	244039.5	.37	.017
μ_R'	.60	2850.00	.200	-.020	244039.5	.37	.017

Table D-1

μ_P	.60	2850.00	.200	-.020	243166.4	.02	.017
μ_P'	.60	2850.00	.200	-.020	243166.4	.02	.017
δ_T	.60	2850.00	.060	-.020	243684.6	.23	.017
K	.60	2850.00	2850.000	-285.000	243411.0	.12	.019
Baseline	.70	2850.00	0.000	0.000	281306.6	0.00	.017
a	.70	2850.00	12.750	-.020	281138.4	-.06	.012
a'	.70	2850.00	12.750	-.020	281677.9	.13	.012
b	.70	2850.00	1.250	-.020	281305.1	0.00	.037
b'	.70	2850.00	1.250	-.020	280890.2	-.15	-.003
c	.70	2850.00	6.750	-.020	281443.9	.05	.021
c'	.70	2850.00	6.750	-.020	281224.1	-.03	.022
d	.70	2850.00	.410	-.020	281184.3	-.04	.037
d'	.70	2850.00	.410	-.020	281399.8	.03	-.003
dr	.70	2850.00	.810	-.020	280979.6	-.12	-.004
dr'	.70	2850.00	.810	-.020	280979.6	-.12	.037
dp	.70	2850.00	.371	-.020	281566.1	.09	.017
dp'	.70	2850.00	.371	-.020	281566.1	.09	.017
dpv	.70	2850.00	.624	-.020	281321.9	.01	.017
dpv'	.70	2850.00	.624	-.020	281321.9	.01	.017
r	.70	2850.00	8.250	-.020	280643.3	-.24	.017
xc	.70	2850.00	0.000	-.020	281130.2	-.06	.056
yc	.70	2850.00	6.000	-.020	280142.1	-.41	.026
Δx	.70	2850.00	0.000	-.020	293474.6	4.33	-.002
Δy	.70	2850.00	0.000	-.020	279822.2	-.53	.017
k	.70	2850.00	.497	-.020	293203.9	4.23	.016
rc0	.70	2850.00	.561	-.020	281053.2	-.09	.017
R _B	.70	2850.00	.747	-.020	281520.4	.08	.017
S _L	.70	2850.00	5.500	-.020	280402.8	-.32	.017

Table D-1

μ_B	.70	2850.00	.100	-.020	284770.1	1.23	.017
μ_R	.70	2850.00	.200	-.020	282213.5	.32	.017
μ_R'	.70	2850.00	.200	-.020	282213.5	.32	.017
μ_P	.70	2850.00	.200	-.020	281353.5	.02	.017
μ_P'	.70	2850.00	.200	-.020	281353.5	.02	.017
δ_T	.70	2850.00	.060	-.020	281279.9	-.01	.017
K	.70	2850.00	2850.000	-285.000	281103.6	-.07	.018

Table D-1

Table D-2. Parameter Sensitivity Calculations for +0.020 Variations.

Parameter	μ Lining	Chamber Force (lbs)	Parameter Value	Variation	Torque (in-lbs)	% Torque Change	$\delta_L - \delta_T$ (in)
Baseline	.30	712.50	0.000	0.000	31151.7	0.00	.004
a	.30	712.50	12.750	.020	31179.4	.09	.009
a'	.30	712.50	12.750	.020	31101.3	-.16	.009
b	.30	712.50	1.250	.020	31145.6	-.02	-.015
b'	.30	712.50	1.250	.020	31164.6	.04	.024
c	.30	712.50	6.750	.020	31091.1	-.19	0.000
c'	.30	712.50	6.750	.020	31158.6	.02	0.000
d	.30	712.50	.410	.020	31158.7	.02	-.015
d'	.30	712.50	.410	.020	31159.1	.02	.024
dr	.30	712.50	.810	.020	31175.4	.08	.025
dr'	.30	712.50	.810	.020	31170.3	.06	-.016
dp	.30	712.50	.371	.020	31092.6	-.19	.004
dp'	.30	712.50	.371	.020	31092.6	-.19	.004
dpv	.30	712.50	.624	.020	31147.9	-.01	.004
dpv'	.30	712.50	.624	.020	31147.9	-.01	.004
r	.30	712.50	8.250	.020	31225.2	.24	.004
xc	.30	712.50	0.000	.020	31147.9	-.01	-.035
yc	.30	712.50	6.000	.020	31175.9	.08	-.006
Δx	.30	712.50	0.000	.020	30619.3	-1.71	.024
Δy	.30	712.50	0.000	.020	32041.9	2.86	.004
k	.30	712.50	.497	.020	29867.8	-4.12	.005
rc0	.30	712.50	.561	.020	31176.0	.08	.004
R _B	.30	712.50	.747	.020	31132.3	-.06	.004
S _L	.30	712.50	5.500	.020	31222.5	.23	.004
μ_B	.30	712.50	.100	.020	30974.3	-.57	.004

μ_R	.30	712.50	.200	.020	31009.1	-.46	.004
μ_R'	.30	712.50	.200	.020	31009.1	-.46	.004
μ_P	.30	712.50	.200	.020	31140.0	-.04	.004
μ_P'	.30	712.50	.200	.020	31140.0	-.04	.004
δ_T	.30	712.50	.060	.020	31143.2	-.03	.004
K	.30	712.50	2850.000	285.000	31109.7	-.13	.004
Baseline	.40	712.50	0.000	0.000	41106.0	0.00	.004
a	.40	712.50	12.750	.020	41140.0	.08	.009
a'	.40	712.50	12.750	.020	41106.4	0.00	.010
b	.40	712.50	1.250	.020	41100.0	-.01	-.015
b'	.40	712.50	1.250	.020	41131.7	.06	.024
c	.40	712.50	6.750	.020	41055.5	-.12	-.001
c'	.40	712.50	6.750	.020	41124.3	.04	0.000
d	.40	712.50	.410	.020	41118.1	.03	-.015
d'	.40	712.50	.410	.020	41121.4	.04	.024
dr	.40	712.50	.810	.020	41157.5	.13	.024
dr'	.40	712.50	.810	.020	41133.4	.07	-.016
dp	.40	712.50	.371	.020	41030.4	-.18	.004
dp'	.40	712.50	.371	.020	41030.4	-.18	.004
dpv	.40	712.50	.624	.020	41101.2	-.01	.004
dpv'	.40	712.50	.624	.020	41101.2	-.01	.004
r	.40	712.50	8.250	.020	41202.3	.23	.004
xc	.40	712.50	0.000	.020	41104.7	0.00	-.035
yc	.40	712.50	6.000	.020	41170.7	.16	-.006
Δx	.40	712.50	0.000	.020	40212.2	-2.17	.024
Δy	.40	712.50	0.000	.020	42331.1	2.98	.004
k	.40	712.50	.497	.020	39489.5	-3.93	.004
rc0	.40	712.50	.561	.020	41146.0	.10	.004

Table D-2

R _B	.40	712.50	.747	.020	41073.1	-.08	.004
S _L	.40	712.50	5.500	.020	41277.3	.42	.004
μ _B	.40	712.50	.100	.020	40812.3	-.71	.004
μ _R	.40	712.50	.200	.020	40935.1	-.42	.004
μ _R '	.40	712.50	.200	.020	40935.1	-.42	.004
μ _P	.40	712.50	.200	.020	41091.0	-.04	.004
μ _P '	.40	712.50	.200	.020	41091.0	-.04	.004
δ _T	.40	712.50	.060	.020	41092.4	-.03	.004
K	.40	712.50	2850.000	285.000	41143.9	.09	.004
Baseline	.50	712.50	0.000	0.000	50974.6	0.00	.004
a	.50	712.50	12.750	.020	50998.2	.05	.009
a'	.50	712.50	12.750	.020	50875.6	-.19	.009
b	.50	712.50	1.250	.020	50952.3	-.04	-.015
b'	.50	712.50	1.250	.020	50907.5	-.13	.023
c	.50	712.50	6.750	.020	50888.2	-.17	-.001
c'	.50	712.50	6.750	.020	50993.4	.04	-.001
d	.50	712.50	.410	.020	50976.3	0.00	-.015
d'	.50	712.50	.410	.020	50890.9	-.16	.023
dr	.50	712.50	.810	.020	51009.3	.07	.025
dr'	.50	712.50	.810	.020	50998.0	.05	-.016
dp	.50	712.50	.371	.020	50774.2	-.39	.004
dp'	.50	712.50	.371	.020	50774.2	-.39	.004
dpv	.50	712.50	.624	.020	50968.6	-.01	.004
dpv'	.50	712.50	.624	.020	50968.6	-.01	.004
r	.50	712.50	8.250	.020	51092.9	.23	.004
xc	.50	712.50	0.000	.020	50958.6	-.03	-.035
yc	.50	712.50	6.000	.020	51037.9	.12	-.006
Δx	.50	712.50	0.000	.020	49502.0	-2.89	.024

Table D-2

Δy	.50	712.50	0.000	.020	52554.4	3.10	.004
k	.50	712.50	.497	.020	48854.5	-4.16	.004
rc0	.50	712.50	.561	.020	51031.3	.11	.004
R_B	.50	712.50	.747	.020	50922.9	-.10	.004
S_L	.50	712.50	5.500	.020	51080.1	.21	.004
μ_B	.50	712.50	.100	.020	50539.3	-.85	.004
μ_R	.50	712.50	.200	.020	50745.4	-.45	.004
μ_R'	.50	712.50	.200	.020	50745.4	-.45	.004
μ_P	.50	712.50	.200	.020	50955.7	-.04	.004
μ_P'	.50	712.50	.200	.020	50955.7	-.04	.004
δ_T	.50	712.50	.060	.020	50845.9	-.25	.004
K	.50	712.50	2850.000	285.000	50893.6	-.16	.004
Baseline	.60	712.50	0.000	0.000	60545.8	0.00	.004
a	.60	712.50	12.750	.020	60569.9	.04	.009
a'	.60	712.50	12.750	.020	60399.0	-.24	.009
b	.60	712.50	1.250	.020	60521.7	-.04	-.015
b'	.60	712.50	1.250	.020	60587.3	.07	.024
c	.60	712.50	6.750	.020	60474.3	-.12	-.001
c'	.60	712.50	6.750	.020	60580.6	.06	-.001
d	.60	712.50	.410	.020	60551.4	.01	-.015
d'	.60	712.50	.410	.020	60563.6	.03	.024
dr	.60	712.50	.810	.020	60605.6	.10	.024
dr'	.60	712.50	.810	.020	60577.1	.05	-.016
dp	.60	712.50	.371	.020	60435.7	-.18	.004
dp'	.60	712.50	.371	.020	60435.7	-.18	.004
dpv	.60	712.50	.624	.020	60538.8	-.01	.004
dpv'	.60	712.50	.624	.020	60538.8	-.01	.004
r	.60	712.50	8.250	.020	60685.2	.23	.004

Table D-2

xc	.60	712.50	0.000	.020	60531.9	-.02	-.035
yc	.60	712.50	6.000	.020	60656.1	.18	-.006
Δx	.60	712.50	0.000	.020	58526.7	-3.33	.024
Δy	.60	712.50	0.000	.020	62494.2	3.22	.004
k	.60	712.50	.497	.020	58174.0	-3.92	.004
rc0	.60	712.50	.561	.020	60623.9	.13	.004
R _B	.60	712.50	.747	.020	60474.3	-.12	.004
S _L	.60	712.50	5.500	.020	60797.0	.41	.004
μ_B	.60	712.50	.100	.020	59946.6	-.99	.004
μ_R	.60	712.50	.200	.020	60270.6	-.45	.004
μ_R'	.60	712.50	.200	.020	60270.6	-.45	.004
μ_P	.60	712.50	.200	.020	60524.0	-.04	.004
μ_P'	.60	712.50	.200	.020	60524.0	-.04	.004
δ_T	.60	712.50	.060	.020	60514.1	-.05	.004
K	.60	712.50	2850.000	285.000	60587.0	.07	.004
Baseline	.70	712.50	0.000	0.000	69919.9	0.00	.004
a	.70	712.50	12.750	.020	69946.0	.04	.009
a'	.70	712.50	12.750	.020	69926.6	.01	.009
b	.70	712.50	1.250	.020	69887.5	-.05	-.016
b'	.70	712.50	1.250	.020	69983.9	.09	.023
c	.70	712.50	6.750	.020	69844.5	-.11	-.001
c'	.70	712.50	6.750	.020	70120.7	.29	-.001
d	.70	712.50	.410	.020	69932.7	.02	-.016
d'	.70	712.50	.410	.020	69951.5	.05	.023
dr	.70	712.50	.810	.020	70126.7	.30	.025
dr'	.70	712.50	.810	.020	70107.7	.27	-.016
dp	.70	712.50	.371	.020	69796.6	-.18	.004
dp'	.70	712.50	.371	.020	69796.6	-.18	.004

Table D-2

dpv	.70	712.50	.624	.020	69912.1	-.01	.004
dpv'	.70	712.50	.624	.020	69912.1	-.01	.004
r	.70	712.50	8.250	.020	70079.6	.23	.004
xc	.70	712.50	0.000	.020	69901.2	-.03	-.035
yc	.70	712.50	6.000	.020	70203.2	.41	-.006
Δx	.70	712.50	0.000	.020	67283.4	-3.77	.024
Δy	.70	712.50	0.000	.020	72258.5	3.34	.004
k	.70	712.50	.497	.020	67180.8	-3.92	.004
rc0	.70	712.50	.561	.020	70022.0	.15	.004
R _B	.70	712.50	.747	.020	69826.7	-.13	.004
S _L	.70	712.50	5.500	.020	70203.7	.41	.004
μ_B	.70	712.50	.100	.020	69128.1	-1.13	.004
μ_R	.70	712.50	.200	.020	69773.8	-.21	.004
μ_R'	.70	712.50	.200	.020	69773.8	-.21	.004
μ_P	.70	712.50	.200	.020	69895.5	-.03	.004
μ_P'	.70	712.50	.200	.020	69895.5	-.03	.004
δ_T	.70	712.50	.060	.020	69880.0	-.06	.004
K	.70	712.50	2850.000	285.000	69954.9	.05	.004
Baseline	.30	1425.00	0.000	0.000	62372.9	0.00	.009
a	.30	1425.00	12.750	.020	62395.1	.04	.014
a'	.30	1425.00	12.750	.020	62289.5	-.13	.014
b	.30	1425.00	1.250	.020	62354.6	-.03	-.011
b'	.30	1425.00	1.250	.020	62307.2	-.11	.028
c	.30	1425.00	6.750	.020	62171.2	-.32	.004
c'	.30	1425.00	6.750	.020	62341.8	-.05	.004
d	.30	1425.00	.410	.020	62369.5	-.01	-.011
d'	.30	1425.00	.410	.020	62295.6	-.12	.028
dr	.30	1425.00	.810	.020	62423.1	.08	.029

Table D-2

dr'	.30	1425.00	.810	.020	62366.3	-.01	-.012
dp	.30	1425.00	.371	.020	62160.1	-.34	.008
dp'	.30	1425.00	.371	.020	62160.1	-.34	.008
dpv	.30	1425.00	.624	.020	62366.5	-.01	.009
dpv'	.30	1425.00	.624	.020	62366.5	-.01	.009
r	.30	1425.00	8.250	.020	62520.7	.24	.009
xc	.30	1425.00	0.000	.020	62345.1	-.04	-.031
yc	.30	1425.00	6.000	.020	62381.7	.01	-.001
Δx	.30	1425.00	0.000	.020	61275.1	-1.76	.028
Δy	.30	1425.00	0.000	.020	64137.5	2.83	.009
k	.30	1425.00	.497	.020	59872.5	-4.01	.009
rc0	.30	1425.00	.561	.020	62416.7	.07	.009
R _B	.30	1425.00	.747	.020	62339.7	-.05	.009
S _L	.30	1425.00	5.500	.020	62514.8	.23	.009
μ_B	.30	1425.00	.100	.020	61994.7	-.61	.009
μ_R	.30	1425.00	.200	.020	62051.8	-.51	.009
μ_R'	.30	1425.00	.200	.020	62051.8	-.51	.009
μ_P	.30	1425.00	.200	.020	62352.9	-.03	.009
μ_P'	.30	1425.00	.200	.020	62352.9	-.03	.009
δ_T	.30	1425.00	.060	.020	62272.5	-.16	.008
K	.30	1425.00	2850.000	285.000	62349.6	-.04	.008
Baseline	.40	1425.00	0.000	0.000	82262.4	0.00	.008
a	.40	1425.00	12.750	.020	82430.8	.20	.013
a'	.40	1425.00	12.750	.020	82294.5	.04	.013
b	.40	1425.00	1.250	.020	82220.4	-.05	-.011
b'	.40	1425.00	1.250	.020	82325.3	.08	.028
c	.40	1425.00	6.750	.020	82147.6	-.14	.003
c'	.40	1425.00	6.750	.020	82389.1	.15	.004

Table D-2

d	.40	1425.00	.410	.020	82254.9	-.01	-.011
d'	.40	1425.00	.410	.020	82304.3	.05	.028
dr	.40	1425.00	.810	.020	82434.9	.21	.029
dr'	.40	1425.00	.810	.020	82399.6	.17	-.012
dp	.40	1425.00	.371	.020	82102.6	-.19	.009
dp'	.40	1425.00	.371	.020	82102.6	-.19	.009
dpv	.40	1425.00	.624	.020	82254.7	-.01	.008
dpv'	.40	1425.00	.624	.020	82254.7	-.01	.008
r	.40	1425.00	8.250	.020	82456.3	.24	.008
xc	.40	1425.00	0.000	.020	82327.5	.08	-.031
yc	.40	1425.00	6.000	.020	82439.9	.22	-.001
Δx	.40	1425.00	0.000	.020	80479.0	-2.17	.028
Δy	.40	1425.00	0.000	.020	84696.0	2.96	.009
k	.40	1425.00	.497	.020	78966.9	-4.01	.009
rc0	.40	1425.00	.561	.020	82333.1	.09	.008
R _B	.40	1425.00	.747	.020	82209.4	-.06	.008
S _L	.40	1425.00	5.500	.020	82616.4	.43	.009
μ_B	.40	1425.00	.100	.020	81828.2	-.53	.009
μ_R	.40	1425.00	.200	.020	82007.6	-.31	.009
μ_R'	.40	1425.00	.200	.020	82007.6	-.31	.009
μ_P	.40	1425.00	.200	.020	82238.5	-.03	.008
μ_P'	.40	1425.00	.200	.020	82238.5	-.03	.008
δ_T	.40	1425.00	.060	.020	82241.3	-.03	.009
K	.40	1425.00	2850.000	285.000	82376.9	.14	.008
Baseline	.50	1425.00	0.000	0.000	101913.7	0.00	.008
a	.50	1425.00	12.750	.020	101937.9	.02	.013
a'	.50	1425.00	12.750	.020	101935.0	.02	.013
b	.50	1425.00	1.250	.020	101841.6	-.07	-.011

Table D-2

b'	.50	1425.00	1.250	.020	101982.0	.07	.028
c	.50	1425.00	6.750	.020	101764.7	-.15	.003
c'	.50	1425.00	6.750	.020	102122.5	.20	.004
d	.50	1425.00	.410	.020	101886.9	-.03	-.011
d'	.50	1425.00	.410	.020	101949.1	.03	.028
dr	.50	1425.00	.810	.020	101960.5	.05	.029
dr'	.50	1425.00	.810	.020	102069.9	.15	-.012
dp	.50	1425.00	.371	.020	101726.8	-.18	.009
dp'	.50	1425.00	.371	.020	101726.8	-.18	.009
dpv	.50	1425.00	.624	.020	101904.2	-.01	.008
dpv'	.50	1425.00	.624	.020	101904.2	-.01	.008
r	.50	1425.00	8.250	.020	102152.3	.23	.008
xc	.50	1425.00	0.000	.020	101985.5	.07	-.031
yc	.50	1425.00	6.000	.020	102144.0	.23	-.001
Δx	.50	1425.00	0.000	.020	99050.1	-2.81	.028
Δy	.50	1425.00	0.000	.020	105052.1	3.08	.009
k	.50	1425.00	.497	.020	97838.1	-4.00	.009
rc0	.50	1425.00	.561	.020	102014.6	.10	.008
R _B	.50	1425.00	.747	.020	101795.7	-.12	.009
S _L	.50	1425.00	5.500	.020	102360.4	.44	.009
μ_B	.50	1425.00	.100	.020	101018.0	-.88	.008
μ_R	.50	1425.00	.200	.020	101610.2	-.30	.009
μ_R'	.50	1425.00	.200	.020	101610.2	-.30	.009
μ_P	.50	1425.00	.200	.020	101883.9	-.03	.008
μ_P'	.50	1425.00	.200	.020	101883.9	-.03	.008
δ_T	.50	1425.00	.060	.020	101887.5	-.03	.009
K	.50	1425.00	2850.000	285.000	102039.2	.12	.008
Baseline	.60	1425.00	0.000	0.000	121181.8	0.00	.008

Table D-2

a	.60	1425.00	12.750	.020	121207.0	.02	.013
a'	.60	1425.00	12.750	.020	121219.2	.03	.013
b	.60	1425.00	1.250	.020	121106.0	-.06	-.011
b'	.60	1425.00	1.250	.020	121285.3	.09	.028
c	.60	1425.00	6.750	.020	121030.2	-.13	.003
c'	.60	1425.00	6.750	.020	121461.2	.23	.004
d	.60	1425.00	.410	.020	121163.0	-.02	-.011
d'	.60	1425.00	.410	.020	121247.5	.05	.028
dr	.60	1425.00	.810	.020	121250.5	.06	.029
dr'	.60	1425.00	.810	.020	121385.0	.17	-.012
dp	.60	1425.00	.371	.020	121003.2	-.15	.008
dp'	.60	1425.00	.371	.020	121003.2	-.15	.008
dpv	.60	1425.00	.624	.020	121170.6	-.01	.008
dpv'	.60	1425.00	.624	.020	121170.6	-.01	.008
r	.60	1425.00	8.250	.020	121463.8	.23	.008
xc	.60	1425.00	0.000	.020	121093.7	-.07	-.032
yc	.60	1425.00	6.000	.020	121501.6	.26	-.001
Δx	.60	1425.00	0.000	.020	117061.6	-3.40	.027
Δy	.60	1425.00	0.000	.020	125048.3	3.19	.009
k	.60	1425.00	.497	.020	116342.6	-3.99	.009
rc0	.60	1425.00	.561	.020	121317.2	.11	.008
R _B	.60	1425.00	.747	.020	121066.3	-.10	.008
S _L	.60	1425.00	5.500	.020	121753.7	.47	.008
μ_B	.60	1425.00	.100	.020	120024.8	-.95	.008
μ_R	.60	1425.00	.200	.020	120866.1	-.26	.009
μ_R'	.60	1425.00	.200	.020	120866.1	-.26	.009
μ_P	.60	1425.00	.200	.020	121146.8	-.03	.008
μ_P'	.60	1425.00	.200	.020	121146.8	-.03	.008

Table D-2

δ_T	.60	1425.00	.060	.020	121181.2	0.00	.009
K	.60	1425.00	2850.000	285.000	121293.6	.09	.008
Baseline	.70	1425.00	0.000	0.000	140145.1	0.00	.008
a	.70	1425.00	12.750	.020	140122.6	-.02	.013
a'	.70	1425.00	12.750	.020	140154.9	.01	.013
b	.70	1425.00	1.250	.020	140021.5	-.09	-.011
b'	.70	1425.00	1.250	.020	140249.3	.07	.028
c	.70	1425.00	6.750	.020	139951.4	-.14	.003
c'	.70	1425.00	6.750	.020	140456.9	.22	.004
d	.70	1425.00	.410	.020	140090.8	-.04	-.011
d'	.70	1425.00	.410	.020	140185.1	.03	.028
dr	.70	1425.00	.810	.020	140191.6	.03	.028
dr'	.70	1425.00	.810	.020	140359.2	.15	-.012
dp	.70	1425.00	.371	.020	139938.0	-.15	.008
dp'	.70	1425.00	.371	.020	139938.0	-.15	.008
dpv	.70	1425.00	.624	.020	140132.1	-.01	.008
dpv'	.70	1425.00	.624	.020	140132.1	-.01	.008
r	.70	1425.00	8.250	.020	140468.9	.23	.008
xc	.70	1425.00	0.000	.020	140009.0	-.10	-.031
yc	.70	1425.00	6.000	.020	140611.1	.33	-.002
Δx	.70	1425.00	0.000	.020	134814.5	-3.80	.028
Δy	.70	1425.00	0.000	.020	144779.7	3.31	.009
k	.70	1425.00	.497	.020	134558.5	-3.99	.009
rc0	.70	1425.00	.561	.020	140319.7	.12	.008
R_B	.70	1425.00	.747	.020	139988.8	-.11	.008
S_L	.70	1425.00	5.500	.020	140802.8	.47	.008
μ_B	.70	1425.00	.100	.020	138646.1	-1.07	.008
μ_R	.70	1425.00	.200	.020	139782.1	-.26	.008

Table D-2

μ_R'	.70	1425.00	.200	.020	139782.1	-.26	.008
μ_P	.70	1425.00	.200	.020	140104.5	-.03	.008
μ_P'	.70	1425.00	.200	.020	140104.5	-.03	.008
δ_T	.70	1425.00	.060	.020	140129.1	-.01	.008
K	.70	1425.00	2850.000	285.000	140229.8	.06	.008
Baseline	.30	2137.50	0.000	0.000	93541.1	0.00	.013
a	.30	2137.50	12.750	.020	93724.2	.20	.018
a'	.30	2137.50	12.750	.020	93557.1	.02	.018
b	.30	2137.50	1.250	.020	93453.9	-.09	-.006
b'	.30	2137.50	1.250	.020	93565.9	.03	.033
c	.30	2137.50	6.750	.020	93342.3	-.21	.008
c'	.30	2137.50	6.750	.020	93574.5	.04	.008
d	.30	2137.50	.410	.020	93490.6	-.05	-.007
d'	.30	2137.50	.410	.020	93571.7	.03	.033
dr	.30	2137.50	.810	.020	93721.4	.19	.033
dr'	.30	2137.50	.810	.020	93600.8	.06	-.007
dp	.30	2137.50	.371	.020	93377.0	-.18	.013
dp'	.30	2137.50	.371	.020	93377.0	-.18	.013
dpv	.30	2137.50	.624	.020	93479.9	-.07	.013
dpv'	.30	2137.50	.624	.020	93479.9	-.07	.013
r	.30	2137.50	8.250	.020	93764.1	.24	.013
xc	.30	2137.50	0.000	.020	93535.9	-.01	-.026
yc	.30	2137.50	6.000	.020	93619.3	.08	.003
Δx	.30	2137.50	0.000	.020	91881.8	-1.77	.032
Δy	.30	2137.50	0.000	.020	96165.8	2.81	.013
k	.30	2137.50	.497	.020	89899.3	-3.89	.014
rc0	.30	2137.50	.561	.020	93600.1	.06	.013
R_B	.30	2137.50	.747	.020	93451.9	-.10	.013

Table D-2

S _L	.30	2137.50	5.500	.020	93977.6	.47	.013
μ _B	.30	2137.50	.100	.020	93111.3	-.46	.013
μ _R	.30	2137.50	.200	.020	93180.4	-.39	.013
μ _R '	.30	2137.50	.200	.020	93180.4	-.39	.013
μ _P	.30	2137.50	.200	.020	93465.8	-.08	.013
μ _P '	.30	2137.50	.200	.020	93465.8	-.08	.013
δ _T	.30	2137.50	.060	.020	93556.1	.02	.013
K	.30	2137.50	2850.000	285.000	93518.7	-.02	.012
Baseline	.40	2137.50	0.000	0.000	123740.4	0.00	.013
a	.40	2137.50	12.750	.020	123703.2	-.03	.017
a'	.40	2137.50	12.750	.020	123533.6	-.17	.018
b	.40	2137.50	1.250	.020	123643.8	-.08	-.007
b'	.40	2137.50	1.250	.020	123543.3	-.16	.032
c	.40	2137.50	6.750	.020	123542.9	-.16	.008
c'	.40	2137.50	6.750	.020	123771.2	.02	.009
d	.40	2137.50	.410	.020	123648.4	-.07	-.007
d'	.40	2137.50	.410	.020	123506.9	-.19	.032
dr	.40	2137.50	.810	.020	123692.1	-.04	.033
dr'	.40	2137.50	.810	.020	123835.9	.08	-.007
dp	.40	2137.50	.371	.020	123285.6	-.37	.013
dp'	.40	2137.50	.371	.020	123285.6	-.37	.013
dpv	.40	2137.50	.624	.020	123730.0	-.01	.013
dpv'	.40	2137.50	.624	.020	123730.0	-.01	.013
r	.40	2137.50	8.250	.020	124033.1	.24	.013
xc	.40	2137.50	0.000	.020	123562.5	-.14	-.027
yc	.40	2137.50	6.000	.020	123937.6	.16	.003
Δx	.40	2137.50	0.000	.020	120730.6	-2.43	.032
Δy	.40	2137.50	0.000	.020	127357.1	2.92	.013

Table D-2

k	.40	2137.50	.497	.020	118708.0	-4.07	.014
rc0	.40	2137.50	.561	.020	123832.4	.07	.013
R _B	.40	2137.50	.747	.020	123422.0	-.26	.013
S _L	.40	2137.50	5.500	.020	124084.8	.28	.013
μ _B	.40	2137.50	.100	.020	122823.8	-.74	.013
μ _R	.40	2137.50	.200	.020	123085.5	-.53	.013
μ _R '	.40	2137.50	.200	.020	123085.5	-.53	.013
μ _P	.40	2137.50	.200	.020	123708.0	-.03	.013
μ _P '	.40	2137.50	.200	.020	123708.0	-.03	.013
δ _T	.40	2137.50	.060	.020	123512.4	-.18	.013
K	.40	2137.50	2850.000	285.000	123466.2	-.22	.012
Baseline	.50	2137.50	0.000	0.000	153175.2	0.00	.012
a	.50	2137.50	12.750	.020	153404.6	.15	.018
a'	.50	2137.50	12.750	.020	152923.7	-.16	.018
b	.50	2137.50	1.250	.020	152950.3	-.15	-.007
b'	.50	2137.50	1.250	.020	153202.6	.02	.032
c	.50	2137.50	6.750	.020	152822.5	-.23	.008
c'	.50	2137.50	6.750	.020	153314.5	.09	.008
d	.50	2137.50	.410	.020	153018.4	-.10	-.007
d'	.50	2137.50	.410	.020	153235.6	.04	.033
dr	.50	2137.50	.810	.020	153107.1	-.04	.033
dr'	.50	2137.50	.810	.020	153235.3	.04	-.007
dp	.50	2137.50	.371	.020	152981.8	-.13	.013
dp'	.50	2137.50	.371	.020	152981.8	-.13	.013
dpv	.50	2137.50	.624	.020	153163.4	-.01	.012
dpv'	.50	2137.50	.624	.020	153163.4	-.01	.012
r	.50	2137.50	8.250	.020	153536.2	.24	.012
xc	.50	2137.50	0.000	.020	153245.6	.05	-.027

Table D-2

yc	.50	2137.50	6.000	.020	153464.6	.19	.003
Δx	.50	2137.50	0.000	.020	148637.1	-2.96	.032
Δy	.50	2137.50	0.000	.020	157837.5	3.04	.013
k	.50	2137.50	.497	.020	146938.2	-4.07	.013
rc0	.50	2137.50	.561	.020	153304.9	.08	.013
R_B	.50	2137.50	.747	.020	153071.8	-.07	.013
S_L	.50	2137.50	5.500	.020	153583.5	.27	.013
μ_B	.50	2137.50	.100	.020	151893.5	-.84	.012
μ_R	.50	2137.50	.200	.020	152673.3	-.33	.013
μ_R'	.50	2137.50	.200	.020	152673.3	-.33	.013
μ_P	.50	2137.50	.200	.020	153138.1	-.02	.012
μ_P'	.50	2137.50	.200	.020	153138.1	-.02	.012
δ_T	.50	2137.50	.060	.020	152914.7	-.17	.013
K	.50	2137.50	2850.000	285.000	153081.7	-.06	.012
Baseline	.60	2137.50	0.000	0.000	182008.5	0.00	.013
a	.60	2137.50	12.750	.020	182325.3	.17	.017
a'	.60	2137.50	12.750	.020	182000.9	0.00	.018
b	.60	2137.50	1.250	.020	182179.6	.09	-.007
b'	.60	2137.50	1.250	.020	182035.2	.01	.032
c	.60	2137.50	6.750	.020	181641.2	-.20	.008
c'	.60	2137.50	6.750	.020	182232.1	.12	.008
d	.60	2137.50	.410	.020	182273.3	.15	-.007
d'	.60	2137.50	.410	.020	181980.9	-.02	.032
dr	.60	2137.50	.810	.020	182443.4	.24	.033
dr'	.60	2137.50	.810	.020	182483.8	.26	-.008
dp	.60	2137.50	.371	.020	181799.5	-.11	.012
dp'	.60	2137.50	.371	.020	181799.5	-.11	.012
dpv	.60	2137.50	.624	.020	181995.9	-.01	.013

Table D-2

dpv'	.60	2137.50	.624	.020	181995.9	-.01	.013
r	.60	2137.50	8.250	.020	182436.4	.24	.013
xc	.60	2137.50	0.000	.020	182015.6	0.00	-.027
yc	.60	2137.50	6.000	.020	182669.5	.36	.003
Δx	.60	2137.50	0.000	.020	175996.0	-3.30	.032
Δy	.60	2137.50	0.000	.020	187765.5	3.16	.013
k	.60	2137.50	.497	.020	175063.4	-3.82	.013
rc0	.60	2137.50	.561	.020	182226.0	.12	.013
R _B	.60	2137.50	.747	.020	181874.7	-.07	.013
S _L	.60	2137.50	5.500	.020	182962.7	.52	.012
μ_B	.60	2137.50	.100	.020	180330.5	-.92	.012
μ_R	.60	2137.50	.200	.020	181434.6	-.32	.013
μ_R'	.60	2137.50	.200	.020	181434.6	-.32	.013
μ_P	.60	2137.50	.200	.020	181968.8	-.02	.013
μ_P'	.60	2137.50	.200	.020	181968.8	-.02	.013
δ_T	.60	2137.50	.060	.020	182092.2	.05	.012
K	.60	2137.50	2850.000	285.000	181853.6	-.09	.012
Baseline	.70	2137.50	0.000	0.000	210809.0	0.00	.012
a	.70	2137.50	12.750	.020	210466.8	-.16	.017
a'	.70	2137.50	12.750	.020	210289.5	-.25	.017
b	.70	2137.50	1.250	.020	210569.2	-.11	-.007
b'	.70	2137.50	1.250	.020	210881.8	.03	.032
c	.70	2137.50	6.750	.020	210385.0	-.20	.008
c'	.70	2137.50	6.750	.020	210884.1	.04	.008
d	.70	2137.50	.410	.020	210436.0	-.18	-.007
d'	.70	2137.50	.410	.020	210771.8	-.02	.032
dr	.70	2137.50	.810	.020	210547.5	-.12	.033
dr'	.70	2137.50	.810	.020	210712.9	-.05	-.008

Table D-2

dp	.70	2137.50	.371	.020	210051.9	-.36	.013
dp'	.70	2137.50	.371	.020	210051.9	-.36	.013
dpv	.70	2137.50	.624	.020	210792.1	-.01	.012
dpv'	.70	2137.50	.624	.020	210792.1	-.01	.012
r	.70	2137.50	8.250	.020	211299.3	.23	.012
xc	.70	2137.50	0.000	.020	210786.3	-.01	-.027
yc	.70	2137.50	6.000	.020	211114.3	.14	.003
Δx	.70	2137.50	0.000	.020	202541.6	-3.92	.032
Δy	.70	2137.50	0.000	.020	217720.2	3.28	.013
k	.70	2137.50	.497	.020	202262.7	-4.05	.013
rc0	.70	2137.50	.561	.020	211036.4	.11	.012
R_B	.70	2137.50	.747	.020	210106.1	-.33	.013
S_L	.70	2137.50	5.500	.020	211377.1	.27	.013
μ_B	.70	2137.50	.100	.020	208143.4	-1.26	.013
μ_R	.70	2137.50	.200	.020	209632.3	-.56	.013
μ_R'	.70	2137.50	.200	.020	209632.3	-.56	.013
μ_P	.70	2137.50	.200	.020	210756.0	-.03	.012
μ_P'	.70	2137.50	.200	.020	210756.0	-.03	.012
δ_T	.70	2137.50	.060	.020	210344.3	-.22	.012
K	.70	2137.50	2850.000	285.000	210497.4	-.15	.011
Baseline	.30	2850.00	0.000	0.000	124929.5	0.00	.017
a	.30	2850.00	12.750	.020	125116.7	.15	.022
a'	.30	2850.00	12.750	.020	124735.7	-.16	.022
b	.30	2850.00	1.250	.020	124747.9	-.15	-.002
b'	.30	2850.00	1.250	.020	125024.9	.08	.037
c	.30	2850.00	6.750	.020	124724.8	-.16	.013
c'	.30	2850.00	6.750	.020	124927.5	0.00	.013
d	.30	2850.00	.410	.020	124799.0	-.10	-.002

Table D-2

d'	.30	2850.00	.410	.020	124993.9	.05	.037
dr	.30	2850.00	.810	.020	125125.8	.16	.038
dr'	.30	2850.00	.810	.020	125132.0	.16	-.003
dp	.30	2850.00	.371	.020	124502.5	-.34	.017
dp'	.30	2850.00	.371	.020	124502.5	-.34	.017
dpv	.30	2850.00	.624	.020	124921.9	-.01	.017
dpv'	.30	2850.00	.624	.020	124921.9	-.01	.017
r	.30	2850.00	8.250	.020	125228.4	.24	.017
xc	.30	2850.00	0.000	.020	124960.4	.02	-.022
yc	.30	2850.00	6.000	.020	125049.8	.10	.008
Δx	.30	2850.00	0.000	.020	122641.1	-1.83	.037
Δy	.30	2850.00	0.000	.020	128393.1	2.77	.018
k	.30	2850.00	.497	.020	119822.1	-4.09	.018
rc0	.30	2850.00	.561	.020	124997.3	.05	.017
R _B	.30	2850.00	.747	.020	124888.8	-.03	.017
S _L	.30	2850.00	5.500	.020	125340.6	.33	.017
μ_B	.30	2850.00	.100	.020	124129.7	-.64	.018
μ_R	.30	2850.00	.200	.020	124441.5	-.39	.017
μ_R'	.30	2850.00	.200	.020	124441.5	-.39	.017
μ_P	.30	2850.00	.200	.020	124905.3	-.02	.017
μ_P'	.30	2850.00	.200	.020	124905.3	-.02	.017
δ_T	.30	2850.00	.060	.020	124760.2	-.14	.017
K	.30	2850.00	2850.000	285.000	124756.8	-.14	.016
Baseline	.40	2850.00	0.000	0.000	165197.3	0.00	.017
a	.40	2850.00	12.750	.020	165274.0	.05	.022
a'	.40	2850.00	12.750	.020	164814.4	-.23	.022
b	.40	2850.00	1.250	.020	165010.7	-.11	-.002
b'	.40	2850.00	1.250	.020	165213.1	.01	.037

Table D-2

c	.40	2850.00	6.750	.020	164889.9	-.19	.013
c'	.40	2850.00	6.750	.020	165126.1	-.04	.013
d	.40	2850.00	.410	.020	164878.7	-.19	-.002
d'	.40	2850.00	.410	.020	165158.9	-.02	.037
dr	.40	2850.00	.810	.020	165337.1	.08	.038
dr'	.40	2850.00	.810	.020	165349.9	.09	-.003
dp	.40	2850.00	.371	.020	164647.2	-.33	.017
dp'	.40	2850.00	.371	.020	164647.2	-.33	.017
dpv	.40	2850.00	.624	.020	164846.7	-.21	.017
dpv'	.40	2850.00	.624	.020	164846.7	-.21	.017
r	.40	2850.00	8.250	.020	165248.3	.03	.017
xc	.40	2850.00	0.000	.020	165109.6	-.05	-.022
yc	.40	2850.00	6.000	.020	165242.8	.03	.007
Δx	.40	2850.00	0.000	.020	161224.9	-2.40	.037
Δy	.40	2850.00	0.000	.020	169978.9	2.89	.017
k	.40	2850.00	.497	.020	158372.6	-4.13	.018
rc0	.40	2850.00	.561	.020	165303.3	.06	.017
R _B	.40	2850.00	.747	.020	164799.7	-.24	.017
S _L	.40	2850.00	5.500	.020	165741.6	.33	.017
μ_B	.40	2850.00	.100	.020	163951.3	-.75	.017
μ_R	.40	2850.00	.200	.020	164220.4	-.59	.017
μ_R'	.40	2850.00	.200	.020	164220.4	-.59	.017
μ_P	.40	2850.00	.200	.020	164830.5	-.22	.017
μ_P'	.40	2850.00	.200	.020	164830.5	-.22	.017
δ_T	.40	2850.00	.060	.020	164966.3	-.14	.017
K	.40	2850.00	2850.000	285.000	164881.5	-.19	.016
Baseline	.50	2850.00	0.000	0.000	204360.7	0.00	.017
a	.50	2850.00	12.750	.020	204558.4	.10	.022

Table D-2

a'	.50	2850.00	12.750	.020	204449.7	.04	.022
b	.50	2850.00	1.250	.020	204393.6	.02	-.002
b'	.50	2850.00	1.250	.020	204687.3	.16	.037
c	.50	2850.00	6.750	.020	204217.6	-.07	.012
c'	.50	2850.00	6.750	.020	204561.9	.10	.012
d	.50	2850.00	.410	.020	204503.2	.07	-.002
d'	.50	2850.00	.410	.020	204645.8	.14	.037
dr	.50	2850.00	.810	.020	204830.8	.23	.038
dr'	.50	2850.00	.810	.020	204598.1	.12	-.003
dp	.50	2850.00	.371	.020	204113.8	-.12	.017
dp'	.50	2850.00	.371	.020	204113.8	-.12	.017
dpv	.50	2850.00	.624	.020	204275.3	-.04	.017
dpv'	.50	2850.00	.624	.020	204275.3	-.04	.017
r	.50	2850.00	8.250	.020	204771.6	.20	.017
xc	.50	2850.00	0.000	.020	204540.2	.09	-.022
yc	.50	2850.00	6.000	.020	204769.8	.20	.007
Δx	.50	2850.00	0.000	.020	198444.1	-2.90	.036
Δy	.50	2850.00	0.000	.020	210539.6	3.02	.018
k	.50	2850.00	.497	.020	196351.5	-3.92	.017
rc0	.50	2850.00	.561	.020	204498.5	.07	.017
R _B	.50	2850.00	.747	.020	204197.0	-.08	.017
S _L	.50	2850.00	5.500	.020	205012.7	.32	.017
μ_B	.50	2850.00	.100	.020	202602.7	-.86	.017
μ_R	.50	2850.00	.200	.020	203506.7	-.42	.017
μ_R'	.50	2850.00	.200	.020	203506.7	-.42	.017
μ_P	.50	2850.00	.200	.020	204254.5	-.05	.017
μ_P'	.50	2850.00	.200	.020	204254.5	-.05	.017
δ_T	.50	2850.00	.060	.020	204483.9	.06	.017

Table D-2

K	.50	2850.00	2850.000	285.000	204287.7	-.04	.016
Baseline	.60	2850.00	0.000	0.000	243128.7	0.00	.017
a	.60	2850.00	12.750	.020	243247.6	.05	.021
a'	.60	2850.00	12.750	.020	243163.0	.01	.022
b	.60	2850.00	1.250	.020	243104.2	-.01	-.003
b'	.60	2850.00	1.250	.020	243497.4	.15	.037
c	.60	2850.00	6.750	.020	242891.0	-.10	.012
c'	.60	2850.00	6.750	.020	243529.4	.16	.012
d	.60	2850.00	.410	.020	243202.2	.03	-.003
d'	.60	2850.00	.410	.020	243078.0	-.02	.036
dr	.60	2850.00	.810	.020	243357.4	.09	.037
dr'	.60	2850.00	.810	.020	243343.7	.09	-.003
dp	.60	2850.00	.371	.020	242908.8	-.09	.017
dp'	.60	2850.00	.371	.020	242908.8	-.09	.017
dpv	.60	2850.00	.624	.020	243116.2	-.01	.017
dpv'	.60	2850.00	.624	.020	243116.2	-.01	.017
r	.60	2850.00	8.250	.020	243704.8	.24	.017
xc	.60	2850.00	0.000	.020	243267.1	.06	-.023
yc	.60	2850.00	6.000	.020	243537.2	.17	.007
Δx	.60	2850.00	0.000	.020	234816.4	-3.42	.036
Δy	.60	2850.00	0.000	.020	250750.6	3.13	.017
k	.60	2850.00	.497	.020	233689.1	-3.88	.017
rc0	.60	2850.00	.561	.020	243310.6	.07	.017
R _B	.60	2850.00	.747	.020	242989.9	-.06	.017
S _L	.60	2850.00	5.500	.020	243900.2	.32	.017
μ_B	.60	2850.00	.100	.020	240945.3	-.90	.017
μ_R	.60	2850.00	.200	.020	242209.7	-.38	.017
μ_R'	.60	2850.00	.200	.020	242209.7	-.38	.017

Table D-2

μ_P	.60	2850.00	.200	.020	243088.9	-.02	.017
μ_P'	.60	2850.00	.200	.020	243088.9	-.02	.017
δ_T	.60	2850.00	.060	.020	242656.3	-.19	.017
K	.60	2850.00	2850.000	285.000	242982.3	-.06	.015
Baseline	.70	2850.00	0.000	0.000	281306.6	0.00	.017
a	.70	2850.00	12.750	.020	281236.5	-.02	.021
a'	.70	2850.00	12.750	.020	281189.5	-.04	.022
b	.70	2850.00	1.250	.020	281065.4	-.09	-.003
b'	.70	2850.00	1.250	.020	281249.8	-.02	.036
c	.70	2850.00	6.750	.020	280877.6	-.15	.012
c'	.70	2850.00	6.750	.020	281645.3	.12	.012
d	.70	2850.00	.410	.020	281205.0	-.04	-.003
d'	.70	2850.00	.410	.020	281052.4	-.09	.036
dr	.70	2850.00	.810	.020	281386.7	.03	.037
dr'	.70	2850.00	.810	.020	281476.1	.06	-.003
dp	.70	2850.00	.371	.020	280349.1	-.34	.016
dp'	.70	2850.00	.371	.020	280349.1	-.34	.016
dpv	.70	2850.00	.624	.020	281291.1	-.01	.017
dpv'	.70	2850.00	.624	.020	281291.1	-.01	.017
r	.70	2850.00	8.250	.020	281969.4	.24	.017
xc	.70	2850.00	0.000	.020	280974.3	-.12	-.023
yc	.70	2850.00	6.000	.020	281607.8	.11	.007
Δx	.70	2850.00	0.000	.020	270147.6	-3.97	.036
Δy	.70	2850.00	0.000	.020	290453.7	3.25	.017
k	.70	2850.00	.497	.020	270392.1	-3.88	.018
rc0	.70	2850.00	.561	.020	281543.2	.08	.017
R _B	.70	2850.00	.747	.020	281107.1	-.07	.017
S _L	.70	2850.00	5.500	.020	282059.4	.27	.017

Table D-2

μ_B	.70	2850.00	.100	.020	277753.6	-1.26	.017
μ_R	.70	2850.00	.200	.020	280251.9	-.37	.017
μ_R'	.70	2850.00	.200	.020	280251.9	-.37	.017
μ_P	.70	2850.00	.200	.020	281257.5	-.02	.017
μ_P'	.70	2850.00	.200	.020	281257.5	-.02	.017
δ_T	.70	2850.00	.060	.020	280688.3	-.22	.017
K	.70	2850.00	2850.000	285.000	280971.7	-.12	.015

Table D-2

